Highly Efficient and Flexible Piezoelectric Nanogenerator based on Lead-free Perovskite Modified Self-Poled Poly (vinylidene fluoride) composite

A thesis submitted toward partial fulfilment

of the requirements for the degree of

Master of Technology in Nanoscience and Technology

Submitted by

SASWATA MANDAL

ROLL NO.: M4NST22002

Registration No. 154571 of 2020-2021

Under the guidance of

Prof. Kalyan Kumar Chattopadhyay

School of Materials Science and Nanotechnology

Jadavpur University

Kolkata -700032

Course affiliated to

Faculty of Engineering and Technology

Jadavpur university

Kolkata-700032

India

2022

M.Tech. (Nanoscience and Technology) course affiliated to

Faculty of Engineering and Technology

Jadavpur
University

Kolkata, India

CERTIFICATE OF RECOMMENDATION

This is to certify that the thesis entitled "**Highly Efficient and Flexible Piezoelectric Nanogenerator based on Lead-free Perovskite Modified Self-Poled Poly (vinylidene fluoride) composite**" is a bonafide work carried out by **Saswata Mandal** under our supervision and guidance for partial fulfillment of the requirement of Master of Technology in Nanoscience and Technology in School of Materials Science and Nanotechnology during the academic session 2020-2022.

29.8.22

THESIS ADVISOR

Prof. Kalyan Kumar Chattopadhyay

HOD Dept. of Physics

School of Materials and Nanotechnology,

Jadavpur University,

Kolkata-700 032

Dr. K. K. Chattopadhyay
Professor
Head, Department of Physics
Jadavpur University
Kolkata-700 032

24/8/22

DIRECTOR

Dr. Sourav Sarkar

School of Materials Science and Nanotechnology,

Jadavpur University,

Kolkata-700 032

Dr. Sourav Sarkar
Director
Associate Professor
School of Materials Science & Nanotechnology
Jadavpur University
Kolkata - 700032

24/08/2022

DEAN

Faculty Council of

Interdisciplinary Studies, Law and Management

Jadavpur University,

Kolkata-700 032

Dean
Faculty of Interdisciplinary Studies
Law & Management
Jadavpur University, Kolkata-700032

2

M.Tech. (Nanoscience and Technology) course affiliated to

Faculty of Engineering and Technology

Jadavpur University

Kolkata, India

CERTIFICATE OF APPROVAL **

This foregoing thesis is hereby approved as a credible study of an engineering subject carried out and presented in a manner satisfactory to warrant its acceptance as a prerequisite to the degree for which it has been submitted. It is understood that by this approval the undersigned does not dose or approve any statement made or opinion expressed or conclusion drawn therein but approves the thesis only for the purpose for which it has been submitted.

Committee of final examination ----------

for evaluation of Thesis ----------

** Only in case the thesis is approved.

DECLARATION OF ORIGINALITY AND COMPLIANCE OF ACADEMIC ETHICS

I hereby declare that this thesis contains a literature survey and original research work by the undersigned candidate, as part of his Master of Nano science and Technology) studies during academic session 2020-2022. All information in this document has been obtained and prefollowingce with academic rules and ethical conduct.

I also declare that, as required by this rules and conduct, I have fully cited and referred all material and results that are not original to this work.

NAME: Saswata Mandal

ROLL NUMBER: M4NST22002

Registration No.: 154571 of 2020-2021

THESIS TITLE: Highly Efficient and Flexible Piezoelectric Nanogenerator based on Lead-free Perovskite Modified Self-Poled Poly (vinylidene fluoride) composite

SIGNATURE: Saswata Mandal DATE: 24/8/2022

Acknowledgment

In the first place, I would like to express my profound gratitude to my supervisor **Prof (Dr). Kalyan Kumar Chattopadhyay** for his advice and guidance from the very early stage of this research as well as for giving me extraordinary experiences throughout the work. Above all and the most needed, he with provided me constant encouragement and support in various ways. Thank you also for the amicable environment conducive to extensive research work at Thin Film and Nanoscience Lab, in which you have welcomed me. All of these provided me with great support, helping me to confront the difficult periods of my project, which I do not think I would have completed it otherwise.

I would like to express my special heartiest thanks to my co-guide (Mr). Suvankar Mondal for his advice, guidance, and crucial contribution throughout my work. His involvement with his originality has triggered and nurtured the scholarly development that I will benefit from, for a long time to come. I really cannot value his support and generous cooperation. He was like an elder brother to me always by my side whenever I need him. Without his guidance, it would have been impossible for me to complete this project.

I would also like to express my sincere thanks to Dr. Chandan Kumar Ghosh, Dr. Mahua Ghosh Chowdhury, and Dr. Sourav Sarkar, for their help, support, encouragement, suggestion, and advice during the research. Their enthusiasm provided me with a helpful and effective way of learning which in turn inspired me to follow the research project with great enthusiasm.

I would also really like to thank all the staff members of the School of Materials Science and Nanotechnology and the Department of Physics for carrying out the critical characterization parts of the synthesized samples that composed a very important part of the thesis.

I extend my heartiest thanks to all my seniors in ‘Thin Film & Nano Science’ lab especially Suvankar Poddar da, Pulak da, Nabamita di, Nabamita di, Dimitra Di, Riyaz da, Souvik da, Biswojit Da, Ratna Di, and everyone in this lab for extending their helping hands. I would also like to thank all my friends Mrinmoy, Avinash, Saswata, Tanay, Manas, and Imran for their encouragement and cooperation.

Abstract

Piezoelectric nanoparticles provide a chance for the development of self-powered systems through energy collection. The usage of a system or device that performs a function without the requirement for an external power source, such as a battery or any other sort of source, is made possible by the newly developing technology known as self-powered systems. For instance, employing the piezoelectric effect, this technology may harness energy from sources such as ambient mechanical vibrations, noise, human movement, etc., and transform it into electrical energy. The size of conventional batteries is inappropriate for nanoscale devices and will result in the loss of the "nano" notion. This is a result of the traditional sources' provided power's vast size and comparatively large magnitude. The development of a nanogenerator (NG) to convert energy from the environment into electric energy would facilitate the development of some self-powered systems relying on nano- devices.

Making piezoelectric Cesium copper chloride ($CsCuCl_3$) and PVDF composite-based NGs for use in low-frequency energy harvesting applications is **the major goal of this thesis**. To test them under various low frequency mechanical deformations, many varieties of NGs based on this nanostructure have been thoroughly constructed and investigated. Using a low temperature and power, well-aligned $CsCuCl_3$ nanowires (NWs) with a high piezoelectric coefficient were created on flexible substrates. Then, several low-frequency energy harvesting systems were shown using these composite based NWs in various topologies.

The first chapter contains the fundamentals of nanoscience and technology, their applications, and the definitions of perovskite material and nanogenerators as well as their dielectric characteristics. The discussion of the researchers' work on various Perovskite-based nanogenerator types and perovskite dopes in PVDF or composite-based nanogenerators is covered in **the second chapter**. Their essay demonstrates a variety of cheap and simple

methods. In their publications, they demonstrate a variety of excellent daily applications. The fundamental synthesis process and characterization were detailed in **the third chapter**, covering how the machine operates and which equipment uses our synthesis method and electrical characterization. Polyvinylidene fluoride (PVDF) and cesium copper chloride (CsCuCl3) hybrid films are explained in the fourth chapter as desirable functional materials for piezoelectric-based mechanical energy harvesters. A piezoelectric nanogenerator (PNG) made of PVDF and CsCuCl3 demonstrated impressive output performance. PVDF has high crystallinity and electroactive β-phase nucleation of 92%. In composites, perovskite concertation was improved to achieve benchmark level output responsiveness. PNG with 4.0 wt% CsCuCl3 in PVDF produced an instantaneous output voltage and current of 220 V and 14 μA, respectively. It also demonstrated endurance under adverse circumstances and long-cycle stability (1,000 cycles). Furthermore, electricity from PNG was used to power 30 LEDs and charge a capacitor. The results that were obtained are quite significant and reveal the viability of developing revolutionary smart devices employing this class of perovskites.

Contents

4.2.2 Characterization

4.3 Results and discussion

4.4. Conclusion

Chapter 5

Grand conclusion & Grand conclusion

5.1 Grand conclusion

5.2 Scope for future works

Chapter 1

Introduction

1.1 Nanoscience & Nanotechnology:

The 1980s saw the early development of the multidisciplinary scientific and technology discipline known as nanoscience and technology. The nanoscale, which ranges in size from 1 to 100 nanometers, is the focus of engineering, science, and technology. One nanometer, or 10-9 of a metre, is one billionth of a metre. The atomic, molecular, and supramolecular manipulation of matter is known as nanotechnology. Molecular biology, surface science, semiconductor physics, energy storage, organic chemistry, microfabrication, molecular engineering, etc. are only a few examples of the many scientific disciplines that fall under the broad definition of nanotechnology, which is determined by scale. The related research and applications are as wide, ranging from wholly new strategies based on molecular self-assembly to extensions of predictable device physics, from creating new materials with nanoscale dimensions to direct control of matter on the atomic scale.

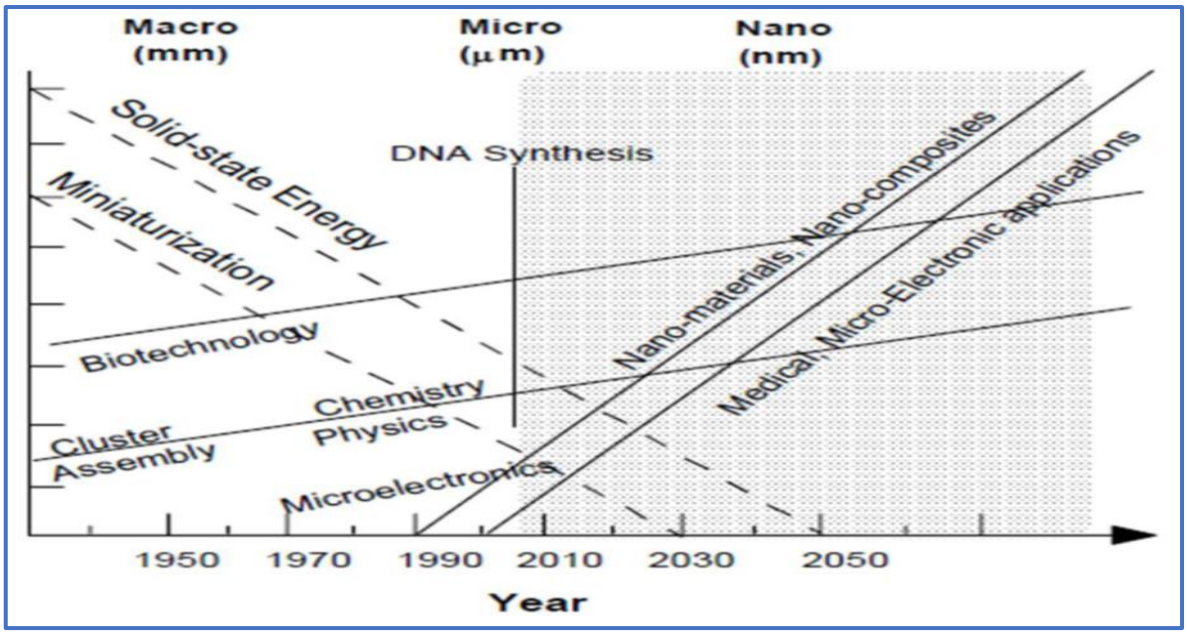

Figure 1.1: Introduction to Nanotechnology

1.1.1 What is Nanotechnology:

Maximum definitions focus on the investigation and management of events and substances at

length scales below 100 nm, and they frequently draw comparisons with human hair, which has a width of 80,000 nm. Professor Norio Taniguchi of the University of Tokyo coined the term "Nanotechnology" in 1971. The original meaning of "Nanotechnology" in English is the manufacturing technology to get extremely exact measurements with extremely tiny tolerances, i.e., precision and fineness on the order of 1 nm (nanometer), 10-9 metres in length [1]. Drexler refined Feynman's description of nanotechnology in 1986 and stated that "Nanotechnology" is the principle of atom-by-atom manipulation through molecular level control of matter structure [2]. In a wider sense, we define a material as being in the nanoscale if it has a structural thickness of fewer than 100 nanometers in at least one dimension. This kind of nanostructure, such as a thin film, can be identified as a 2D nanostructure, where one dimension is on the nanoscale and the other two are on the microscale. We acquire a 1D nanostructure, such as nanorods and nanowires, if two dimensions are fewer than 100 nanometers apart and one dimension is in the microscale. Nanoparticles, colloids, quantum dots, and other terms are used to describe materials with nano dimensions in all directions.

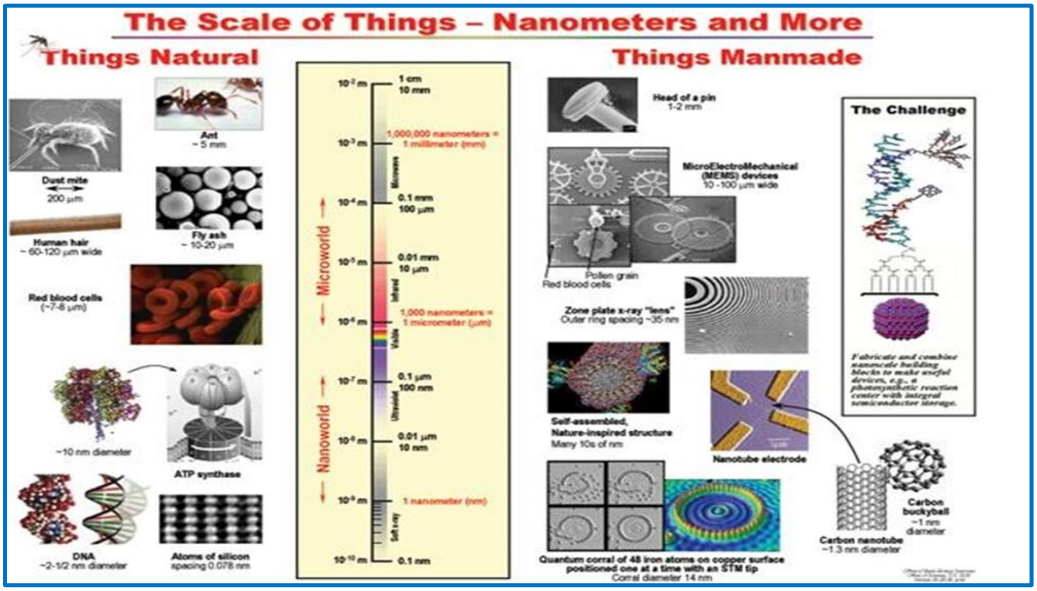

Figure1.2 Area of Nanoscience and Technology

1.1.2 History of Nanotechnology:

- The early 2000s also saw the beginnings of commercial applications of nanotechnology, although these were limited to the bulk application of nanomaterials.

- The first ever concept was presented in 1959 by the famous professor of physics Dr. Richard Feynman.

- **1974:** "Nanotechnology"- Professor Norio Taniguchi for the first time uses the term nanotechnology [3].

- **1981:** IBM develops Scanning Tunnelling Microscope [4].

- **1985:** "Buckyball"- Scientists at Rice University and the University of Sussex discover Fullerene (C60) [5].

- **1986**: "Engines of Creation"- First book on nanotechnology by K. Eric Drexler [6].

- **1989:** IBM logo made with individual atoms.

- **1991:** Carbon Nanotubes discovered by S. Ijima.

- **1999: "**Nanomedicine"- First Nanomedicine book by R. Freitas.

- **2000:** National Nanotechnology Initiative was launched.

- **2003**: 21st-century nanotechnology research report published.

- **2005:** DNA-based computer discovered and algorithmic self-assembly.

- **2007:** Lithium-ion battery with a common type of virus was discovered.

- **2009:** Several DNA-like robotic nanoscale assembly devices were discovered.

- **2010:** Invention of Graphene.

- **2014:** Updated 2014 strategic plan was released by the NNI.

1.1.3 What is Nanometer Scale:

The usual scale for the nanometer is 1 to 100 nm. One billionth of a metre is a nanometer. To prevent designing single atoms or extremely small groups of atoms as nano-objects, the size range is often defined to be at least 1 nm. Therefore, at least 1 nm-sized cluster of atoms are involved in nanoscience and nanotechnology. Usually, the highest limit is 100 nm, although this is a "fluid" restriction; frequently, things with larger dimensions—even 200 nm—are classified as nanomaterials. The question "why 100 nm and not 150 nm?" or even "why not 1 to 1000 nm?" is one that students may legitimately pose. The definition itself concentrates on the effect that the dimension has on a given material, such as the emergence of a quantum-particle phenomenon, rather than on the precise dimension at which this effect develops, which is why the "1 to 100 nm range" is characterized as approximative. Nan science is not the study of little things; rather, it is the study of how materials with small dimensions exhibit novel physical phenomena known as the quantum effect that are both size-dependent and vastly unlike the characteristics of materials with larger scales.

1.2 What are Nanomaterials:

A group of compounds known as nanoscale materials is those whose minimum dimension is less than or equal to 100 nanometers. 100,000 times smaller than the diameter of a human hair, a nanometer is one-millionth of a millimeter The unique optical, magnetic, electrical, and other characteristics that appear at this size in nanomaterials make them interesting. Electronics, medicine, and other disciplines stand to benefit greatly from these emerging features.

Figure 1.3- Nanomaterial (For example Carbon nanotube)

History of Nanomaterials:

The formation of nanostructures in the first meteorites marked the beginning of the history of nanomaterials shortly after the big bang. Many more nanostructures, including skeletons and seashells, were eventually developed by nature. When early people used fire, tiny smoke particles were created. But the history of nanomaterials in science didn't start until much later. Michael Faraday's 1857 creation of colloidal gold particles is one of the first examples of scientific research. For more than 70 years, researchers have also studied nanostructured catalysts. Precipitated and fumed silica nanoparticles were being produced and offered as an alternative to ultrafine carbon black for rubber reinforcements in the USA and Germany by the early 1940s. Nanosized amorphous silica particles are widely used in a variety of common consumer goods, including non-dairy coffee creamer, tires, optical fibers, and catalytic supports. Metallic nanopowders for magnetic recording, and cassettes, were created in the 1960s and 1970s. Granqvist and Buhrman initially described nanocrystals made using the now-common inert-gas evaporation method in 1976. Maya blue paint has just been discovered to be a nanostructured hybrid material. Studies of genuine samples from Jaina Island show that the material is made of needle-shaped palygorskite (clay) crystals that form a superlattice with a period of 1.4 nm, with intercalates of amorphous silicate substrate containing inclusions of

metal (Mg) nanoparticles. The origin of its color and its resistance to acids and biocorrosion is still unknown. The creation of synthetic samples has demonstrated that the lovely blue hue can only be attained when both these nanoparticles and the superlattice are present. An item is considered a nanomaterial if at least one of its dimensions is on the nanometer scale. First, all nanomaterials are made up of incredibly tiny particles. The first benefit of nanomaterials and nanotechnologies is that they facilitate the development of superminiaturization. Nanostructures may be crammed very tightly together due to their tiny size. As a consequence, more functional nanodevices may be found on a given unit of area, which is crucial for nanoelectronics. Their high packing density has the ability to increase information storage capacity in terms of volume and surface area as well as processing speed.

Today, nanophase engineering is used to manipulate the mechanical, catalytic, electric, magnetic, optical, and electronic characteristics of a constantly expanding range of structural and functional materials, both inorganic and organic. The development of distinct tiny clusters that are later fused into a bulk-like material or on their embedding into compact liquid or solid matrix materials is often the basis for the manufacture of nanophase or cluster-assembled materials. For instance, nanophase silicon, which has different physical and electrical characteristics from regular silicon, might be used in macroscopic semiconductor processes to make novel devices. For instance, the common glass may be transformed into a high-performance optical medium with potential uses in optical computing by doping it with quantized semiconductor "colloids."

Classification of Nanomaterials:

Nanomaterials are very tiny, with at least one dimension being 100 nanometers or less. Nanoscale materials come in one or more dimensions, such as surface coatings, strands, fibers, or three dimensions (e.g. particles). They come in spherical, tubular, and irregular shapes and can be found alone, fused, aggregated, or agglomerated. Typical examples of nanomaterials

include fullerenes, quantum dots, dendrimers, and nanotubes. Nanomaterials are used in the field of nanotechnology and differ from conventional chemicals in terms of their physical-chemical properties (i.e., silver nano, carbon nanotube, fullerene, photocatalyst, carbon nano, and silica). Thin films, nanowires, nanoparticles, and other sorts of nanoscale formations are only a few examples. The term "quantum dot" is frequently used to refer to nanoparticles, which are essentially zero-dimensional structures. The new characteristics of the aforementioned systems are simply the result of basic physics, and theoretical study has provided a clear explanation for how this works. It is crucial to briefly describe the densities of states (DOS) of quantum dots (0 dimensions), quantum wires (1 dimension), and quantum wells (2 dimensions) in order to comprehend these systems.

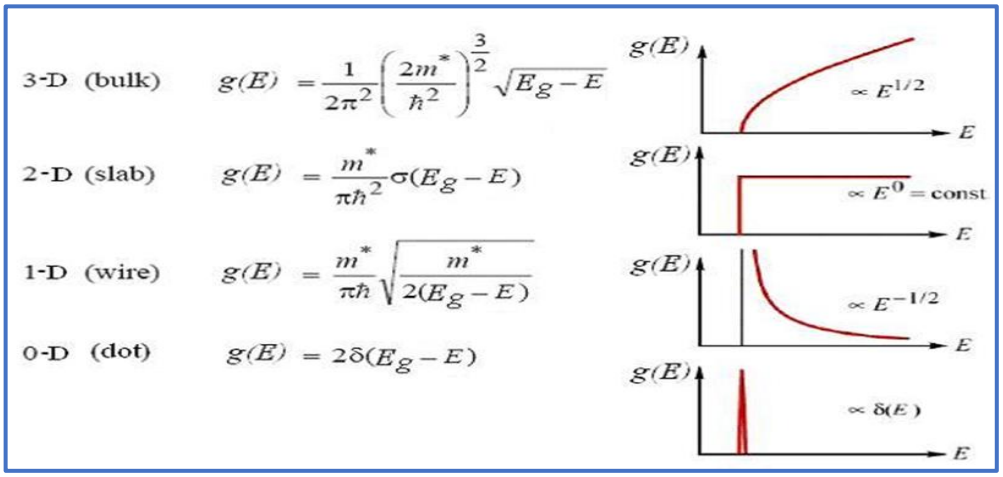

Table 1.1. Density of states

Nanomaterials are substances with ultra-fine grains (50 nm) or with dimensions no larger than 50 nm. Richard W. Siegel's definition of nanomaterials includes zero (atomic clusters, filaments, and cluster assemblies), one (multilayers), two (ultrafine-grained overlayers or buried layers), and three (buried layers) (nanophase materials consisting of equiaxed nanometer-sized grains).

Classification	Examples
Dimension ▪ 1 dimension ▪ 2 dimension ▪ 3 dimension	Films, coatings, multilayer, etc. Tubes, fibers, wires, platelets, etc. Particles, quantum dots, hallow spheres, etc.
Phase Composition ▪ Single-phase solid ▪ Multi-phase solid ▪ Multi-phase system	Crystalline, amorphous, particles and layers, etc. Matrix composites, coated particles, etc. Colloid, aerogels, ferrofluids, etc.
Manufacturing Process ▪ Gas phase reaction ▪ Liquid phase reaction ▪ Mechanical procedures	Flame synthesis, condensation, CVD, etc. Sol-gel, precipitation, hydrothermal processing, etc. Ball milling, plastic deformation, etc.

Table1.2 Classification of nanomaterial about different parameters.

1.2.3 Why so much interested in Nanomaterial:

These materials have created a high interest in recent years by their unusual mechanical, electrical, optical, and magnetic properties. Some examples are given below:

- Because they are more ductile at high temperatures than coarse-grained ceramics, nanophase ceramics are of great interest.
- It is well known that nanostructured semiconductors exhibit a variety of non-linear optical characteristics. Quantum confinement effects in semiconductor Q-particles can also result in unique features, such as luminescence in silicon powders and silicon-germanium quantum dots used as infrared optoelectronic devices. Solar cells' window layers are made of nanostructured semiconductors.
- Metallic powders that are nanoscale in size have been utilized to create porous coatings, dense components, and gas-tight materials. Their ductility and cold welding characteristics make them appropriate for metal-metal bonding, particularly in the electronic sector.
- Single nanoscale magnetic particles are mono-domains, therefore it stands to reason that in magnetic nanophase materials, the grains correspond to domains while the borders, on

the other hand, are disordered walls. In addition to the superparamagnetic behavior, very small particles have unique atomic structures with discrete electronic states that give rise to unusual features. High-density information storage, magnetic refrigeration, and ferrofluids are just a few applications for magnetic nanocomposites.

- Nanostructured metal clusters and colloids of mono- or plus metallic composition have a special impact in catalytic applications. They may serve as precursors for a new type of heterogeneous catalysts (Cortex-catalysts) and have been shown to offer substantial advantages concerning activity, selectivity, and lifetime in chemical transformations and electrocatalysis (fuel cells). Enantioselective catalysis was also achieved using chiral modifiers on the surface of nanoscale metal particles.
- The development of gas sensors with improved sensitivity and selectivity for NOx, CO, CO2, CH4, and aromatic hydrocarbons is gaining attention thanks to nanostructured metal-oxide thin films. Applications for nanostructured metal oxide (MnO2) include rechargeable automobile or consumer product batteries. Nanostructured titanium oxide porous films for their high transmission and large surface area enhancement leading to strong absorption in dye-sensitized solar cells, and nanocrystalline silicon films for very transparent contacts in thin-film solar cells.
- Polymer-based composites with a high content of inorganic particles leading to a high dielectric constant are interesting materials for photonic bandgap structure.

Nanomaterial Synthesis and Processing:

There are several techniques to make nanostructures, including the artificial synthesis of macromolecules, nanoparticles, buckyballs, nanotubes, and other structures for certain materials. As a result, we can create nanomaterials by either assembling atoms or disassembling (breaking or dissociating) bulk solids into smaller fragments until they are composed of just a few atoms.

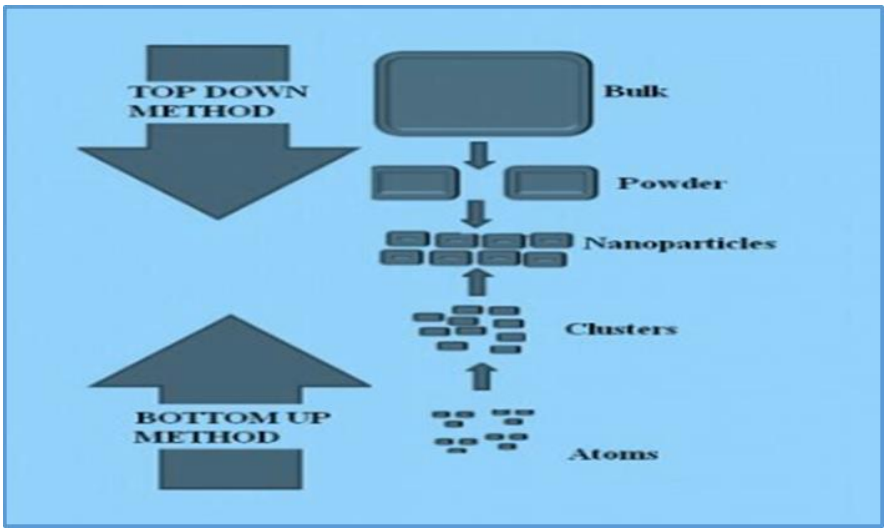

Fig 1.4. Top-down and bottom-up.

(1) Mechanical grinding:

Mechanical attrition is a common illustration of a "top-down" method of synthesis of nanomaterials, where the material is generated by structural disintegration of coarser-grained structures as a result of intense plastic deformation rather than cluster construction. Due to its ease of use, the relatively low cost of the required equipment, and its potential to be used in the synthesis of virtually all kinds of materials, this technique has grown in popularity for producing nanocrystalline materials. The most common methods for mechanical milling are high-energy shakers, planetary ball mills, and tumbler mills. The amount of energy that refractory or steel balls impart to the powder relies on the rotational (vibrational) speed, size, and quantity of the balls, the mass ratio of the balls to the powder, the milling period, and the milling environment. A nanoparticle is created.

(2) Sol-gel process:

Through the creation of a colloidal suspension (sol) and the gelation of the sol to create a network in a continuous liquid phase, the sol-gel process includes the evolution of inorganic networks (gel). The precursors used to create these colloids typically include a metal or metalloid element encircled by a variety of reactive ligands. When the beginning material

comes into contact with water or diluted acid, the processed starting material transforms into a sol. The gel is produced when the liquid is taken out of the sol, and the sol/gel transition regulates the particle size and form. Oxide is created during the calcination of the gel. Alkoxide-based precursors like $Si(OEt)_4$ are hydrolyzed and condensed during the sol-gel manufacturing process (tetraethyl orthosilicate, or TEOS). The reactions involved in the sol-gel chemistry based on the hydrolysis and condensation of metal alkoxides M(OR)z can be described as follows:

$$MOR + H2O \rightarrow MOH + ROH \text{ (hydrolysis)}$$

$$MOH + ROM \rightarrow M\text{-}O\text{-}M + ROH \text{ (condensation)}$$

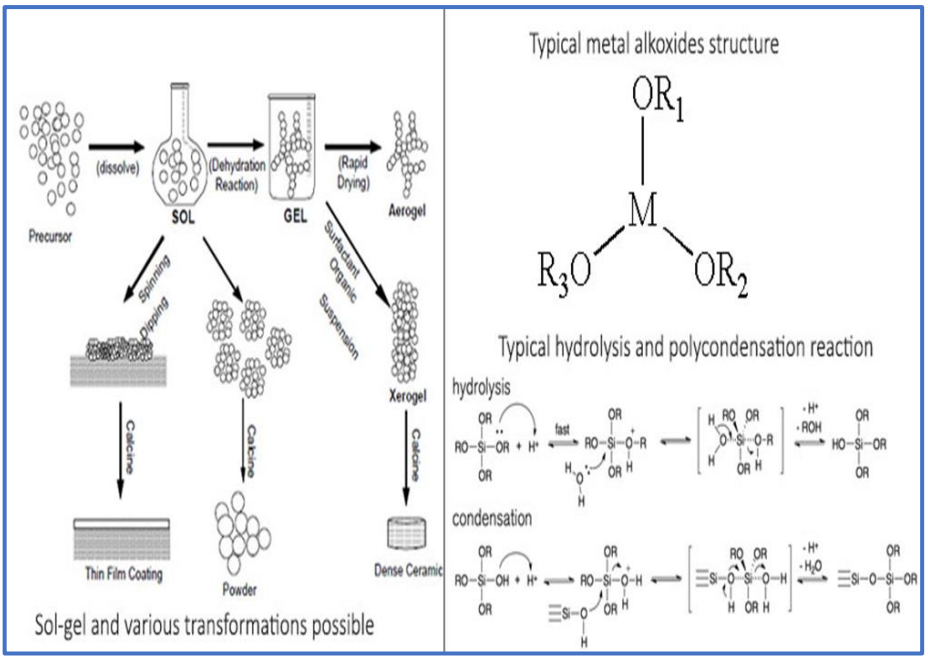

Fig 1.5. Sol-Gel process [7]

(3) Gas-Phase synthesis of nanomaterials:

The gas-phase synthesis methods are of increasing interest because they allow an elegant way to control process parameters to be able to produce size, shape, and chemical composition controlled nanostructures. Before we discuss a few selected pathways for the gas-phase

formation of nanomaterials, some general aspects of gas-phase synthesis need to be discussed. In conventional chemical vapor deposition (CVD) synthesis, gaseous products either are allowed to react homogeneously or heterogeneously depending on a particular application.

(4) Solid States:

The simplest fashion to produce nanoparticles is by heating the desired material in a heat-resistant crucible containing the desired material. This method is appropriate only for materials that have a high vapor pressure at heated temperatures that can be as high as 2000 °C.

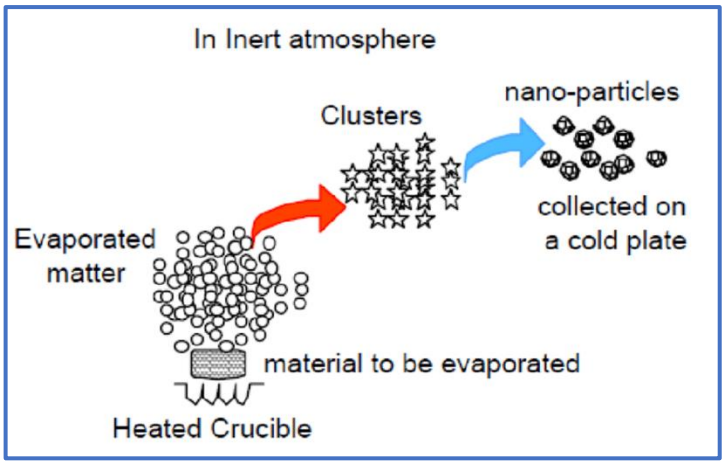

Figure 1.6. Schematic representation of a gas-phase process of synthesis [8]

(5) Chemical Vapour Condensation (CVC):

In Chemical vapor deposition the evaporative source used in GPC is replaced by a hot wall reactor in the Chemical Vapour Condensation or the CVC process. Depending on the processing parameters nucleation of nanoparticles is observed during chemical vapor deposition (CVC) of thin films and poses a major problem in obtaining good film qualities.

The original idea of the novel CVC process which is schematically shown below where was intended to adjust the parameter field during the synthesis to suppress film formation and enhance the homogeneous nucleation of particles in the gas flow. It is readily found that the residence time of the precursor in the reactor determines if films or particles are formed. In a certain range of residence time, both particle and film formation can be obtained.

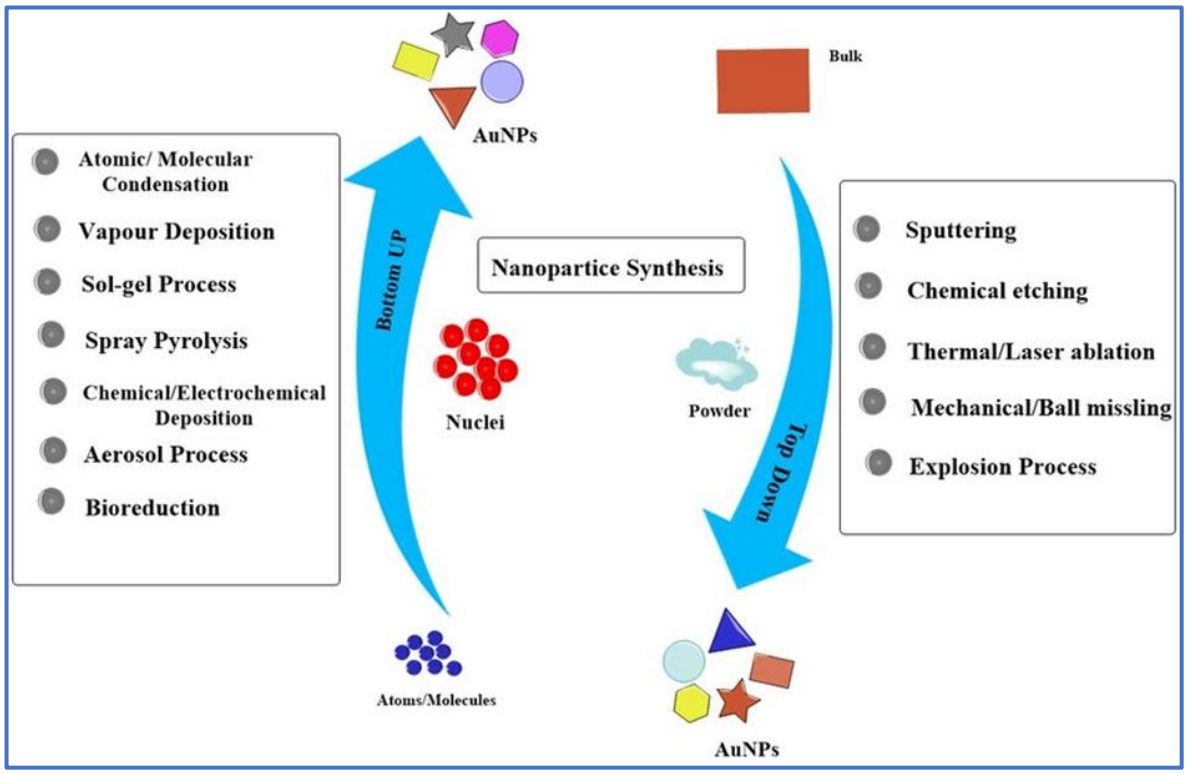

Figure 1.7. Schematic of Nanoparticle Synthesis.

1.2.5 Properties of Nanomaterials:

Nanomaterials have structural features in between those of atoms and the bulk materials. While most microstructured materials have similar properties to the corresponding bulk materials, the properties of materials with nanometer dimensions are significantly different from those of atoms and bulk materials. This is mainly due to the nanometer size of the materials which renders them: (i) a large fraction of surface atoms; (ii) high surface energy; (iii) spatial confinement; (iv) reduced imperfections, which do not exist in the corresponding bulk materials[9]. Due to their small dimensions, nanomaterials have an extremely large surface area to volume ratio, which makes a large to be the surface or interfacial atoms, resulting in more “surface” dependent material properties. Especially when the sizes of nanomaterials are comparable to length, the entire material will be affected by the surface properties of nanomaterials. This in turn may enhance or modify the properties of the bulk materials. For

example, metallic nanoparticles can be used as very active catalysts. Chemical sensors from nanoparticles and nanowires enhanced the sensitivity and sensor selectivity. The nanometer feature sizes of nanomaterials also have a spatial confinement effect on the materials, which brings the quantum effects [10].

(1) Optical properties:

One of the most fascinating and useful aspects of nanomaterials is their optical properties. Applications based on optical properties of nanomaterials include an optical detector, laser, sensor, imaging, phosphor, display, solar cell, photocatalysis, photo-electrochemistry, and biomedicine. The optical properties of nanomaterials depend on parameters such as feature size, shape, surface characteristics, and other variables including doping and interaction with the surrounding environment or other nanostructures [11]. It may also be controlled by dopant incorporation which changes the band gaps. The variation of bandgap generally occurs due to the change of lattice parameters by annealing [12-13] or impurity doping [14-15].

(2) Electrical Properties:

Electrical Properties of Nanoparticles" discuss fundamentals of electrical conductivity in nanotubes and nanorods, carbon nanotubes, photoconductivity of nanorods, and the electrical conductivity of nanocomposites. One interesting method which can be used to demonstrate the steps in conductance is the mechanical thinning of a nanowire and measurement of the electrical current at a constant applied voltage. The important point here is that, with decreasing diameter of the wire, the number of electron wave modes contributing to the electrical conductivity is becoming increasingly smaller by well-defined quantized steps. The charge transport phenomenon for materials with nanoscale dimensions mainly depends on the grain boundary [16]. The effects of grain boundary play a very significant role as its interface contains a density of defects like vacancies, dangling bonds, vacancy clusters, etc [17].

(3) Mechanical Properties:

Mechanical Properties of Nanoparticles" deals with bulk metallic and ceramic materials, the influence of porosity, the influence of grain size, superplasticity, filled polymer composites, particle-filled polymers, polymer-based nanocomposites filled with platelets, carbon nanotube-based composites. The discussion of mechanical properties of nanomaterials is, to some extent, only of quite basic interest, the reason being that it is problematic to produce macroscopic bodies with a high density and a grain size in the range of less than 100 nm. However, two materials, neither of which is produced by pressing and sintering, have attracted much greater interest as they will undoubtedly achieve industrial importance. These materials are polymers that contain nanoparticles or nanotubes to improve their mechanical behaviors, and severely plastic-deformed metals, which exhibit astonishing properties. However, because of their larger grain size, the latter is generally not accepted as nanomaterials.

(4) Magnetic properties:

Bulk gold and Pt are non-magnetic, but at the nano size, they are magnetic. Surface atoms are not only different from bulk atoms, but they can also be modified by interaction with other chemical species, that is, by capping the nanoparticles. This phenomenon opens the possibility to modify the physical properties of the nanoparticles by capping them with appropriate molecules. It should be possible that non-ferromagnetic bulk materials exhibit ferromagnetic-like behavior when prepared in the nano range. One can obtain magnetic nanoparticles of Pd, Pt, and the surprising cause of Au (that is diamagnetic in bulk) from non-magnetic bulk materials. In the case of Pt and Pd, ferromagnetism arises from the structural changes associated with side effects [18].

1.3 Applications:

1.3.1 Fuel cells:

A fuel cell is an electrochemical energy conversion device that converts the chemical energy from fuel (on the anode side) and oxidant (on the cathode side) directly into electricity. The heart of the fuel cell is the electrodes. The performance of a fuel cell electrode can be optimized in two ways; by improving the physical structure and by using a more active electrocatalyst. A good structure of electrode must provide ample surface area, provide maximum contact of catalyst, reactant gas, and electrolyte, facilitate gas transport, and provide good electronic Carbon nanotubes (CNTs) have chemical stability, good mechanical properties, and high surface area, making them ideal for the design of sensors and provide very high surface area due to its structural network. Since carbon nanotubes are also suitable supports for cell growth, electrodes of microbial fuel cells can be built using CNT. Conductance. In this fashion, the structure should be able to minimize losses [19].

1.3.4 Next-Generation Computer Chips:

The microelectronics industry has been emphasizing miniaturization, whereby the circuits, such as transistors, resistors, and capacitors, are reduced in size. By achieving a significant reduction in their size, the microprocessors, which contain these components, can run much faster, thereby enabling computations at far greater speeds. However, there are several technological impediments to these advancements, including lack of the ultrafine precursors to manufacture these components; poor dissipation of tremendous amount of heat generated by these microprocessors due to faster speeds; short mean time to failures (poor reliability), etc. Nanomaterials help the industry break these barriers down by providing the manufacturers with nanocrystalline starting materials, ultra-high purity materials, materials with better thermal conductivity, and longer-lasting, durable interconnections (connections between various components in the microprocessors). For example, Nanowires for junctionless transistors:

1.3.5 Super-capacitor:

A supercapacitor is a high-capacity capacitor with capacitance values much higher than other

capacitors (but lower voltage limits) that bridge the gap between electrolytic and rechargeable. They typically store 10 to 100 times more energy per unit volume than electrolytic capacitors, can accept and deliver charge much faster than batteries, and tolerate many more charge and discharge cycles than rechargeable batteries. A transition metal oxide exhibits high amounts of pseudo capacitance [21].

1.3.6 Elimination of Pollutants:

Nanomaterials possess extremely large grain boundaries relative to their grain size. Hence, they are very active in terms of their chemical, physical, and mechanical properties. Due to their enhanced chemical activity, nanomaterials can be used as catalysts to react with such noxious and toxic gases as carbon monoxide and nitrogen oxide in automobile catalytic converters and power generation equipment to prevent environmental pollution arising from burning gasoline and coal.

1.3.7 Sensors:

Sensors rely on the highly active surface to initiate a response with a minute change in the concentration of the species to be detected. Engineered monolayers (a few Angstroms thick) on the sensor surface area exposed to the environment and the peculiar functionality (such as a change in potential as the CO/anthrax level is detected) are utilized in sensing.

1.3.8 Medical and Healthcare application:

Nanotechnology is already broadening the medical tools, knowledge, and therapies currently available to clinicians. Nanomedicine, the application of nanotechnology in medicine, draws on the natural scale of biological phenomena to produce precise solutions for disease prevention, diagnosis, and treatment. Below are some examples of recent advances in this area

- Commercial applications have adapted gold nanoparticles as probes for the detection of

targeted sequences of nucleic acids, and gold nanoparticles are also being clinically investigated as potential treatments for cancer and other diseases.

- Nanotechnology researchers are working on several different therapeutics where a nanoparticle can encapsulate or otherwise help to deliver medication directly to cancer cells and minimize the risk of damage to healthy tissue. This has the potential to change the way doctors treat cancer and dramatically reduce the toxic effects of chemotherapy.
- Research in the use of nanotechnology for regenerative medicine spans several application areas, including bone and neural tissue engineering. For instance, novel materials can be engineered to mimic the crystal mineral structure of human bone or used as a restorative resin for dental applications. Researchers are looking for ways to grow complex tissues with the goal of one day growing human organs for transplant. Researchers are also studying ways to use graphene nanoribbons to help repair spinal cord injuries; preliminary research shows that neurons grow well on the conductive graphene surface.

1.3.9 Future transport:

Nanotechnology offers the promise of developing multifunctional materials that will contribute to building and maintaining lighter, safer, smarter, and more efficient vehicles, aircraft, spacecraft, and ships. In addition, nanotechnology offers various means to improve the transportation infrastructure:

- Nano-engineered materials in automotive products include polymer nano-composite structural parts; high-power rechargeable battery systems; thermoelectric materials for temperature control; lower rolling-resistance tires; high-efficiency/low-cost sensors and electronics; thin-film smart solar panels; and fuel additives and improved catalytic converters for cleaner exhaust and extended range.

Nanoscale sensors, communications devices, and other innovations enabled by nanoelectronics

can also support an enhanced transportation infrastructure that can communicate with vehicle-based systems to help drivers maintain lane position, avoid collisions, adjust travel routes to avoid congestion, and improve drivers' interfaces to onboard electronics.

2. INTRODUCTION OF PEROVSKITE

Nowadays people widely use nonrenewable energies that are limited as a result of the price of this rapidly increasing. For reduce to use, researchers are working on it. Researchers choose renewable energies. In recent years Perovskite materials earn great attention to use as energy harvesting because of their ferroelectric properties.

These materials are great useful as light-emitting diodes, 2 Light-Emitting Electrochemical Cells, lasing, and photodetector [22].

Scientist found the chemical form of perovskite that is ABX_3. Where A-Organic/Inorganic cation ex-CH_3NH_2, $NCH_3CH_2NH_2$. B-Heavy metal cation EX-Pb/Bi with usually co-ordination no of 6 and X-halogen (like Cl, Br, I).

Basically, both the sides having the A and B which is having the different size and in between having the X which is holding the hand of the A and B [22].

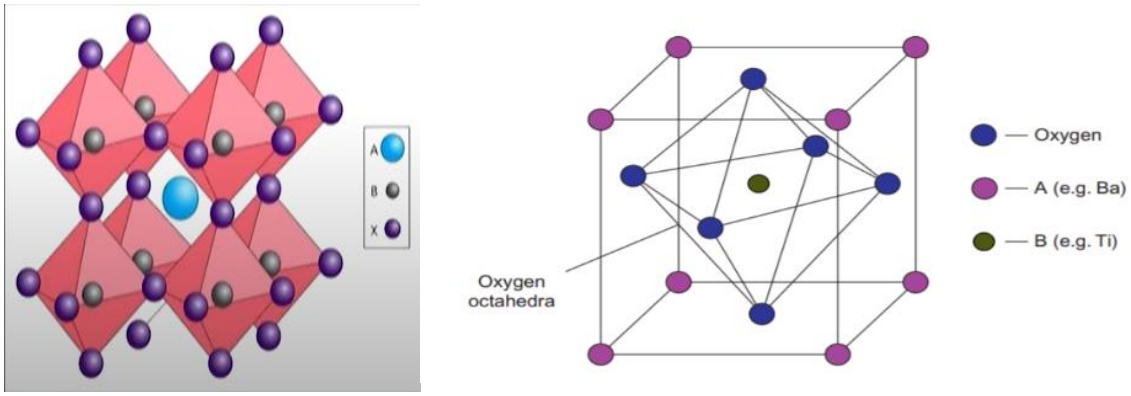

Fig 2.1 and 2.2: Perovskite crystal structure of ABX_3 [23] [34].

Earlier $BatiO_3$, $CatiO_3$ are widely used as perovskite but now researchers find alternative materials or alternative organic cation or change the structure, use hybrid materials to improve the efficiency, reduce cost, increase stability, and better optoelectrical properties.

2.1 AIMS AND OBJECTIVES OF THE THESIS

- To know the history and past to present statistics of the efficiency of Perovskite materials
- To understand that why we are choosing the perovskite materials by their properties
- Understanding the classification of the perovskite crystalline
- To know How does it work with structure?
- To discuss the classification of synthesis procedures of the perovskite materials
- To know the advantages and disadvantages and what will do in future with Perovskite materials

1. HISTORY

Gustavo Rose in 1839 first found this material in the Russia, named after mineralogist Lev Perovski. So, to give him respect to the name of the founder is, a material known as perovskite material [24]. Therefore, if you look at the complete history, we can find that in 1839 it was founded by Gustavo Rose and discovered the property of the perovskite building.

YEAR	INVENTOR	DESCRIPTION
1839	Gustavo Ros	First found this material
2008	Miyasaka	Use as in solar cell and succeed 3.8% [25]
2012	Henry Snaith and Mike Lee	they succeed the solid-state hole transporter such as Spiro-OMeTAD [26]

2013	Burschka	succeed 15 % efficiency by two step solution processing technique [27]
2014	researchers at KRICT	achieved 20.1 % efficiency from PSC [28]
2018	researchers at the Chinese academy of science	certified efficiency of 23.3% from PSC [29]
2021	Jeong, Jaeki, et al.	25.6% efficiency [30]

So, we can see every year efficiency of this materials are increasing.

2. why we are choosing the perovskite materials? [31]

These materials having

- high absorption coefficient,
- high carrier mobility,
- long charge carrier diffusion length,
- band gap tuning,
- highly crystalline structure
- the low exciting binding energy.

Therefore, all these structures are useful in making any type of solar cells. A lot of building materials are available in the market, people have done a lot of research on other things already.

Characteristics	CdTe	CIGS	Crystalline – Si	Perovskite
Raw material cost	Low	Medium	Low	Low
Finished material cost	Low	High	High	Low
Fabrication cost	Medium	Medium	High	Low
Energy payback period	Medium	High	High	Low
Levelized cost of energy (LCOE)	Medium	High	High	Low
Efficiency	Medium	Medium	High	High

Figure 2.3 comparisons between CdTe, CIGS, Crystalline-si, perovskite [32]

3 CLASSIFICATION

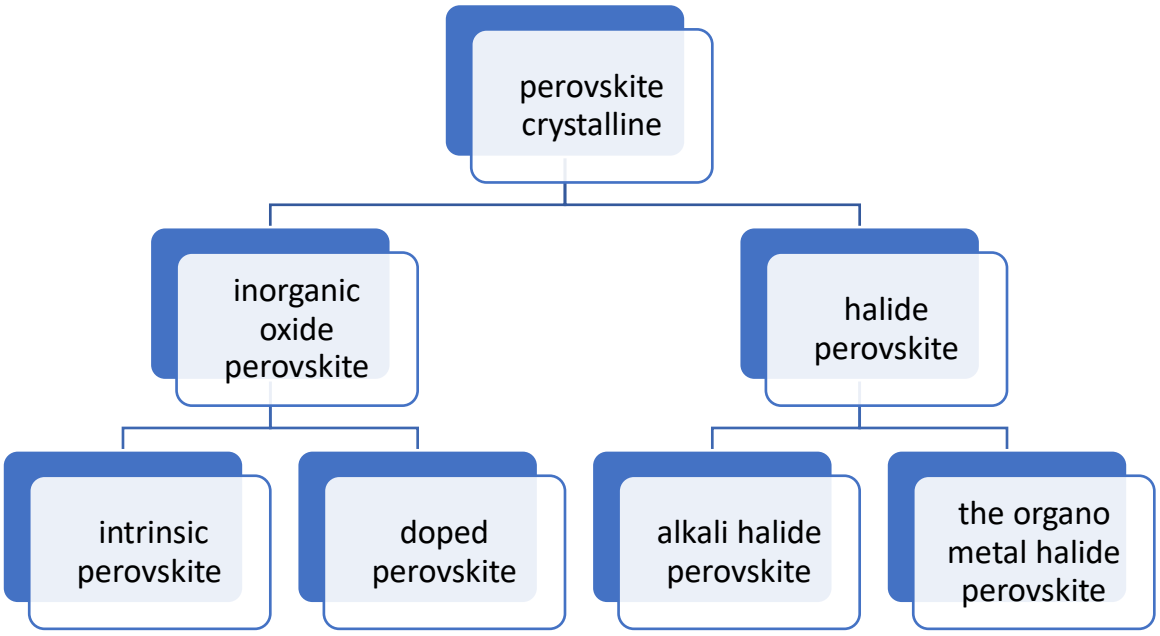

The perovskite structure is ABX_3 perovskite crystalline systems are basically divided into two parts; one is called inorganic oxide perovskite where the basic formula is ABO_3 as example. $CaTiO_3$, $BaTiO_3$, etc., the other is called halide perovskite ABX_3, the different X groups of halides will come as I, Br, Cl, F as follows. Then the perovskite of inorganic oxide is also

divided into two parts; one is called intrinsic perovskite (ABO_3 to complex systems) and the other is called doped perovskite (Axa1-xByb1-yOzo3-z.) this is a very complex structure and halide perovskite is also divided into two parts; one is called alkali-halide perovskite and the other is called organo-metal halide perovskite or possibly 3D and layer structure [33].

3. How does it work with structure?

Basically, the device structure, related materials, and interfacial modifications are key factors in performance of the solar cells.

Typical structures can be constructed;

- one is called the mesoscopic structure
- another one is called the planar structure

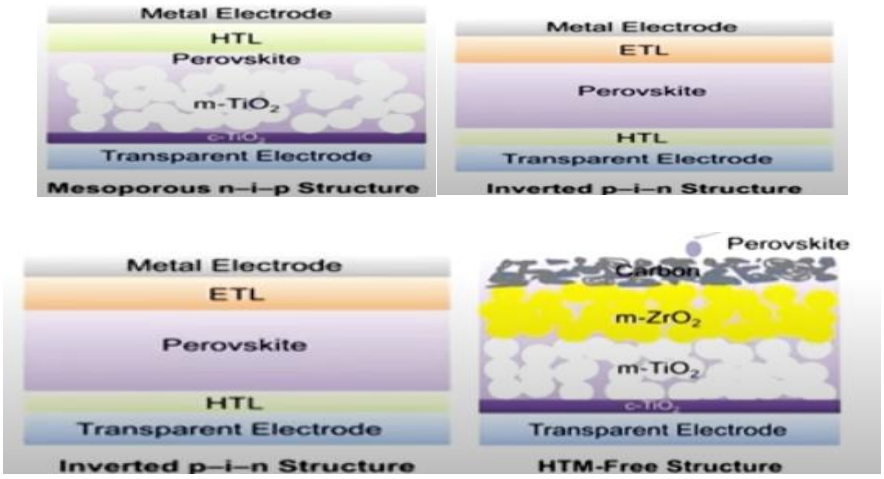

Fig 2.4 electron transport layer and HTL layer [34].

electron transport layer is used to

- collect and
- transport the electrons

HTL or Hole Transporting Layer which is use for

- transport the holes and
- collecting.

in this image we have shown many different structures such as the mesoporous nip structure, in this case we are using perovskite m-TiO_2 materials in this planar, when we are using perovskite materials here between HTL and ETL in this. Inverted, inverted PIN format means the opposite. automatically the top is ETL and the bottom is called HTL. it is the opposite of the planar nip structure. Then when we talk about the free HTM structure, therefore, in this case we are using two single layer elements are m-TiO_2 and m-ZrO_2 and above that set. carbon and more are used perovskite materials. it is basically a structure-like sandwich. what positions are basically using perovskite materials and how you use the floor or maybe upstairs and how it works based on the fact that we offer a different nomenclature of this sandwich as a structure. [15]

electron transport layer

the basic function of the electron transport layer is to:

• creates a special electron contact with a layer that absorbs light perovskite

• improve the efficiency of extracting auto-generated electrons

• block the hole from moving to the counting electrode

• reduce the reunion of electrons and holes

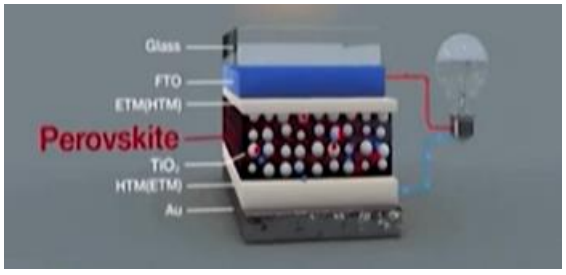

Figure 2.1 electron transport layer [35]

from this particular image you can understand that this is perovskite cell materials,

what we have first is that gold (Au) moreover we have HTM or maybe ETM materials on top of that we put TiO_2 and then we put our perovskite material and then if the bottom will be ETM already, the top will be HTM or it may be on the contrary we place the FTO glass and on top of that we place the glass substrate over there, this way you can basically see the perovskite material between us. ETM and HTM or maybe different [36].

Properties required for the selection of materials for the electron transport layer systems:

• high electron carrier movement,

• shines in visible light,

• The structure of the band should be perforated with perovskite materials,

• adjustment to possible conditions and low temperatures [16].

EXAMPLES are inorganic materials like zinc oxide, titanium dioxide. Organic materials like PCBM, (one of the fullerene derivatives that is called the –phenyl-C61-butyric acid methyl ester) and PFN (poly [9,9 dioctylfluorine-9,9-bis (N, N in dimethylpropyl) fluorine]) etc.

So, it's a complex kind of structure we can say.

HOLE TRANSPORT LAYER

when an electron moves from one place to another it easily leaves one hole there. Therefore, by default everything will be transferred from one side to the other. just like this the whole thing will go or maybe all will go just the opposite of the electron. Premises required for selection of Hole Transport Layer (HTL) materials the flow of the top hole, wide band gap, a simple solvent treatment process, high film design capability [36].

EXAMPLES: Inorganic materials like NiO, copper iodide, CsSnI3, copper gallium oxide.Organic materials like Spiro-OMeTAD, P_3HT, PEDOT:PSS.

These all are may be the polystyrene sulfonate, this or these all are the examples of hole transport layer.

4. THE CLASSIFICATION OF SYNTHESIS PROCEDURES OF THE PEROVSKITE materials:

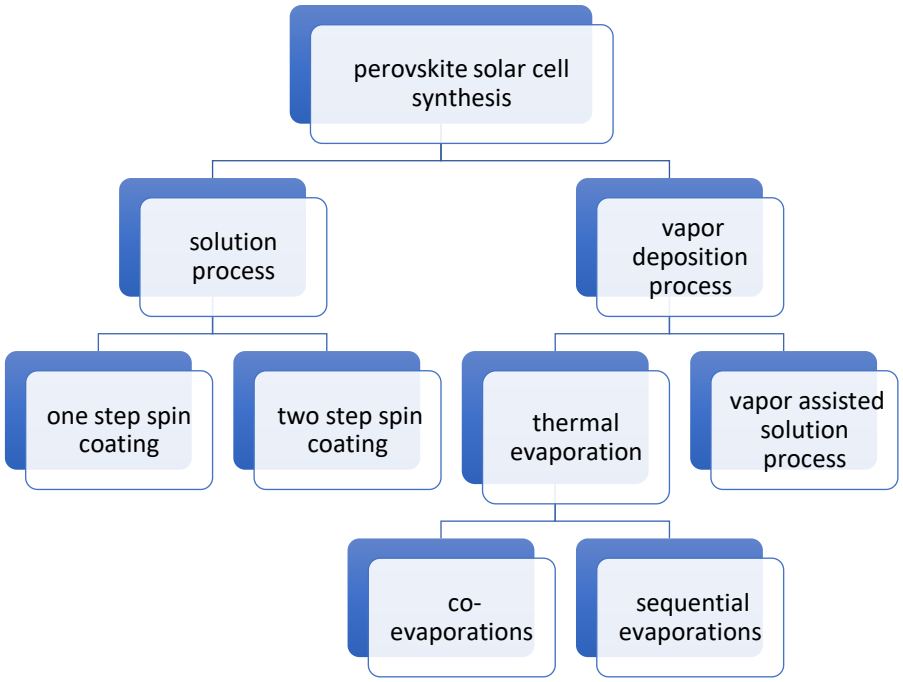

a. Solution Process

It is basically a simple process for the synthesis of perovskite nanaomaterials. Therefore, perovskite solar cells can be easily made with a simple solution process, a cheaper method like spin coating usually performs this particular procedure using a spin coater. Therefore, simple and inexpensive techniques such as spin coating can be used. The formation of a perovskite solar cell using spin coating can be done in two ways the other is called one step spin coating, the other is called two-step spin coating.

But the obstacles to solar cell making are that complete making must be done in a glove box under a controlled environment. because the biggest problem with dealing with perovskite solar cells is that, if you do not do the integration of certain areas, then, by default decreasing the quality of the this, very fast. that is to say, the predefined air we create with ineffective gas and especially that space we have to make a combination of that thing, we have to make the formation of solar cells, and only then can we test the full efficiency. of those materials used. Then, after we have done all the work of the solar cell, we can then take that particular solar cell out of the glove box or perhaps out of the room.[37]

a. i. One-Step Spin Coating

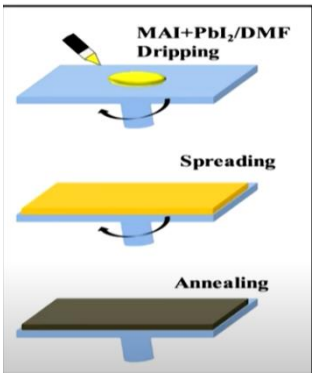

Figure2. 2 ONE-STEP SPIN COATING [16]

In this case put MAI, we put PbI_2 in DMF solutions, we mix everything together well and then if possible, using a dropper, we put those things. on titanium dioxide substrate. And then we use a spin coater; that means the substrate rotates at a very high rpm, so that these substances are evenly distributed on my substrate material and after that simple we do the extraction process, which means we hit that particular drying material and the preparations are completed.

The one-step method is simple, but it is not easy to control the morphology and size of the crystals being made. That is a small way or maybe one of the obstacles to this one step spin coating process.

a. ii. the two-step spin coating

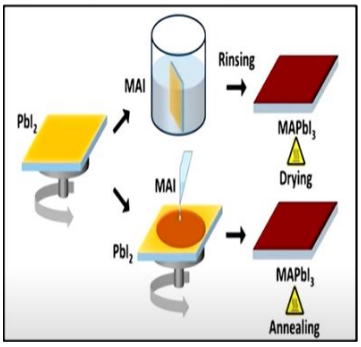

Figure 2.3: the two-step spin coating [36].

In this deposition process, PbI_2 basically begins to be spin coated into the TiO_2 layer from the solution under ideal conditions. The yellow substrates are changed to perovskite by immersion or possibly spin coating in MAI solutions into isopropanol. After setting at the appropriate temperature PbI_2 reacts with MAI and the perovskite layers are compacted

(MAI is the CH3NH3 and I CH3NH3 cations.) The two-step method is useful for making perovskite films under high humidity. So, A B material before put it on a substrate that we mix both and then the mixer that we put on the substrate does the one step steps. In this case have a substrate at first I put A's things, then drying, and then after a while I put B's things back and then drying and in between they are evenly distributed and evenly spaced. to do everything on the substrate itself and then the final step is to annealing. Therefore, dry all the building materials and the perovskite material will form on the substrate itself [36].

b. Vapor Deposition Process.

i)thermal evaporation process

1) co evaporation process

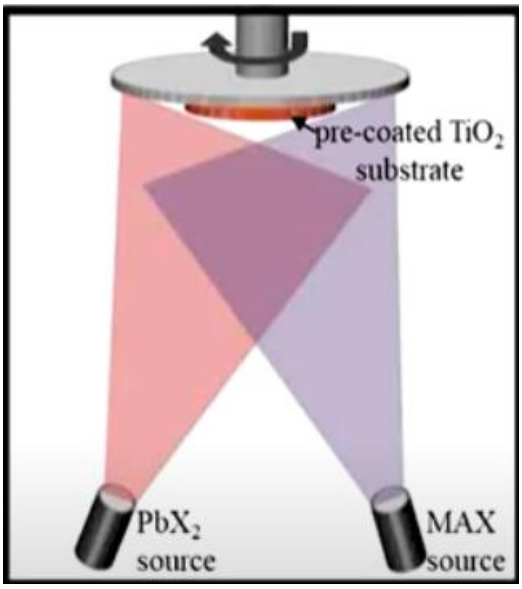

Figure 2.4 co evaporation process [36]

the word itself can be understood to be a kind of thermal evaporation process. that is also divided into several parts, the first of which is known as the co-evaporation process.

Therefore, the mechanism of vapor deposition of perovskite-absorbing layer is usually carried out under high vacuum conditions. Therefore, a high vacuum means that perovskite materials are less likely to be damaged. PbX_2 and MAX are instantaneously embedded in a pre-cover titanium dioxide substrate by thermal evaporation from both sources of PbX_2 and MAX.

I have that substrate. Easy I have one MAX source I have PbX_2 both evaporates coming and depositing on my own substrate. Therefore, $MAPbX_3$ is formed at ideal temperature and atmosphere and is then coated in a perovskite film, requiring high temperatures to evaporate solid PbI_2 into vapor.[36]

b. i. 2. Sequential Evaporations.

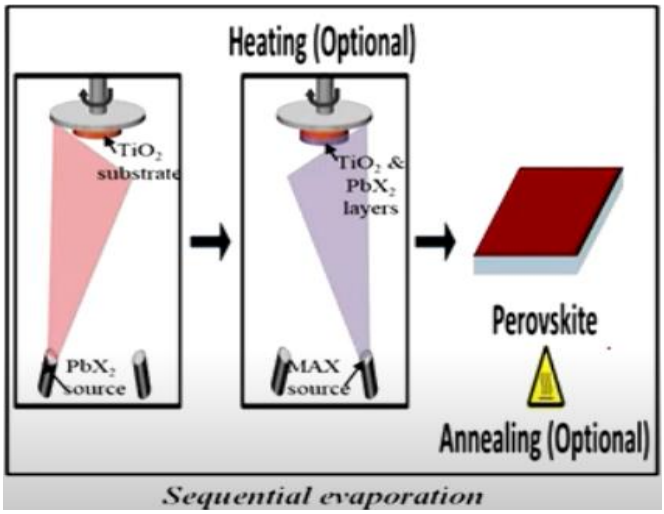

Figure 2.5 sequential evaporations [36].

It is similar with the two-step spinning process. So, one by one, Basically, in sequential vapor deposition, PbX_2 was first exposed to thermal vapor followed by MAX evaporation. In the previous phase both evaporates and condenses on the substrate itself. Now in both cases the source of the vapor comes separately and then puts on top of each other and after that last phase we do the process of annealing and drying and releasing the material. Therefore, this sequential placement was improved due to the struggle of viewing the MAX suspension rate in the evaporation process. The photovoltaic performance of devices prepared for successive installations has been found to be highly dependent on substrate temperature. The need for a high vacuum is a major limitation of the thermal vapor process.[38]

b.ii. Vapor Assisted Solution Process.

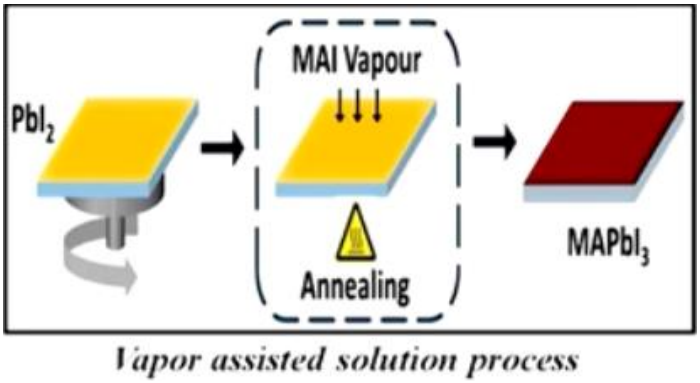

Figure 2.6 Vapor Assisted Solution Process [16].

It is designed to avoid barriers to solution and vapor deposition method. In this process inorganic films pre-coated or PbX_2 (with spin or dip coating) are applied as a substrate and are followed by MAX vapor exposure. There is nothing wrong with mixing both thermal and solution process. in this case the first step we take with the solution process is like using spin coating and the second is that we apply steam over those objects. Therefore, here the growing of perovskite film occurs in situ reaction area of the film coated as PbX_2 with organic vapors. The resulting film shows a well-defined grain growth up to a few micrometer sizes that fill the entire surface [39].

5. WHAT ARE THE BENEFITS?

• have very high efficiency and low cost of production

• Develop production methods based on low temperature, high absorption,

• high distribution length,

• high charge carrier flexibility,

• Very high open voltage voltages are usually found.

6. WHAT ARE THE DIFFICULTIES?

- mass production of solar cells with metal oxide is expensive

- degradation of peroxide will occur when uncovered to an outdoor environment, an object in a controlled atmosphere or perhaps in a highly maintained vacuum.
- lead base perovskite solar cell devices produce toxic gases in the environment.
- Those are so flexible, so this may be break down by natural issues like heavy rain, Strom.

that is why the scientist are working on it to improve [40].

7. APPLICATIONS

- many optoelectronic applications can be applied, such as FETs, the single photon emitters, photo detectors [12].
- Perovskite is flexible and light weight, so can apply on screens, drones and other device.

With this solar cell many scientists working on space application.

2 INDROUCTION OF NANOGENERATORS

Nowadays mankind is effortlessly reliant on non-renewable energy like fossil fuels, however, the repository of these sources is bounded in the earth. As a result of the diminishing of these fossil fuels, the prices are rising constantly, the majority of the non-sustainable energies emit CO2 gas as a by-product which is a terrible impact on climate changes and the human body, persistently contaminated in the environment. Conquering these issues, researchers continue to work on eco-friendly harvesting energies like solar energy, geothermal energy, Hydro energy, etc. But still, among the discoveries of research of renewable energy, nanogenerator is excellent, this is minimal expenses, portable compare to others mechanical harvesting energies. Z. L. Wang and L.Sang first introduced the nanogenerator in 2006[44]

what is nanogenerators?

A nanogenerator is nothing more than a type of gadget that transforms energy from one form to another, let's say. Thus, the material may produce electricity either by the application of pressure or pounding, or it may produce electricity through the rubbing of two materials. When we apply heat to a certain substance, the material may occasionally produce electricity as a result. Sometimes an electromagnetic force of some type exists between two materials, and this electromagnetic force can turn into electrical energy. As a result, different materials behave differently. In order for the material to convert those forces into energy, certain circumstances demand for applying a specific sort of pressure, others for applying a specific type of friction, and yet others for applying a specific type of electromagnetic force.[41]

how it has come?

Therefore, according to academicians of the Chinese Academy of Science, the discovery of nanogenerators is among the top ten scientific discoveries in the world. They think that this idea of a nanogenerator is one of the adaptable things, or perhaps one of the most recent discoveries, that can be listed among the top 10 inventions in the world as of right now. Therefore, as I mentioned before, we are essentially divided into different segments. Based on that which type of materials we are going to use and what type of energy basically using on those particular materials to get the electricity. But output for all the cases is remain same that is the electricity, and input are variable like heat, pressure, magnetic force, friction, so, these all are the cases.

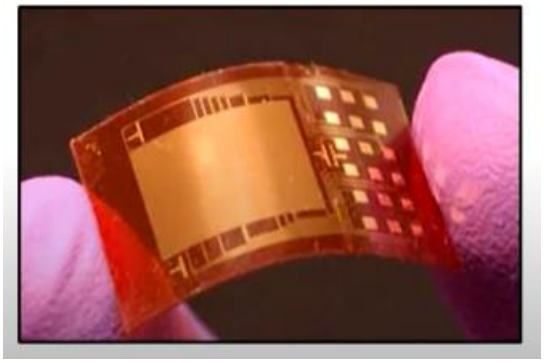

Figure 3.1 Nanogenerator

nanogenerators has been divided into several parts, one is called the piezoelectric, triboelectric, pyroelectric, thermoelectric and electromagnetic.

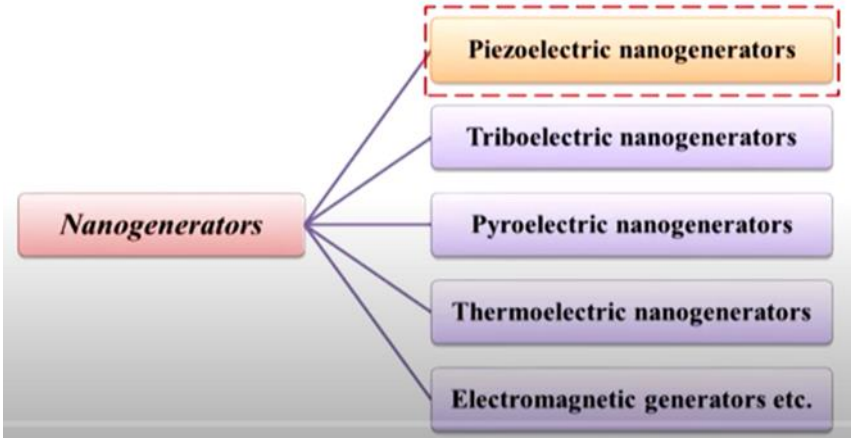

Figure 3.2 Different Types Of NG

- **WHAT ARE PIEZOELECTRIC MATERIALS?**

when we have particular materials available. Therefore, such materials may create electricity if we apply a specific pressure to them in certain locations or even at a specific angle. This is the beauty of those particular materials. And the materials that exhibit these characteristics are referred to be piezoelectric materials. Therefore, in a nutshell, piezoelectric materials are those that have the capacity to produce electrical charges in response to mechanical pressure. Therefore, if you have one material and apply pressure to it, those materials will be able to produce electricity through the piezoelectric effect, which is why this phenomenon is known as the piezoelectric effect. Piezoelectricity literally translates as "pressure electricity" since you

are applying pressure to certain materials. The prefix term piezo in this context comes from the Greek word piezein, which means to pressure. Cady provided a more complex definition of piezoelectricity as an electrical polarisation caused by mechanical strain because when you apply a certain amount of load or pressure to some materials, the material will automatically produce mechanical strength, which is why the material is giving off electricity. When we squeeze certain crystals from a particular class of materials, not all of the materials produce electricity. It should be able to do that or have the characteristics it possesses, which is why it only provides power to us after receiving pressure or a load. The Curie brothers Jacques and Pierre investigated the impact of pressure on the creation of electrical charge by various natural crystals, such as quartz or maybe tourmaline, in 1880. During this time, they made the discovery of piezoelectricity. In essence, therefore, they are the materials. So, they have developed, they have seen these phenomena first time in the year of 1880. And then after that, the piezoelectric materials has come into the market. Now, scientist has done so many research on that; they have tried to make some new materials so that the electrical efficiency will be increased. [42]

PIEZOELECTRIC EFFECT

So, the piezoelectric effect in piezoelectric crystals manifests itself in two ways:

1. direct piezoelectric effect - When electrical charge

is generated as a result of a mechanical stress applied to the crystal,

2. the converse piezoelectric effect when a strain is generated as a result of an electrical

field applied to the crystal.

In fact, this material has excellent beauty, so if you apply pressure to it or even a load, it will produce energy. Additionally, if you apply electricity to certain materials, they will experience

stress or maybe strain. The fact that it will alter its size and shape indicates that the materials will be deformed in some way, thus the situation there is essentially the opposite of that. In this instance, you can see that when I give the voltage input and output while concurrently giving the strain input and output over there, it immediately goes into deformations.[43]

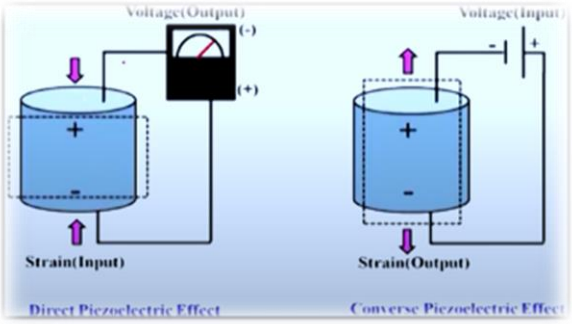

Figure 3.3 Piezoelectric Effect

or maybe the under the strain. So, theoretically, these two effects are described by two basics equations which relate the elastic variables, stress (T) and the strain(S), to the electric variables that is field (E) and displacement(D). So, basically the two equations of states are written as follows say capital

$D = dT + \varepsilon^T ED$ which is nothing but known as the direct effect.

$S=s^ET+dE$ so that is known as the converse effect.

here d is the piezoelectric coefficient or maybe the charge constant, and s is the elastic compliance, and e is the dielectric constant which is nothing but known as the permittivity of that particular material. So, by these equations, we can calculate.

- **What Are The Parameters Or Maybe The Constants Which Affect The Performance Of Any Piezoelectric Materials?**

- Not all materials can exhibit this type of characteristic. In essence, for a material to exhibit the piezoelectric effect, certain internal qualities must exist. What are they, starting with that
- electromechanical coupling factors which are nothing but known as the k,
- piezoelectric strain charge constants which are denoting by d,
- piezoelectric voltage constants which are denoting by g,
- then mechanical quality factor Q_m,
- electrical loss tanδ,
- the dielectric constant that is e which is nothing but the relative permittivity.

So, basically, these all are known as the piezoelectric constants. So, now discuss one by one.

- **ELECTROMECHANICAL COUPLING FACTOR OR K.**

It serves as a gauge of how well a piezoelectric material turns electrical energy into mechanical energy, or vice versa, when mechanical energy is converted into electrical energy.

$$K^2 = \frac{mechanical\ energy\ converted\ to\ electrical\ energy}{input\ mechanical\ energy}$$ ...direct piezo effect

It is providing efficiency-related things. So, the direct piezoelectric effect or maybe the ratio is determined by how many input parameters you place inside the materials and how much efficiency essentially or perhaps output you are obtaining as a result of that particular input parameters. Or maybe the vice versa things, K^2 = (mechanical energy converted to electrical energy)/(input electrical energy) that is known as the converse piezoelectric effect. Generally denoted by $k_{i\,j,}$ where i is the electric field directions, j is the longitudinal vibration direction [43].

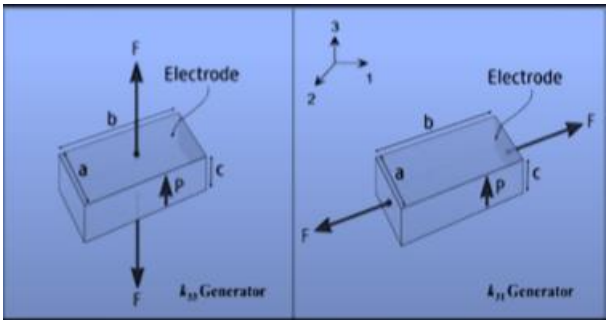

Figure 3.4 Electromechanical Coupling Factor

Depending on the structure, a typical piezoelectric ceramic may transfer 25 to 50% of the energy supplied to it in one form into another. You can now see that the conversion rate is between 25 and 50 percent. If you apply pressure and assume that it is 100 percent, then 50 percent of the pressure will be converted to electrical energy. If we apply 100% of whatever the electrical input is to that specific material, if you think of it as 100%, then you may get a mechanical strain of 25% to 50%. Or perhaps it works the other way around. Therefore, that depends on the characteristics of the material and its crystal structure.

So, a high k usually is desirable for efficient energy conversion

PIEZOELECTRIC STRAIN CONSTANT (d).

the piezoelectric charged constant is the ratio between the electric charge generated per unit area and an applied force and is expressed in Coulomb/Newton.

So, now, d is the charge density (open circuit) / the applied stress, which is nothing but the direct piezoelectric effect.

d = strain developed / the applied field that is converse piezoelectric effect.

$$\mathbf{d = kx\sqrt{\varepsilon_0 \varepsilon s^E}}\ (C/N)$$

So, where k is nothing but the electromechanical coupling factor;

ε_0 is the relative permittivity of the free space;

ε is the dielectric constant which is nothing but the relative permittivity, and

s^E is nothing but the compliance which value is basically 10^{-12} m^2/ N.

generally denoted by d i j;

i – induced polarization directions, and j is the stress applied directions.

d is an important indicator of a material suitability for the strain-dependent or maybe

the actuator applications.

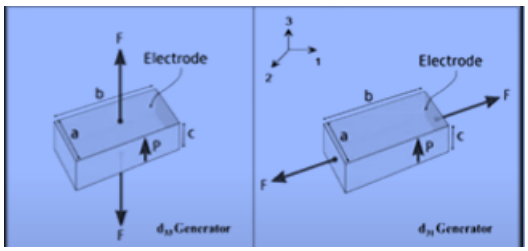

Figure 3.5 Piezoelectric Strain Constant

Basically, what is happening suppose you are choosing certain area over there, now you are giving the pressure in this area, or maybe giving the pressure in this area, or maybe whatever the pressure is giving, or maybe the load you are giving which is acting on the whole area, depending upon that material efficiency will be changing.

PIEZOELECTRIC VOLTAGE CONSTANTS. (G)

The piezoelectric voltage constant, denoted as Vm/Newton, is the reciprocal of the electric field generated to the mechanical stress applied. For the direct piezoelectric effect, it is fundamentally characterised by tiny g, which is nothing more than the field created by the applied mechanical stress; in contrast, the reverse piezoelectric effect is nothing more than the strain created by the applied charge density.

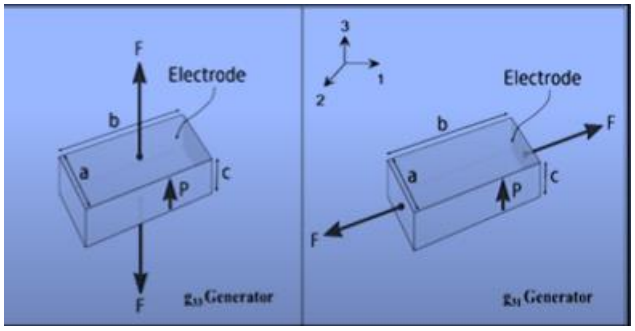

Figure 3.6 Piezoelectric Voltage Constants

It is generally denoted by $\mathbf{g}_{ij}$, where i is the induced electrical field directions, and j is the stress applied directions. So, in this particular case, what happened small g is important for assessing a material suitability for sensor or maybe the sensing applications.

MECHANICAL QUALITY FACTOR, QM.

the mechanical quality factor is defined as $Qm = 2\pi f (U_e / P_d)$

So, where Ue is the store mechanical energy of the system, that means, whatever the mechanical energy before any giving load or pressure has been consumed by that particular material.

P_d power dissipated that is of course in watts,

$2\pi f$ is the angular frequency.

For piezoelectric nanogenerators, high Qm piezoelectric materials are preferred since, if we apply even a small amount of load or pressure, there is a risk that the material would break. In order to apply a constant load to those specific materials and have them produce electricity; the material must have a high mechanical strength.

ELECTRICAL LOSS TAN δ,

the dielectric loss factor is defined as the tangent of the loss angle, which is nothing but known as tan δ.

The loss factor is inverse of mechanical quality factor Qm. basically, the tand is nothing but 1/ Qm.

- **DIELECTRIC CONSTANTS OR ε (RELATIVE PERMITTIVITY):**

the dielectric constant is defined as the ratio of the permittivity of the material

to the permittivity of free space.

$$\varepsilon = \frac{C_0 h}{\epsilon_0 A}$$

, where e is the relative permittivity of the material,

e_0 is the relative permittivity of free space which is nothing but 8.854 C 10^{-12} Farad / meter,

h is the distance between electrodes which is in meter,

A is the area of the electrodes that is in m^2,

C_0 is the measured capacitance at 1 kilohertz which is nothing but in Farad value.

Discuss about the piezoelectric constants of the various materials. As a result, the various input parameters have been discussed up to this point. Going to talk about the materials now

that can fulfil all of those input parameters there.

Piezoelectric constants of different materials:

Type of material	PZT-4	$PbNbO_3$	PVDF	$LiNb0_3$	AlN thin film	PMN-PT
Electromechanical coupling coefficient (k)	0.47	0.33	0.19	0.16	0.24	0.57
Piezoelectric strain constant (d)	290	85	25	5.9	5.5	1400
Piezoelectric voltage constant (g)	26	32	230	22	52	30
Mechanical quality factor (Q_m)	High	Low	Low	Very high	Very high	Low
Electrical loss tangent ($\tan\delta$)	0.004	0.01	0.3	0.001	0.0005	0.01
Relative permittivity at constant stress (ε)	1270	300	8.4	29.8	12.0	3950

Figure 3.7 Piezoelectric Constant of Different Materials

So, now based on this you can choose your materials which can give you the maximum efficiency or maybe how much surface area you have to cover to get that maximum efficiency, or maybe the what is the piezoelectric voltage constant, so that means, you can get lots of information from these particular materials. And based on these, you choose your own materials or maybe the combinations of materials to get the maximum efficiency.

3.2 PIEZOELECTRIC NANOGENERATORS:

piezoelectric nanogenerators, we are calling it as a PENG.

So, a piezoelectric nanogenerator is an energy harvesting device capable of converting external mechanical energy into electrical energy via action by a nanostructure piezoelectric material,

So, based on mode of operations, PENG can be divided into

- force exerted perpendicular to the axis of the nano wire,
- force exerted parallel to the axis of the nanowire.

applying pressure or even vibrations to those materials in this specific example. As a result, it is producing power. Now, in this specific situation, how you are storing your materials—whether you are storing them vertically or horizontally—is important. Therefore, based on them, there are two types whether it is vertical types, depending on whether you are applying strain, stress, or both in these directions. Therefore, there are two distinct phenomena depending on that. As a result, given the structural configuration,

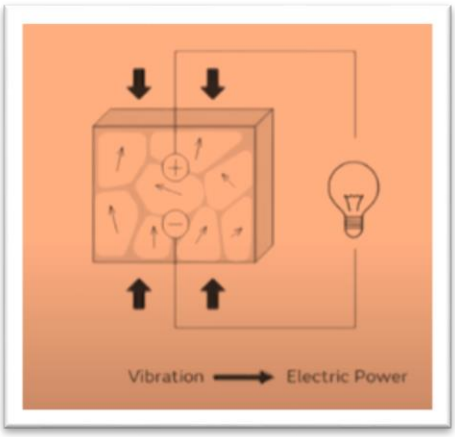

Figure 3.8 PNG Worked By Vibration

PENG can be divided into three parts; one is called

1. the vertical nanowire integrated nanogenerator that is VING,
2. lateral nanowire integrated nanogenerator that is the LING and
3. the nanocomposite electrical generators that is the NEG.

- **FORCE EXERTED PERPENDICULAR TO THE AXIS OF THE NANOWIRE**.

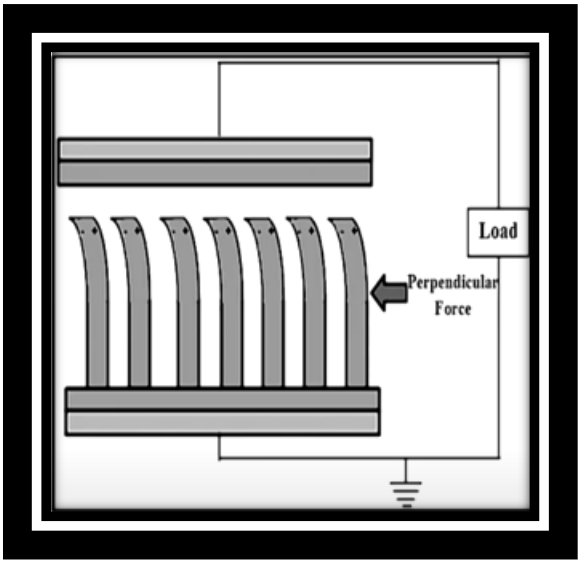

Figure 3.9: Force Exerted Pedicular To The Axis Of The Nanowire

When a piezoelectric structure is exposed to an external force by a moving point in a perpendicular direction, the entire structure deforms. So, in this instance, the information is as follows. The structure will attempt to lie down like this when you apply a perpendicular force over here. In this specific instance, applying a perpendicular force causes the entire structure to deform automatically. Simply put, we are giving you the load in this manner. Therefore, distortion is occurring throughout the whole structure. Thus, the positive electrical potentials will be displayed by the stretch portion with the positive strain, while the negative electrical potentials will be displayed by the compressed part with the negative strain. The electric field created at the tip of the nanostructure is neutralised by the Ohmic contact that develops between the bottom metal electrode and the nanostructures. This is referred to as the Ohmic effect. it appears to be functioning over here.

The Schottky behaviour, which is simply the formation of an electric current, is caused by the Schottky contact those forms between the top metal electrode and the tip of the nanostructure.

FORCE EXERTED PARALLEL TO THE AXIS OF THE NANOWIRE.

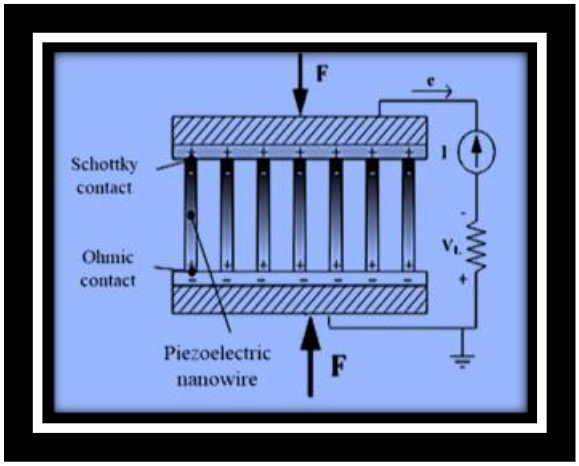

Figure 3.10 Force Exerted Parallel to The Axis of The Nanowire.

Because you are pressing the materials in this specific instance, when the force is directed toward the nanowires' tips, uniaxial compressive is produced in the nanowires. In this specific instance, the Schottky barrier or maybe the Schottky contact is also known as the Ohmic contact. As a result of exerting force, the material between the two electrodes is squeezed. The nanowire's tip will thus have a negative piezoelectric potential as a result of the piezoelectric action. Due to the movement of electrons from the top tip to the bottom, a positive electric potential is formed at the other tip. In this specific instance, this is the positive and this is the negative since here is the minus one and automatically this will obtain the positive ion. Therefore, the current will naturally flow from this direction to this way. Therefore, the produced piezoelectric effect rapidly disappears when the external force is withdrawn. Therefore, it stands to reason that there won't be any electrical generation when you release the pressure.

The migration of accumulated electrons from the bottom electrode to the top electrode of the nanostructure via the external circuit, or more specifically through this circuit, neutralises the positive potentials at the bottom tip of the nanostructure. They are thereby counteracting one another. Now, in general, there are several PENG types based on structural arrangements.

- **VERTICAL NANOWIRE INTEGRATED NANOGENERATOR (VING)**.

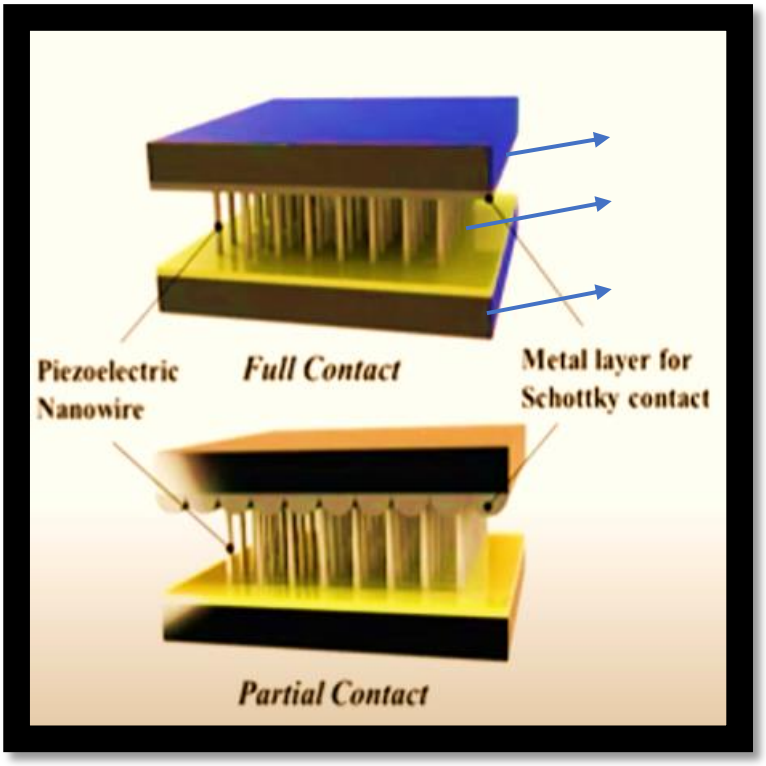

Figure 3.11 Vertical Nanowire Integrated Nanogenerator (VING).

VING is a 3-D configuration consisting of a stack of three layers.

First one is the base electrodes, then 2nd is vertically grown piezoelectric nanostructure and 3rd is the counter electrode. One is the electrode, which is the base electrode and is made of the piezoelectric nanostructure-containing material. Additionally, there are counter electrodes and vertically formed piezoelectric crystals on top of it. Additionally, each electrode has a certain type of backplate. Essentially, in this example, the grey and yellow electrodes are the ones in

question. By using various synthesising procedures, the piezoelectric nanostructure is typically produced from the base electrode. It can be seen from this view that all of the piezoelectric crystals are upright. The counter electrode's tip is then fully or partially mechanically in touch with them before they are integrated with it. Now apply pressure in the manner shown.

- **LATERAL NANOWIRE INTEGRATED NANOGENERATOR OR LING.**

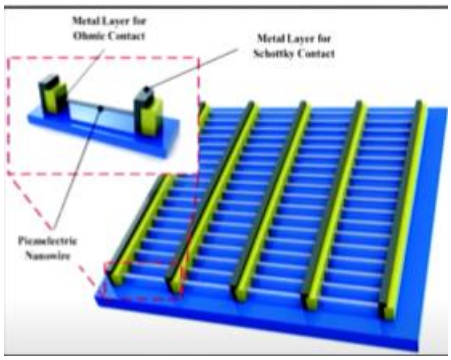

Figure 3.11 **Lateral Nanowire Integrated Nanogenerator Or LING**

LING is a two-dimensional configuration consisting of three sections,

- base electrode,
- laterally grown piezoelectric nanostructures, and
- the top metal electrode.

The Schottky contact is established using the first metal electrode, and the Ohmic contact is established using the second metal electrode. By connecting more LING in series, the voltage produced by a LING may be raised.

this is one electrode, and this is the second electrode over there, so that is why basically it is known as the lateral nanowire integrated nanogenerator or maybe the LING.

Nanocomposite Electrical Generators, NEG.

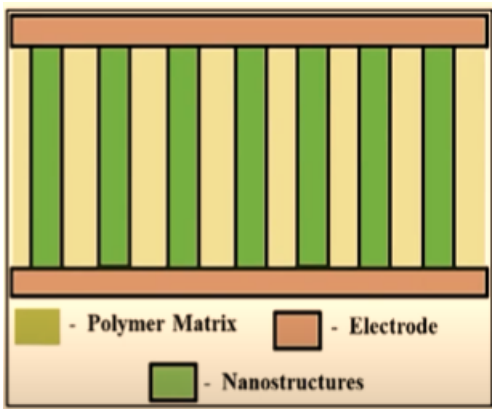

Figure3.12 Nanocomposite Electrical Generators, NEG.

NEG is a three-dimensional configuration consisting of three main parts.

- Metal plate electrodes, having two electrodes over there right, so that is metal plate.
- Now, in between these, it is like composites. In the composites, that polymer matrix as well as the nanostructured materials.
- Next vertically grown piezoelectric nanostructure and the polymer matrix.

The gaps between the piezoelectric nanostructures are filled with polymer matrix. This resembles a pillar, and the polymeric matrix fills the space between the pillars.

It was demonstrated that the NEG is more effective than the original nanogenerator designs in which an AFM tip bends a zinc oxide nanowire.

It has also been demonstrated that it offers a more sustainable energy source.

what kind of materials we are using for these piezoelectric nanogenerators?

The electromechanical characteristics of the material and the development of the Schottky contact between the nanostructure's tip and the second metal electrode provide the foundation of the power generating process.

These two factors are the most important ones. Now, wurtzite-structured piezoelectric semiconductor materials, such as zinc oxide, gallium nitride, and cadmium sulphide, since they concurrently show semiconducting and piezoelectric qualities

Because they are brittle and have a poor degree of formability, inorganic materials are only useful in a few numbers of applications.

In cases where a lightweight generator design is needed, polymers, particularly PVDF, are employed as alternatives to metals. There are concurrently three major classes of piezoelectric properties based on the unit cell structure.

- perovskite group, (ABO_3)
- bismuth layer-structure group that is $Bi_2 A_{x-1} B_x O_{3x+3}$
- pyrochlore group that is the $A_2B_2O_7$.

perovkite group (ABO_3).

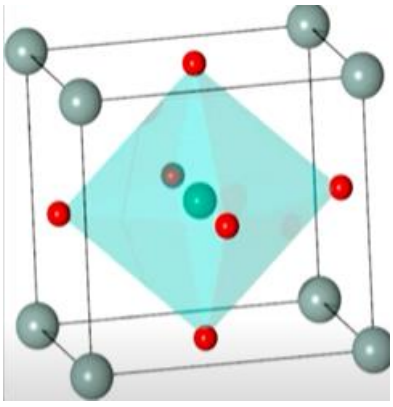

Figure 3.13 Crystal Structure Of Perovskite

• The perovskite group, which has the greatest piezoelectric constants and a huge variety of uses, is by far the most significant class of piezoelectric materials.

• Ceramics of the PZT type are the dominant kind in the perovskite family.

• The structure may be characterised as a straightforward cubic unit cell with oxygen in the middle of each face and massive cations on each corner (A site and B site, respectively). the ABO3 structure is formed.

• the instances of $BaTiO_3$ and $PbTiO_3$

bismuth layered structures $Bi_2A_{x-1}Bx\,O_{3x+3}$ or (BLS).

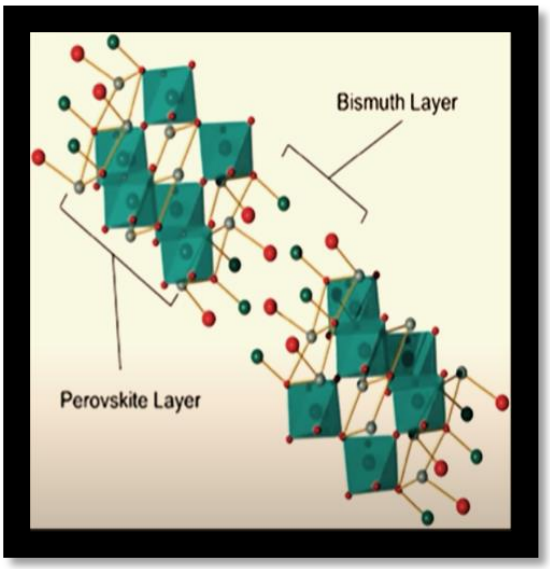

Figure 3.14 Crystal Structure Of Bismuth Layered

- This structure may be seen as an endless layer of perovskite unit cells separated by layers of Bi_2O_2 two ions.
- Thus, the value x in the chemical formula designates a thickness of one or more-unit cells for the perovskite layer.
- In the high-temperature phase, BLS-containing materials exhibit a tetragonal symmetry. Examples are $SrBi_2Ta_2O_9$, Bi_2WO_6, and $PbBi_2Nb_2O_9$.

3.pyrochlore group, $A_2B_2O_7$.

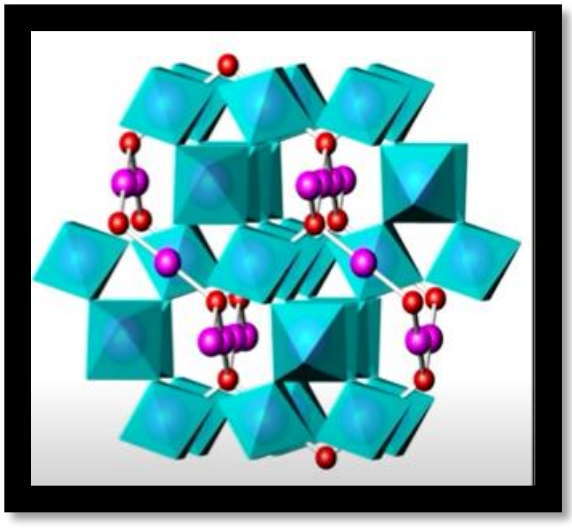

Figure 3.15 Crystal Structure of Pyrochlore Group

• The typical stoichiometry of the pyrochlore structure exhibits cubic symmetry and is $A_2B_2O_7$.

• A is a sizable, low-valence cation, while B is a tiny, highly charged cation that may form coordination or octahedra.

• The normal $A_2B_2O_7$ pyrochlore structure consists of two interconnected structures: blue BO_6, octahedral and A_2O framework oxygen, which is red in this specific hue, and A site cations, which are purple. Therefore, this blue colour is essentially BO_6.

$La_2Ti_2O_7$, $Sr_2Nb_2O_7$, $Gd_2Ti_2O_7$, and $Sm_2Mo_2O_7$ are a few examples.

Challenges

- to increase the efficiency of our materials.
- Second the integration packaging of energy storage unit with the nanogenerators.
- Third optimization on harvesting efficiency of mechanical energy from various working
- conditions
- Optimization of electromechanical conversion efficiency through structural design.
- long-term stability, the chemical stability, mechanical strength.

- Temperature drift during the sensing process for active and the self-powered sensors.
- The integration of active or self-powered system with data processing and the transmitting systems.
- these all are the challenges basically we are facing. And based on these we are trying to make the new materials to solve these kinds of problems.

Advantage

- basically, the piezoelectric nano generator is portable and the wearable.
- PENG an interface with the biological systems.
- PENG has compact configurations; that means, very compactness having in these particular
- materials. So, only you are having the piezoelectric crystals and the two electrode, so very compact
- structure it is having.
- It is compatible with micro electromechanical systems (MEMS).
- PENG, don’t release any harmful gases in there is no any kind of chemical reactions.

Disadvantages

- brittleness in PZT.
- Then uniformity in alignment of the nanowires,
- Need to be protected from the water
- the durability of the structure is less.

applications of the PENG.

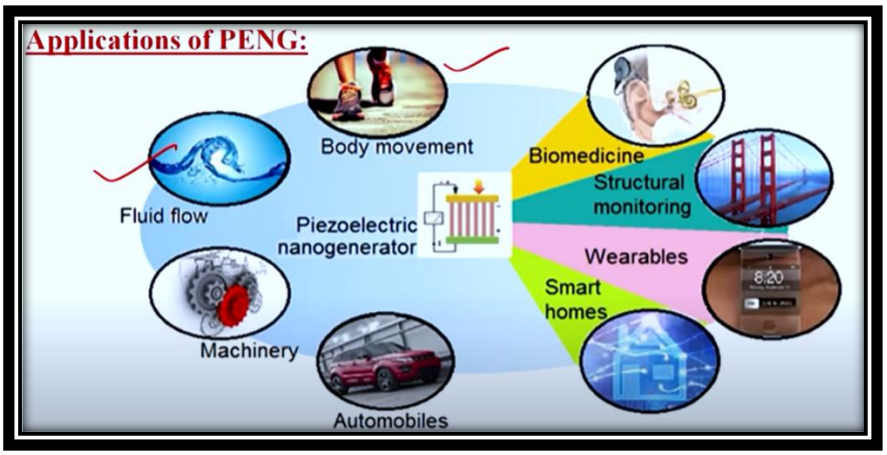

Figure3. 16 Applications Of PENG

Understand that basically where we can place this specific PENG gadget is where we can create the power from the numerous images. Therefore, in this specific instance, if we can put these kinds of materials in our shoes, it will help while we are moving our bodies. Therefore, it may automatically produce energy when we are walking on the surface and pushing our shoes down. If you were to place this type of PENG material in some pipelines, on the sea, or even in a pond, then when a wave of water came as a result of that, the material could be compressed and might produce energy. We may use these sorts of materials in smart homes, wearable technology, structural monitoring, and the biomedical case as well as any kind of machinery applications, mostly for the automobiles or possibly for the tyres or possibly the braking. In general, we may place this specific gadget wherever that any type of force, motion, or movement is creating in order for it to absorb the pressure, motion, or strain and provide you with electricity. So, it is the fundamental idea of employing this type of materials.

References:

[1] N. Taniguchi, \On the Basic Concept of `Nano-Technology' ", Proc. Intl. Conf. Prod. Eng. Tokyo, Part II, Japan Society of Precision Engineering, 1974.

[2] K.E. Drexler, \Engines of Creation", Fourth Estate, London 1990, p. 296.

[3] N. Taniguchi, "On the Basic Concept of 'Nano-Technology'," Proc. Intl. Conf. Prod. Eng. Tokyo, Part II, Japan Society of Precision Engineering, 1974.

[4] G. Binnig et al., Phys. Rev. Lett. 49, 57,(1982).

[5] Smalley, R.E., 1997. Discovering the fullerenes. Reviews of Modern Physics, 69(3),

[6] p.723.

[7] [6] K.E. Drexler, Engines of creation: The coming era of nanotechnology, (Oxford University Press, Oxford, 1986); K.E. Drexler, C. Terson, G. Pergamit, Unbounding the Future: The Nanotechnology Revolution (Morrow, New York, 1991); K.E. Drexler, Nanosystems: Molecular Machinery, Manufacturing, and Computation,(Wiley, New York, 1992).

[8] Burda, C., Chen, X., Narayanan, R. and El-Sayed, M.A., 2005.

[9] Nanomaterials – B. Viswanathan, published by Narosa Publishing House.

Deshpande, S., Patil, S., Kuchibhatla, S.V. and Seal, S., 2005. Size dependency variation in lattice parameter and valency states in nanocrystalline cerium oxide. Applied Physics Letters, 87(13).

[10] Anisotropic nanomaterials: structure, growth, assembly, and functions, P. R. Sajanlal,

[11] T. S. Sreeprasad, A. K. Samal and T. Pradeep, NANO REVIEWS, vol 2, (2011).

Physical Properties of Nanomaterials, Juh Tzeng Lue, Encyclopedia of Nanoscience and Nanotechnology,Volume X: Pages (1–46).

[12] [O. Vigil, F. Cruz, A. Morales-Acevedob, G. Contreras-Puente, Materials

Chemistry and Physics 68 (2001) 249–252.

[13] G. Anil Kumar, M. V. Ramana Reddy, KattaNarasimha Reddy, Journal of Physics: Conference Series 365 (2012) 012031.

[14] H. Merzouk,A. Chelouche,S.Saoudi, D. Djouadi, A. Aksas, ApplPhys A (2012) 109:841–844

[15] B. SrinivasaRao, V. Rajagopal Reddy, B. Rajesh Kumar, T. SubbaRao, International Journal of Nanoscience, Vol. 11, No. 3 (2012) 1240006 (5 pages).

[16] SoumenDhara, P. K Giri, Journal of Experimental Nanoscience, 8(2013) 3, 332–340.

[17] C. Suryanarayana, Bull. Mater. Sci., 17 (1994) 307.

Nanomaterials –An introduction to synthesis, properties and application, Environmental Engineering and Management Journal, 2008, Vol. 7, No.6, 865-870.

[18] [19] Optical properties and spectroscopy of nanomaterials - Jin Zhng Zhang, published by

[19] World Scientific Publishing Co. Pte. Ltd.

K. Nagaveni, G. Sivalingam, M.S. Hegde, Giridhar Madras, Applied Catalysis B: Environmental 48 (2004) 83–93.

[20] [21] Jialin Li , Li Liu, Ying Yu, Yiwen Tang, Huanlun Li, Feipeng Du, Electrochemistry Communications 6 (2004) 940–943.

[21] Assadi, M. Khalaji, et al. "Recent progress in perovskite solar cells." Renewable and Sustainable Energy Reviews 81 (2018): 2812-2822.

[22] Banerjee, Diptonil, and Banerjee, Diptonil, and Kalyan Kumar Chattopadhyay. "Hybrid inorganic organic perovskites: a low-cost-efficient optoelectronic material." Perovskite Photovoltaics. Academic Press, 2018. 123-162. "Hybrid inorganic organic perovskites: a low-cost-efficient optoelectronic material." Perovskite Photovoltaics.

Academic Press, 2018. 123-162

[23] Cubic perovskite ABX3 crystal structure. Published with permission from J.Chen, S. Zhou, S. Jin, H. Li, T.Zhai, Crystal organometal halide perovskites with promising optoelectronic applications, J. Mater. Chem. C 4 (1) (2016) 1127.

[24] Gao, Peng, Michael Grätzel, and Mohammad K. Nazeeruddin. "Organohalide lead perovskites for photovoltaic applications." Energy & Environmental Science 7.8 (2014): 2448-2463.

[25] Kojima, Akihiro, et al. "Organometal halide perovskites as visible-light sensitizers for photovoltaic cells." Journal of the American Chemical Society 131.17 (2009): 6050-6051.

[26] Lee, Michael M., et al. "Efficient hybrid solar cells based on meso-superstructured organometal halide perovskites." Science 338.6107 (2012): 643-647.

[27] Burschka, Julian, et al. "Sequential deposition as a route to high-performance perovskite-sensitized solar cells." Nature 499.7458 (2013): 316-319.

[28] BAI, YuBing, et al. "Progress on perovskite-based solar cells." Chinese Science Bulletin 61.4-5 (2015): 489-500.

[29] Meng, Lei, Jingbi You, and Yang Yang. "Addressing the stability issue of perovskite solar cells for commercial applications." Nature communications 9.1 (2018): 1-4.

[30] Jeong, Jaeki, et al. "Pseudo-halide anion engineering for α-FAPbI 3 perovskite solar cells." Nature 592.7854 (2021): 381-385.

[31] https://www.ossila.com/pages/perovskites-and-perovskite-solar-cells-an-introduction#ref4

[32] Zhao, Yu-Qing, et al. "Tuning superior solar cell performance of carrier mobility and absorption in perovskite CH3NH3GeCl3: A density functional calculations." Journal of Power Sources 313 (2016): 96-103.

[33] http:/ /www.nitttrc.edu.in/nptel/course/video/112107283/lec3.pdf

[34] Guner, Tugrul, and Mustafa M. Demir. "A review on halide perovskites as color conversion layers in white light emitting diode applications." physica status solidi (a) 215.13 (2018): 1800120.

[35] Huang, Like, and Ziyi Ge. "Simple, Robust, and Going More Efficient: Recent Advance on Electron Transport Layer-Free Perovskite Solar Cells." Advanced Energy Materials 9.24 (2019): 1900248.

[36] Zhou, Di, et al. "Perovskite-based solar cells: materials, methods, and future perspectives." Journal of Nanomaterials 2018 (2018).

[37] Mutalikdesai, Amruta, and Sheela K. Ramasesha. "Emerging solar technologies: Perovskite solar cell." Resonance 22.11 (2017): 1061-1083

[38] Lee, Jin-Wook, Hui-Seon Kim, and Nam-Gyu Park. "Lewis acid–base adduct approach for high efficiency perovskite solar cells." Accounts of chemical research 49.2 (2016): 311-319.

[39] [Perovskite solar cells: In pursuit of efficiency and stability : Jasmin S. Shaikh,Navajsharif S. Shaikh, Arif D. Sheikh,Sawanta S. Mali, Abhijeet J.Kale, Pongsakorn Kanjanaboos, Chang Kook Hong,J.H. Kim,Pramod S. Patil,Periodical : Materials & Design, 2017,Page Number : 54-80

[40] Yi, Zijun, et al. "Will organic–inorganic hybrid halide lead perovskites be eliminated from optoelectronic applications?." Nanoscale Advances 1.4 (2019): 1276-1289

[41] Photomechaelectricnanogenerator

panelJinZhao13YinghaoZhang123YifanJia1LixiaBao1LijunYang1SiyuXiao1Jiaying Xie1JiliangWang14

[42] Brignardello-Petersen, Romina. "Piezoelectric instruments used for odontosection or osteotomy may result in less trismus after surgical mandibular third-molar extraction than rotatory instruments." The Journal of the American Dental Association 148.7 (2017): e102.

[43] Jbaily, Abdulrahman, and Ronald W. Yeung. "Piezoelectric devices for ocean energy: a brief survey." *Journal of Ocean Engineering and Marine Energy* 1.1 (2015): 101-118.

[44] Zi, Yunlong, and Zhong Lin Wang. "Nanogenerators: An emerging technology towards nanoenergy." Apl Materials 5.7 (2017): 074103.

Chapter 2:

Review of Past Work

Review of past work:

Abstract

Researchers have been investigating energy harvesting systems as an alternative to traditional power sources (such batteries) for compact and low-power electronic gadgets for more than 25 years. Battery life limitations and the requirement for routine recharging or replacement have consistently been a problem with portable, remote, and implantable devices. Solar, thermal, and vibrational energy are the three main sources of ambient energy. Vibration energy is one of these energy sources that is always present in both natural and man-made structures. Vibrational energy may be transformed into useable electrical energy using a variety of materials and transduction methods, including piezoelectric, electromagnetic, and electrostatic generators. Piezoelectric nanogenerator have been extensively investigated to produce power from vibration energy sources due to its intrinsic electromechanical coupling and high-power density compared to electromagnetic and electrostatic transducers. The authors conducted and published a current review of piezoelectric energy harvesting techniques in this journal in 2007. Numerous researchers have developed new materials, electrical circuits, and analytical models since 2007 in an effort to enhance different aspects of piezoelectric energy harvesting systems. Over the past ten years, other researchers have also identified cutting-edge uses for piezoelectric energy harvesting technologies. This work updates the authors' last review paper by describing the substantial advancements made in the field of piezoelectric energy harvesting over the past ten years, despite the fact that the volume of literature in the subject has increased dramatically since 2007.

In the work in this paper, **Ding, Ran, et al. (2017)** found to increase the performance of nanogenerator with the combination of formamidinium lead halide as perovskite and PVDF and they achieve a good output of NG [1]. They found 12wt% of sample is the best performance for this device and current density and o/p voltage gain up to 6.2ma cm^{-1} and 30V.they can be used to charge the capacitor and LED by using an output power of the device. they had done this device is an easy process and low cost. In this paper I help to find the materials, method of preparation of PENG in an easy way, and how to fabricate the device.

In the work on this paper **Huiying Chen, et all(2019)** found the high performance of electrical and dielectric properties in piezoelectric nanogenerator based on CsPbBr3 attached with PVDF**)** [2]. they have done synthesized in one step electrospinning of solutions of CsPbBr3 and PVDF fiber; in this process, in situ growth of this composite is highly uniform sized and special distribution .in this PENG they published open circuit voltage and density of short circuit current gain up to 103V and 170ma cm-1. they improved the thermal, water, and acid-based stabilities by these PENG-based $CsPbBr_3$ and PVDF composite fibers. Through this work of this PENG-based $CsPbBr_3$ with PVDF composite fibers, they modified better flexibilities, strength, workability, and relatively high permittivity of PVDF. their device after being submerged in water maintains almost 100% for half a year, after being submerged in H_2SO_4 solution and NaOH solution their device preserves respectively 63.53% and 82.35% for 25hours.

In the work on this paper, **Mondal, et al. (2020).** achieved very good performance on piezoelectric nanogenerators which new class of composite of PVDF and perovskite-based $CsPbBr_3$.their colloidal synthesise method and film fabrication method is easy and take less time [3].For reaching the β phase of PVDF, they use CsPbBr3 composite; they found a maximum β phase in 5wt % .They found a higher amount of light absorption and to improve the stability to perovskite rod .output voltage of their PNG 5 produce nearby 120V and open

circuit voltage of finger generated based simple bending is up to 8V.they ensure that conjugation of CsPbBr3 with PVDF detect the visible lights and produces significant changes 3 times in output current and voltage by 2 times. as a result, this device uses of hybrid materials such as piezoelectric energy harvesting and vibration sensor under mobile vibration, air blowers and regular fans.

On this paper **Bhattacharya, et al, (2021).** achieving advantages of mechanical flexibility, light weight, low cost in their device piezoelectric nanogenerators that have effective application as renewable energy harvesting [4]. They used composite of chemically exfoliated tungsten disulfide (WS_2) nanosheets and PVDF that are found effective photosensitive property and made them self-powered optical devices. Here they try to experiment to increase b phase of pvdf composite with exfoliated tungsten disulfide alongside found very good photosensitivity in the nanocomposite. This composite based device produced good high output voltage upto 116 They achieved rampant piezoelectric energy conversion efficiency nearby 25.6%;At zero biased this device display strain depended photocurrent and under the illumination of 410 nm at 0.75% strain shows responsivity of 6.98×10^{-3} A W^{-1}.by this device they use in human regular activism of human (finger tapping, mouse clicking, writing on paper) as harvest energy.

on this paper **Shi, et al, (2020)** prepared successfully nanowire which is composite of PMMA and BaTioO3 by in situ surface-initiated ATRP technology.to make piezoelectric fortify phase of PVDF-TrFE, this PMMA@BaTiO3 composite based nanowire are used with the help of electrospinning **[5]** . Compatibility of PVDF-TrFE and PMMA composite made high, improve the dispersion of BaTiO3 NWs and at the interface between the piezoelectric BaTiO3 NWs and the PVDF-TrFE matrix improve the stress transfer. This device achieved good piezoelectric output, 10wt % of their sample achieved maximum power of 4.35 μW; achieved

voltage of 12.6 V, a current of 1. 30 μA. After 6000 period binding long cycle, PENG generate stable piezoelectric output and exhibits a high longevity.

on this paper **Jiang, et al. (2022)** had displayed in situ preparation of micro/nano fiber film which was composite of $Cs_3Cu_2I_5$ and PVDF by one step electrospinning with blue polarized ratio of 0.5 [6]. Prepared $Cs_3Cu_2I_5$ and PVDF composite based nanofilm show photoluminescence quantum yield if 33.3-86.1% with the highest polarization ratio of 0.4 and high durability. They found that the nanostructures set within the nanofibers show rod shape and specially arranged along the long axis of the nanofibers, that is useful to the high-degree polarization. They suggested that TDM is mainly oriented along Cu-Cu bond of the excited state of Cs3CuI5 and in the future, for the nanofibers the polarization ratio can be further improved by increasing the degree of oriented alignment. Their result suggested that the composite film fiber of $Cs_3Cu_2I_5$ and polymer may useful for optical device applications such as laser, waveguides, displays, information storage.

Wankhade, et al (2020) prepared nanogenerator as energy harvesting device which composite of PVDF and PZT fabricated using nanohybrid preparation process. this is durable, cheap, easily fabricated and good efficient energy harvesting device **[7]**. They examined that the device display very good electrical output due to existence of electroactive filler and by means of 30 wt.% of piezo-filler maximum output is produced. Also, they found that this device generated output voltage of 55 V and output power density of 36 μW/cm−2.From the device they examine that bending feet tapping etc many other methods can produce significant amount of electrical output. they suggested that it can be used in low power consumption electronics devices.

On this paper **Hu, et al. (2018)** prepared a heterostructure double layered and PVDF nanocomposite films with barium titanate nanoparticles by using of spin coating method **[8]**. The nanofillers were concentrated circulated in one layer of semi the film, and the last semi

was arranged PVDF layer. similar content nanoparticles of BT circulated with Single-layer nanocomposite films in whole layer were prepared for comparison. The inductive charges accumulated at the added interlayer interface between BT and PVDF layer and PVDF layer contributes much to enhancing electric capacity of the film. by FT-IR and XRD characterized containing with less content of BT nanoparticles and lower proportion of β-phase in polymer, the PENG devices fabricated by the double-layered films signify higher piezoelectric productions in mechanical-to-electric conversion measurement. They found that the double-layer film contained with 20vol fractions (vol%) BTNPs denote outstanding inclusive performance of 6.7V in output voltage, 2.4μA in output current, and good stability changed in more than one thousand circles within 3%. By this work they examine from the device Profited from good interfacial adhesion and better flexibility, the mechanical property of double-layer films is also upgraded. for self-powered device the double-layer constructure is capable in optimizing nanocomposite film to develop PENGs.

A composite made of very flexible PVDF sheets and perovskite-based CsPbCl3 allowed **Mondal, et al. (2022)** to achieve piezoelectric nanogenerators with outstanding performance as energy harvesters [9]. They look at how differences in electroactive phase nucleation, variations in dielectric properties, and residual polarisation in the hybrid samples occurred in the PVDF sample with small changes in perovskite concentration. According to their findings, a 3wt% perovskite sample yields the hybrid's maximum β phase. They discovered that the highest output voltage and current of PNG 3 were in the range of 168 V and 2 A, whereas those of PVDF film were in the range of 20.0 V and 0.58 A, respectively. They check that this device's output was adequate to turn on 32 nearby green LEDs without the need for additional energy from the outside. This PNGs demonstrates potential value as an active posture sensor that can identify improper posture while seated or standing. Capacitors have been successfully charged by repeated finger taps and releases, indicating that the output voltage of PNG 3 can

be used to power smart electrical devices on its own. They also discovered that PNG 3 based systems were developed, which can convert low-frequency walking motion energy and serve as a power source for small electronic devices, depending on the results of capacitor charging. They also look at the stability and durability tests performed after 10,000 cycle data were collected over a period of 5 months, demonstrating its viability as a long-term energy source.

A unique, high-performance, flexible, multi-layered composite of BTO and PVDF PNG was successfully created by spin coating and layer-by-layer assembly, according **to Li, et al. (2021)**.[10] They discovered that the output voltage and current generated from the BP4-NG with an embedded BTO NPs content of 20 wt% may reach up to 14.22 V and 2.42 A, respectively, by taking use of the composite method and interlaminar electric field effect. With an ideal 5 M load resistance, the BP4-NG device can provide a maximum power of 11.55 W. They look at its Durability and stability of the created multi-layered PNG have been validated by periodic testing and stimulation via diverse deformations. Their study, which is now being presented, not only adds a new multi-layered PNG structure, but also demonstrates how interlaminar electric field effect may be used to create some of the best nanogenerators. Their first electrical tests also demonstrate that BTO/PVDF composite PNG may have potential use in wearable technology and mechanical energy harvesting.

Liu, et al. (2021).[11] Prepared By using the solvothermal approach, the dopamine coated nano-TiO2 is employed to boost the -phase content of PVDF. This article examines the structure, phase formation, piezoelectric and residual polarisation of TiO2/PVDF and DA@TiO2/PVDF films. They look at it the crystallinity and b-phase concentration of DA and TiO2/PVDF clearly increase when compared to TiO2/PVDF. They discovered the d_{33} and P_r of the TiO2-5 weight percent/PVDF film are, respectively, 100% and 265% greater than those of the pure PVDF film. The compatibility of the PVDF matrix and nano-TiO2 is enhanced by the addition of DA. They found that the polar groups (-NH2, -OH) of DA cause the all-trans

conformation of composite films to develop, and the combined action of nano-TiO2 and DA may considerably improve piezoelectric behaviour. The $DA_{2.0}$ @TiO2/PVDF film has d_{33} and P_r values that are 163% and 278% higher, respectively, than the pure PVDF film. The current study allows the PVDF to potentially be used in wearable, portable, and curved panel energy harvesters.

A flexible piezoelectric energy generator based on metal ZnO nanoparticle-P(VDF-TrFE) composite was created by **Jin et al. (2020)** and has improved piezoelectric performance [12]. They methodically assessed how clean, Co, Na, Ag, and Li doped ZnO devices performed. They determined that the 5% Li doped device is the best among all metal dopant devices in terms of voltage production, increasing the voltage output to 9 times that of a pure ZnO device. They showed that the energy captured by finger tapping at 2 Hz can light an ultraviolet (UV) light-emitting diode and charge a capacitor with a significant output power density of 0.45 W/cm3 (LED). By harnessing biomechanical energy and acting as a wearable motion sensor, they showed that the device is a potential prototype for powering tiny devices. In addition to revealing the various impacts of the metal dopant on the piezoelectric performance of flexible PENG, this study also provides a designing technique to enhance the piezoelectric performance of such flexible energy harvesters and motion sensors.

Using a 3D core/shell structure, **Lu, et al. (2022)** created a novel PENG in which 3D-Tb-BCZT-coated 3D-Tb-BCZT/PVDF composite fibres were produced using the coaxial electrospinning technique [13]. The created PENG displays good electrical output performances of 48.5 V and 3.35 A under a vertical force of 30 N at 2 Hz, which are approximately 3.1 and 2.5 times greater than those of the PENG based on the conventional electrospinning procedure (15.6 V and 1.32 A), according to this study. The core/shell structure of piezoelectric particles, Tb-modified BCZT, and 3D structures all contribute to the in situ ternary synergistic improvement of PENG's piezoelectricity. They found that among these, the 3D core/shell

structure design, in which the piezoelectric particles are connected to one another and the stress can directly transmit via adjacent piezoelectric particles, leading to the commendable improvement of stress-transfer efficiency, possesses a dominant effect for improving the output of PENG. They also looked at whether the COMSOL simulation could support the better mechanism of the novel construction. The constructed PENG still displays a consistent output performance and demonstrates good durability and stability even after 5000 cycles and 3 months. They discovered that the developed this PENG may efficiently capture various energies from our daily lives and instantaneously power 16 commercial LEDs without the need for an external energy-storage device. Due to the small weight and soft flexibility of composite fibres, they investigate how both wind flow and sound pressure may create a vibration deformation of prepared PENG to generate output voltage. With a frequency range of 50–200 Hz and an external sound pressure of around 95 dB, PENG output voltages of 2–5 V may be achieved. The output voltages of PENG may reach 12-28 V at various wind speeds between 5 and 14 m/s. Additionally, their PENG can use wind energy to power a commercial digital temperature-humidity metre by interfacing with the circuit management system. They succeeded. The innovative design for composite fibres not only offers a straightforward, affordable method for creating high-performance PENG, but it can also be extensively used on a variety of sceneries to gather micro energy, which is anticipated to be used in self-powered IoT devices in the future.

Ippili, et al. (2019) used an easy method of antisolvent-assisted collision process in ambient air settings to effectively synthesis lead-free $MASnI_3$ perovskite [14]. The $MASnI_3$ films were stable at ambient room settings within 24 hours after being annealed for 1 hour at 180 °C in an argon environment, according to this paper's analysis. They looked at the fact that $MASnI_3$'s phase change from tetragonal to cubic was noted at or below 30 °C and the polycrystalline

$MASnI_3$ films displayed strong P-E hysteresis loops, a low leakage current density of 7 x 10^{-7} A cm^{-2}, and a high dielectric constant of 65 at 100 kHz. These films had a high piezoelectric coefficient of d_{33} = 20.8 pm V^{-1}, representing a 4-fold increase in values for $MAPbI_3$ films that had previously been reported. They discovered Under an applied pressure of 0.5 MPa, the piezoelectric output performance of the poled-$MASnI_3$ PENGs at 20 kV cm^{-1} revealed an output voltage of 3.8 V and current density of 0.35 μA cm^{-2}. The piezoelectric output performance of the $MASnI_3$-based PENGs was further improved using composited $MASnI_3$ sheets made of an ecologically friendly, porous PVDF polymer. They also look at the greatest output voltage and current density of the PVDF-$MASnI_3$ composite-based PENGs poled at 60 kV cm^{-1} were respectively 12.0 V and 4.0 μA cm^{-2}. PVDF-$MASnI_3$ PENGs were able to instantly light a green LED when 0.5 MPa/1 Hz of applied force and frequency were used. The composite PENGs also demonstrated long-term stability for 90 days by maintaining consistent output performance. They succeeded. It is possible to fabricate large-scale, high-performance, and environmentally friendly PENGs based on lead-free organic-inorganic perovskites using this straightforward and affordable solution technique, which may be extensively used in a variety of real-world applications.

Through the carefully regulated evaporation of DMF, **Maity, et al. (2022)** showed how to manufacture PVDF composite film with CPI incorporated using a straightforward solution casting approach [15]. Then they noticed that CPIP's optoelectronic and piezoelectric capabilities were advantageous in piezoelectric NG and PD applications. they discovered The CPI is protected from deterioration by the soft PVDF polymer, which is used as a stabiliser, making it very stable under ambient conditions and increasing the piezoelectric phase content (to 96%) in the CPIP composite. Furthermore, the first principal DFT simulations that probe

the interfacial interaction of the strain-engineered bound system and open the path for further investigation are used to comprehensively study the binding of CPI perovskite and PVDF polymer. In this study, the CPIP-based NG outperforms the Neat PVDF-based NG in terms of mechano-electric conversion efficiency from a straightforward human finger touch (V_{oc} of 20 V and I_{sc} of 6 A). In addition, they discovered that CPIP-based PD has the capacity to detect visible light with a quick reaction time (t_{ON} as 2.4 s and t_{OFF} as 1.1 s) and photo responsiveness of 0.3 mAW1. Finally, they exhibit a substantial improvement in Isc 57% with simultaneous application of compressive strain and light illumination onto the device to show the piezo-phototronic effect in CPIP composite. It presents a tremendous potential for piezotronics and optoelectronic sensors of the upcoming generation. They think that this research offers fresh understanding of the way that CPI and PVDF polymer bond, and that the strain-induced bound complex system with a sufficient bandgap paves the way for highly effective and reliable self-powered electronics. Additionally, they concentrated on further research into other perovskite polymer composites to examine potential piezo-phototronic applications in the near future.

References

1. Ding, Ran, et al. "High-performance piezoelectric nanogenerators composed of formamidinium lead halide perovskite nanoparticles and poly (vinylidene fluoride)." Nano Energy 37 (2017): 126-135.

2. Chen, Huiying, et al. "Piezoelectric Nanogenerator Based on In Situ Growth All-Inorganic CsPbBr3 Perovskite Nanocrystals in PVDF Fibers with Long-Term Stability." Advanced Functional Materials 31.19 (2021): 2011073.
3. Mondal, Suvankar, et al. "Human motion interactive mechanical energy harvester based on all inorganic perovskite-PVDF." Nano Energy 74 (2020): 104870.
4. Bhattacharya, Didhiti, et al. "2D WS 2 embedded PVDF nanocomposites for photosensitive piezoelectric nanogenerators with a colossal energy conversion efficiency of~ 25.6%." *Nanoscale* 13.37 (2021): 15819-15829.
5. Interface induced performance enhancement in flexible BaTiO3/PVDF-TrFE basedpiezoelectricnanogenerators (panelKunmingShiaBinChaiaHaiyangZoubPeiyueShencBinSundPingkaiJiangaZhiwenShicXingyiHuanga)
6. Jiang, Ting, et al. "In Situ Fabrication of Lead-Free Cs3Cu2I5 Nanostructures Embedded in Poly (Vinylidene Fluoride) Electrospun Fibers for Polarized Emission." *ACS Applied Nano Materials* 5.1 (2022): 508-516.
7. Wankhade, Shivaji H., et al. "PVDF–PZT nanohybrid based nanogenerator for energy harvesting applications." *Energy Reports* 6 (2020): 358-364.
8. Hu, Penghao, et al. "Double-layer structured PVDF nanocomposite film designed for flexible nanogenerator exhibiting enhanced piezoelectric output and mechanical property." Composites Science and Technology 168 (2018): 327-335.
9. Mondal, Suvankar, et al. "All-inorganic halide perovskite tuned robust mechanical-energy harvester: Self driven posture monitor and power source for portable electronics." *Applied Materials Today* 26 (2022): 101385.

10. Li, Yinhui, et al. "Multi-layered BTO/PVDF nanogenerator with highly enhanced performance induced by interlaminar electric field." Microelectronic Engineering 244 (2021): 111557.
11. Liu, Lulu, et al. "Piezoelectricity of PVDF composite film doped with dopamine coated nano-TiO2." Journal of Alloys and Compounds 885 (2021): 160829.
12. Jin, Congran, et al. "Flexible piezoelectric nanogenerators using metal-doped ZnO-PVDF films." Sensors and Actuators A: Physical 305 (2020): 111912.
13. Lu, Haowei, et al. "Enhanced Output Performance of Piezoelectric Nanogenerators by Tb-Modified (BaCa)(ZrTi) O3 and 3D Core/shell Structure Design with PVDF Composite Spinning for Microenergy Harvesting." ACS Applied Materials & Interfaces 14.10 (2022): 12243-12256.
14. Ippili, Swathi, et al. "An eco-friendly flexible piezoelectric energy harvester that delivers high output performance is based on lead-free MASnI3 films and MASnI3-PVDF composite films." Nano Energy 57 (2019): 911-923.
15. Maity, Kuntal, et al. "Piezo-phototronic effect in highly stable CsPbI3-PVDF composite for self-powered nanogenerator and photodetector." Nano Energy 92 (2022): 106743.

Chapter 3

Instruments & Apparatus

3.1 Synthesis Apparatus:

3.1.1. Furnace and Oven:

Box furnaces are commonly used for solid state heating. Starting materials are stoichiometrically mixed and annealed in the furnace within the temperature range of 1000 – 1200 0C for 15 – 20 h. Thorough intermediate grinding is an important step for phase uniformity. Synthesis of CuBO2 nanorods through molten salt process have done in blue box-Furnace at 8000c for 3 hours. Alumina boats and crucibles or plain Borosil glass beaker was used for the reaction chamber. The temperature controller usually controls the rate of heating and maintains the temperature with an accuracy of ±0.5 0C. Fig.3.1 (a) and Fig.3.2 shows the digital image of the furnace used. A low temperature oven was used for drying the samples and also for certain hydrothermal reactions. The digital image of a typical oven is shown in Fig.3.1 (b).

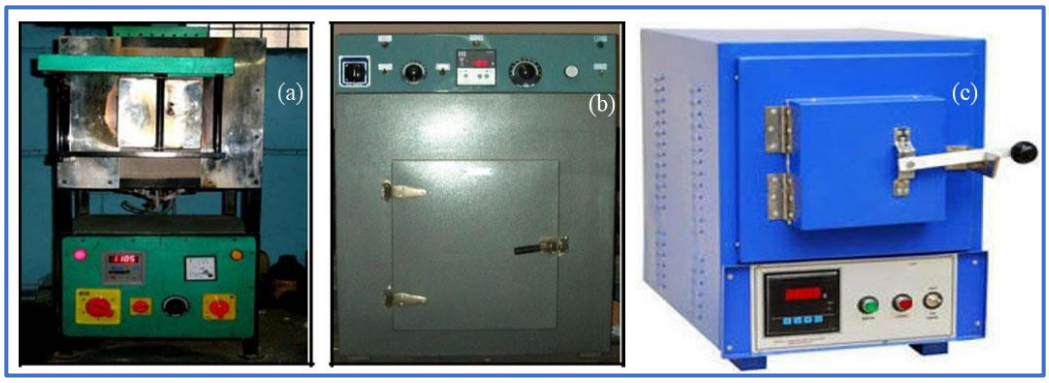

Fig.3.1: Digital images of (a) Furnace and (b) Oven (c) Blue box furnace

3.1.2. Pelletizer:

Pelletizing is an important sample preparation technique, which involves the formation of a solid 'pellet' for analysis via methods that require flat, round samples. The pellets are formed via the agglomeration of fine, amorphous powders in the presence of moisture in a piece of apparatus known as a pelletizer. A solid or liquid binder can also be added before and during pelletizing if needed for process considerations or increasing the hardness of the product. Most common method is the potassium bromide (KBr) pellet method, in which the sample is well mixed with fine alkali halide powder and finely pulverized. The pulverized sample is then fed into a pellet-forming die when applies a vacuum force on the sample to form transparent pellets.

In addition to KBr, cesium iodide may also be used to form pellets. To prepare the pellets we have used a binder because in absence of binder the pellets were found to be very brittle. We have used polyvinyl alcohol (PVA) as the binding agent. In another way To prepare the paste, suitable amount of PVA is mixed with deionized water and is mildly heated with constant stirring until an adhesive gel is formed. One or two drops of this paste are mixed with the oxide powder by a mortar and pestle. Then the powder is pressed into thick films of 12 mm diameter and about 1.5 – 2 mm of thickness under the uniaxial pressure of 1 GPa for 3 min using the pelletizer. The pellets are then sintered at 400 ºC for 3 h to expel the PVA from the sample. Pellets are then connected with electrical contacts to perform characterizations.

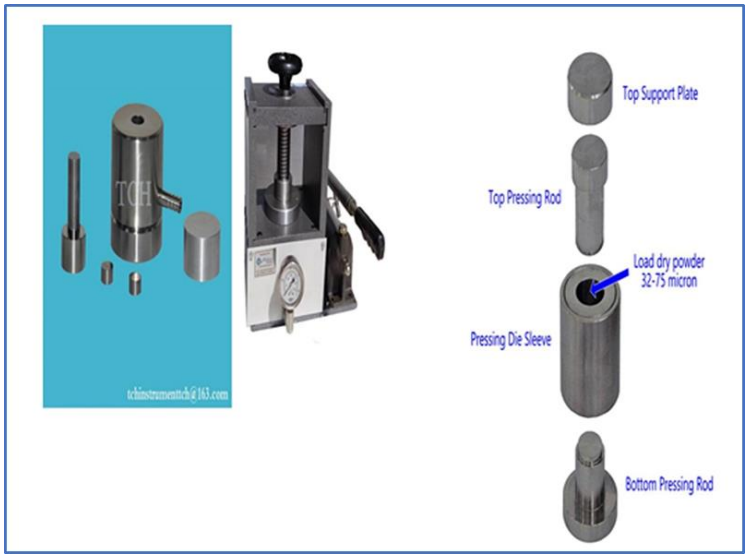

Figure 3.2. Different components of Pelletizer.

3.1.3. Magnetic Stirrer:

The magnetic stirrer can stir the magnetic bit within the solution of the beaker through a revolving magnetic arrangement attached with it. A heater arrangement associated with the stirrer can heat the solution at a desired temperature and the temperature is controlled by a knob as shown in Fig.3.3.

Figure 3.3. Digital image of a magnetic stirrer

3.1.4. Spin coater:

Spin Coating is a procedure used to deposit thin films on flat substrates. Thin films of various thicknesses (μm to nm range) can be deposited on the substrate depending on the rotational velocity of the machine and viscosity of the fluid being deposited. In this process, the solution is first deposited on the substrate, and the substrate is then accelerated quickly to the desired rotational velocity. The liquid on the substrate flows out radially, due to the

centrifugal forces acting on it, and the excess is ejected off the edge of the substrate. The film continues to thin slowly until disjointing pressure effects causes the film to reach an

equilibrium thickness or it turns solid like due to a dramatic rise in viscosity from solvent evaporation. The final thinning of the film is then due to solvent evaporation.

Figure 3.4. the model of the spin coaters at Thin Film and Nano Science Lab, JU, manufactured by Apex Instruments.

3.1.5. Hot Plate:

A hot plate is a tabletop laboratory heater that is generally used to heat glassware and its contents. This apparatus usually features two or more electric heating elements. Most hot plates also contain magnetic stirrers that allow the heated liquid to be stirred simultaneously and automatically. There are a couple of methods other than direct heating that are also used in the laboratory for experimental purposes. One method of heating is to suspend the slightly above the surface of the hot plate with no direct contact. This reduces the temperature of the glass, slows down the rate of heat exchange and encourages even heating. This works well for low boiling point operations. Another method is to suspend glassware above a plate and surround the flask by a skirt of tinfoil. The skirt should start at the neck of the flask and drape down to the surface of the plate, not touching the sides of the flask, but covering the majority of the plates surface. This method is for glassware to be heated at higher temperatures because the flask is warmed indirectly by the hot air collecting under the skirt and unlike simply suspending the glassware, this method is better protected from drafts.

3.1.6: Oscilloscope

An essential weapon in the arsenal of an electronics engineer or tester are oscilloscopes, or scopes. An oscilloscope is a piece of electronics test equipment that makes it possible to view waveforms, greatly facilitating the identification of any issues that may be present in an electronics circuit.

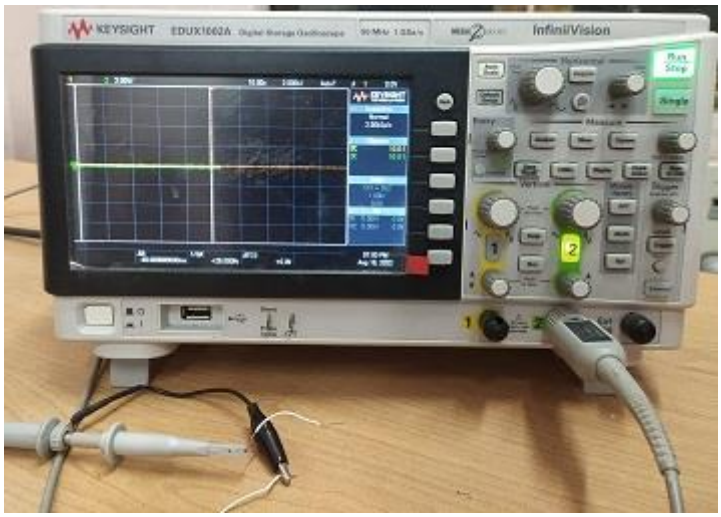

Figure.3.6.1 **Oscilloscope**

Oscilloscopes are a crucial piece of electronics test equipment for any electronics lab or area testing electronics hardware, whether in RF design, general electronics circuit design, electronics manufacturing, service, or repair, or anywhere that electronic circuits and the waveforms on them need to be investigated.

Because it makes oscillations visible, the oscilloscope got its name. The term "cathode-ray oscilloscope," or CRO, was occasionally used. This was due to the fact that the waveforms were shown using cathode ray tubes (CRT). These days, test equipment is most commonly referred to as a scope or an oscilloscope.

The ability to display waveforms on a display is an oscilloscope's primary use. In the default operating mode, amplitude is displayed along the Y axis and time is presented along the horizontal X axis (vertical axis). In this approach, an oscilloscope may display an electrical waveform as it could be imagined. The waveform is comparable to the ripples that develop when a stone is put into a pond and move over its surface.

By observing a waveform in this way, it is able to examine the circuit's operation and identify any potential issues.

How does an oscilloscope work?

The three main oscilloscope systems are trigger, horizontal, and vertical. In order for the oscilloscope to properly reconstruct the electrical signal, these systems work together to offer information about it. An oscilloscope's block diagram is seen in the image below.

The first stage, known as the vertical system since it depends on the vertical scale control, attenuates or amplifies the signal voltage in order to maximise the signal's amplitude. The analog-to-digital converter (ADC) is used to sample the signal voltage and convert it into a digital format value when the signal enters the acquisition block. Each voltage sample receives a precise time (horizontal) coordinate from the horizontal system, which includes a sample clock. The ADC is driven by the sample clock, and the digital output is recorded as a data point in the acquisition memory. A user-specified condition is found in the incoming signal stream by the trigger system, which uses it as a time reference in the waveform record. The waveform data before or after the event, as well as the event that satisfied the trigger requirements, are both presented.

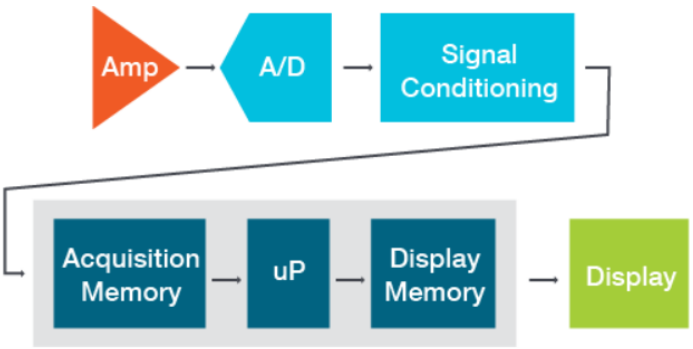

Fig 3.6.2: Block Diagram Of Oscilloscope

3.2. Characterization Apparatus:

3.2.1. X–Ray diffractometer (XRD):

In the year 1895, the German physicist Roentgen discovered X-rays and so named due to the unknown nature at that time. These rays were invisible, traveled in straight lines and affected the photographic plate like ordinary light. Also, these rays show more penetrating power than

light. In the year 1912, the exact nature of X-rays and diffraction phenomenon of x-rays by atomic planes of crystals were properly discovered. This discovery showed the wave nature of X-rays and explored a new direction to investigate the structure of matter. Solid matter can be divided as follows:

- Amorphous: The atoms are arranged in a random way similar to the disorder we find in a liquid. Glasses are amorphous materials.

- Crystalline: The atoms are arranged in a regular pattern, and one smallest volume element that by repetition in three dimensions describe the crystal. This smallest volume element is called a unit cell. The dimensions of the unit cell are described by three axes: a, b, c and the angles between them alpha (α), beta (β), gamma (γ). About 95% of all solids can be described as crystalline. X-rays are electromagnetic radiation of almost same nature as light but having shorter wavelength of 0.5 to 2.5 Å regions. X-rays occupy the region between gamma and ultraviolet rays in the entire spectrum.

X−rays are generated in a cathode ray tube by heating a filament to produce electrons, accelerating the electrons toward a target by applying a voltage, and bombarding the target material with electrons. When electrons have sufficient energy to dislodge inner shell electrons of the target material, characteristic X−ray spectra are produced. These spectra consist of several components, the most common being Kα and Kβ. Kα consists, in part, of Kα1 and Kα2. Kα1 has a slightly shorter wavelength and twice the intensity as Kα2. The specific wavelengths are characteristic of the target material (Cu, Fe, Mo, Cr). Filtering, by foils or crystal monochrometers, is required to produce monochromatic X−rays needed for diffraction. Kα1and Kα2 are sufficiently close in wavelength such that a weighted average of the two is used.

X-rays are electromagnetic radiation of almost same nature as light but having shorter wavelength of 0.5 to 2.5 Å regions. X-rays occupy the region between gamma and ultraviolet rays in the entire spectrum.

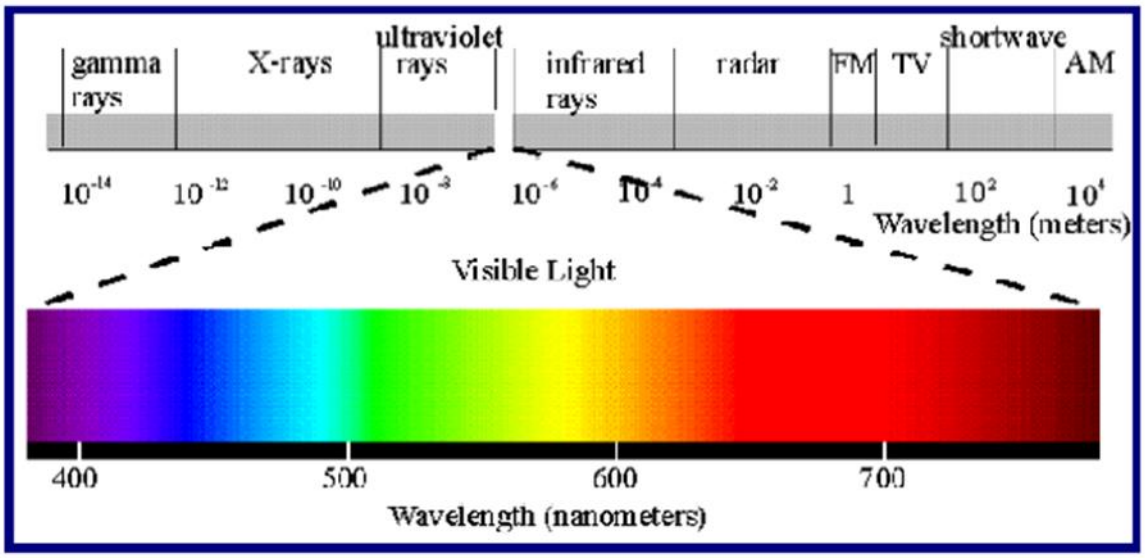

Figure 3.5: Illustration of electromagnetic spectrum

Diffraction is a scattering phenomenon in which a large number of atoms participate and act as scattering center. X-rays scattered by the atoms which are periodically arranged in the lattice, have definite phase relationship in between them. In some scattering direction, destructive interference takes place but, in few directions, constructive interference occurs and forms the diffracted beam. **"A diffracted beam may be defined as a beam composed of a large number of scattered rays mutually reinforcing one another."**

- **Working Principle:**

In XRD, a collimeter beam of X-rays is incident on a specimen and is diffracted by the crystalline phases in the specimen. Using Bragg equation for first order diffraction, lattice spacing may be found from the diffraction angles. Bragg's law is the basic law which governs the X-ray diffraction technique of structural analysis. In Bragg's law, the interaction between x-rays and the electrons of the atoms is described as a process of reflection of x-rays by the atomic planes. When mono chromatic x-rays incident on the atoms in the crystal lattice, atomic

planes allow a part of x-rays to pass through and reflect the other part, there exist a path difference in between the reflected rays from plane 1 and plane 2. These rays will reinforce each other, only when this path difference is equal to an integral multiple of the wavelength.

The ***Bragg's law*** can be written as:

$$2d\sin\theta = n\lambda$$

Where **n** is an integer and **λ** is the wavelength of the x-rays used, **θ** is Bragg angle and **d** is the interplanar spacing.

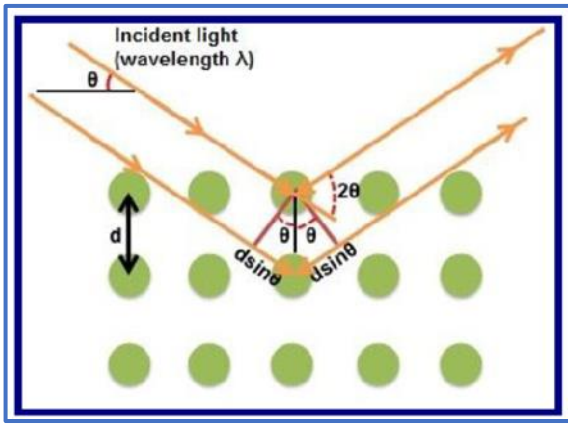

Fig 3.6. Illustration of bragg's law of Diffractometer

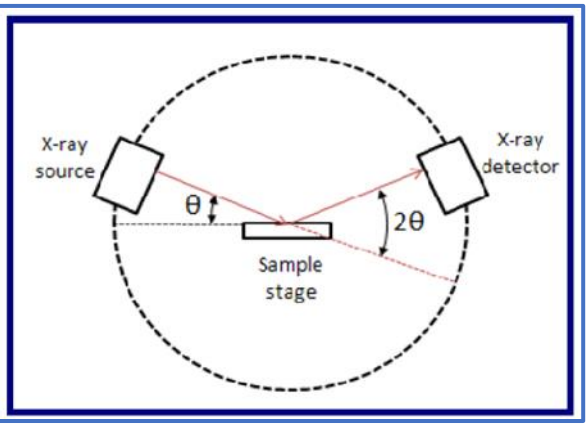

Fig 3.7. Schematic of X-Ray

- **Applications:**

a) Measurement of interplanar spacing between two atomic planes.

b) Determination of orientation of single crystal.

c) Determination of crystal structure for an unknown material.

d) Measurement of particle size, phase and internal stress etc.

A RigakuUltima III X-ray diffractometer was used for recording the diffraction pattern of the samples in θ-2θ configuration with Cu Kα radiation (λ =1.5404 Å) operated at 40 KV voltage and 30 mA current. A photographic image of X-ray diffractometer is shown in **Fig 3.8**

Figure 3.8: Experimental set up of X-Ray Diffractometer

3.2.2. Field Emission Scanning Electron Microscope (FESEM):

An FESEM is microscope instead of light it works with electrons, liberated by a field emission source.

1. **Principle:**

Under vacuum, electrons generated by a Field Emission Source are accelerated in afield gradient. The beam passes through Electromagnetic Lenses, focusing onto the specimen. As result of this bombardment different types of electrons are emitted from the specimen. A detector catches the secondary electrons and an image of the sample surface is constructed by comparing the intensity of these secondary electrons to the scanning primary electron beam. Finally, the image is displayed on a monitor. A FESEM is used to visualize very small topographic details on the surface or entire or fractioned objects. Researchers in biology, chemistry and physics apply this technique to observe structures that may be a ssmall as 1 nanometer (= billion of a millimeter). The FESEM may be employed for example to study organelles and DNA material in cells, synthetical polymers, and coatings on microchips.

2. Preparation:

In order to be observed with SEM objects are first made conductive for current. This is done by coating them with an extremely thin layer (1.5 - 3.0 nm) of gold or gold palladium. Further on, objects must be able to sustain the high vacuum and should not alter the vacuum, for example by losing water molecules or gasses. Metals, polymers and crystals are usually little problematic and keep their structure in the SEM. Biological material, however, requires a prefixation, e.g. with cold slush nitrogen (cryo-fixation) or with chemical compounds. This particular microscope is for seen of a special cryo-unit where frozen objects can be fractured and coated for direct observation in the FESEM. Chemically fixed material needs first to be washed and dried below the critical point to avoid damage of the fine structures due to surface tension. Coating is then performed in a separate device.

Source of electrons:

In standard electron microscopes electrons are mostly generated by heating a tungsten filament by means of a current to a temperature of about 2800°C. Sometimes electrons are produced by a crystal of lanthanum hexaboride (LaB6) that is mounted on a tungsten filament. This modification results in a higher electron density in the beam 81 and abetter resolution than with the conventional device. In a field emission (FE) scanning electron microscope no heating but a so-called "cold" source is employed. An extremely thin and sharp tungsten needle (tip diameter 10–7 –10-8 m) functions as a cathode in front of a primary and secondary anode. The voltage between cathode and anode is in the order of magnitude of 0.5 to 30 KV. Because the

electron beam produced by the FE source is about1000 times smaller than in a standard microscope, the image quality is markedly better. As field emission necessitates an extreme Vacuum (10-8Torr) in the column of the microscope, a device is present that regularly decontaminates the electron source by a current flash. In contrast to a conventional tungsten filament, a FE tip last theoretically for a lifetime, provided the vacuum is maintained stable.

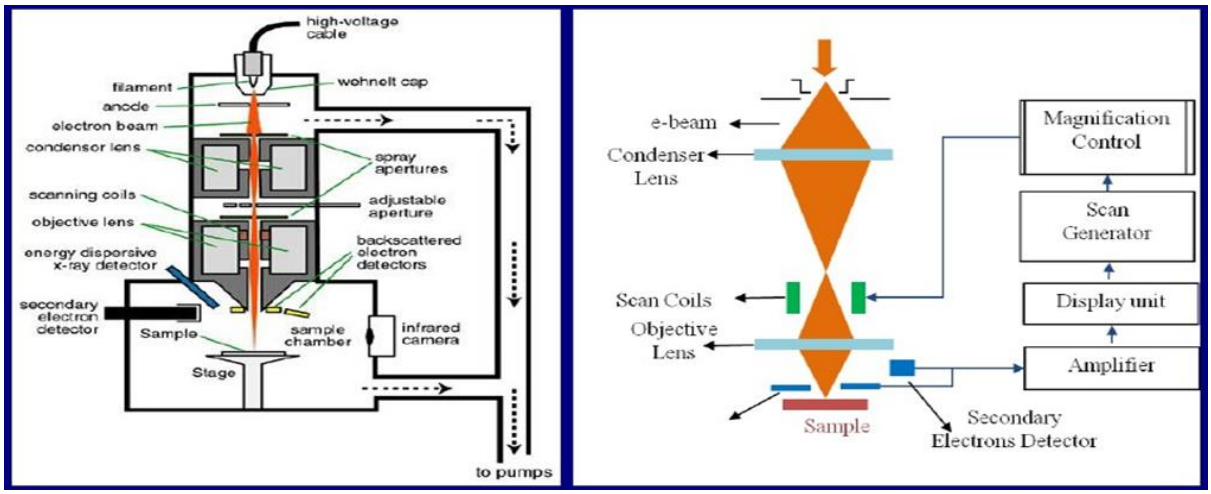

Fig 3.9 Configuration of FESEM and its different components

- **Condenser lens:**

The current in the condenser determines the diameter of the beam: a low current result in a small diameter, a higher current in a larger beam. A narrow beam has the advantage that the resolution is better, but the disadvantage that the signal to noise ratio is worse. The situation is reversed when the beam has a large diameter. The condenser lens is consisting mostly out of two parts.

- **Scan coils:**

The scan coils deflect the electron beam over the object according to a zigzag pattern. The formation of the image on the monitor occurs in synchrony with this scan movement. The scan velocity determines the refreshing rate on the screen and the amount of noise in the image. Scan coils often consist of upper and lower coils, which prevent the formation of a circular shadow at low magnification.

- **The objective lens:**

The objective lens is the lowest lens in the column. The objective focuses the electron beam

on the object (see FOCUS in the virtual FESEM). At a short working distance (object in a higher position, that is closer to the objective lens) the objective lens needs to apply a greater force to deflect the electron beam. The shortest working distance produces the smallest beam diameter, the best resolution, but also the poorest depth of field. (The depth of field indicates which range in vertical direction in the object can still be visualized sharply).

- **The stigmator coils:**

The stigmator coils are utilized to correct irregularities in the x and y deflection of the beam and thus to obtain a perfectly round-shaped beam. When the beam is not circular, but ellipsoidal, the image looks blurred and stretched (see ALIGN X Y in the virtual FESEM).

- **Object chamber:**

After the object has been covered by a conductive layer (see preparation) it i smounted on a special holder. The object is inserted through an exchange chamber into the high vacuum partof the microscope and anchored on a moveable stage. In the virtual FESEM the object can be moved in horizontal and vertical direction on the screen by operating the arrows in the POSITION box. In the real microscope the object can be repositioned in the chamber by means of a joy stick that steer in left right axis, or forward and backward. In addition, the object can be tilted (e.g., for stereo views), rotated and moved in Z direction (= closer or further away to the Objective lens). The “secondary electron emission” detector (scintillator) is located at the rear of the object holder in the chamber.

- **Image formation:**

When the primary probe bombards the object, secondary electrons are emitted from the object surface with a certain velocity that is determined by the levels and angles at the surface of the object. The secondary electrons, which are attracted by the Corona, strike the scintillator (fluorescing mirror) that produces photons. The location and intensity of illumination of the mirror vary depending on the properties of the secondary electrons. The signal produced by the

scintillator is amplified and transduced to a video signal that is fed to a cathode ray tube in synchrony with the scan movement of the electron beam. The contrast in the "real time" image that appears on the screen reflects the structure on the surface of the object. Parallel to the analog image, a digital image is generated which can be further processed.

Fig 3.10 FESEM (Hitachi S-4800) SET UP

3.2.3. Ultraviolet Visible Spectrophotometer:

UV spectroscopy is type of absorption spectroscopy in which light of ultra violet region (200-400 nm) is absorbed by the molecule. Absorption of the ultraviolet radiations results in the excitation of the electrons from the ground state to higher energy state. The energy of the ultraviolet radiation that are absorbed is equal to the energy difference between the ground state and higher energy states ($\Delta E = h\upsilon$).

There are two laws that govern the absorption of light by a medium, known as Lambert's law and Beer's law. Lambert's law predicts that the absorbance is directly proportional to the thickness/path length of the medium. Beer's law explains the effect of concentration of colored components in solution on light transmission or absorption. By combining of these two laws, we get Lambert- Beer's law which is as follows:

$$\log (I0/It) = A = \alpha cd$$

Where, A denotes absorbance, α denotes molar absorptivity, c is concentration and d is path length. From the Lambert-Beer's law it is clear that greater the number of molecules capable of absorbing light of a given wavelength, the greater the extent of light absorption. That is the basic principle of UV spectroscopy.

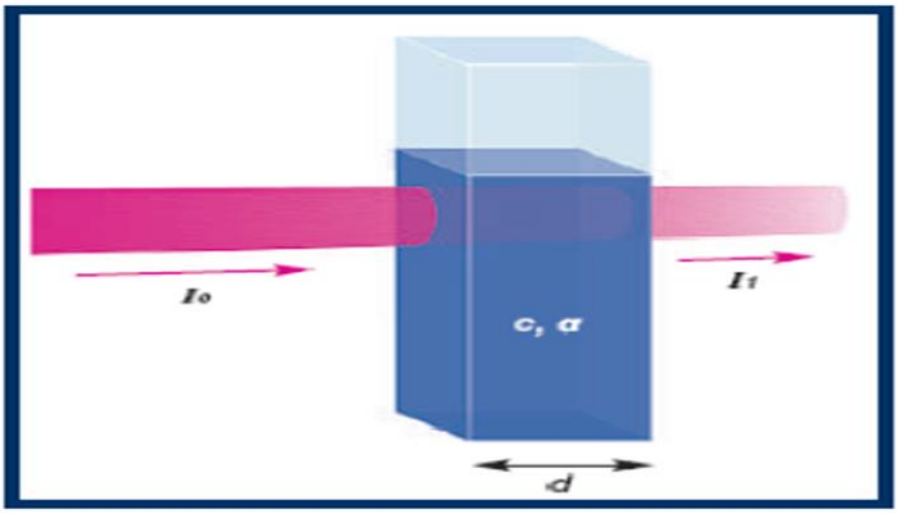

Fig 3.11: Lambert-Beer's law

- **Configuration of instrument:**

A spectrophotometer is an instrument which measures the transmittance or absorbance of a sample as a function of the wavelength of electromagnetic radiation. The main components of a spectrophotometer are:

1. Source

2. Monochromator

3. Sample container

4. Detectors

1. **Source:**

The ideal light source would yield a constant intensity over all wavelengths with low noise and long-term stability. Unfortunately, however, such a source does not exist. Two sources are commonly used in UV-visible spectrophotometers. The electrical excitation of deuterium or hydrogen at low pressure produces a continuous UV spectrum. The mechanism for this involves formation of an excited molecular species, which breaks up to give two atomic species and an ultraviolet photon.

Deuterium lamps emit radiation in the range 160-375 nm. Quartz windows must be used in these lamps, and quartz cuvettes must be used, because glass absorbs radiation of wavelengths less than 350 nm. The tungsten filament lamp is commonly employed as a source of visible light. This type of lamp is used in the wavelength range of 350-2500 nm.

1. **Monochromator:**

All monochromators contain certain components like entrance slit, collimating mirrors, dispersing device (usually a prism or a grating), focusing mirrors and exit slit. Polychromatic radiation (radiation of more than one wavelength) enters the monochromator through the entrance slit. The beam is collimated, and then strikes the dispersing element at an angle. The beam is split into its component wavelengths by the grating or prism. By moving the dispersing element or the exit slit, radiation of only a particular wavelength leaves the monochromator through the exit slit.

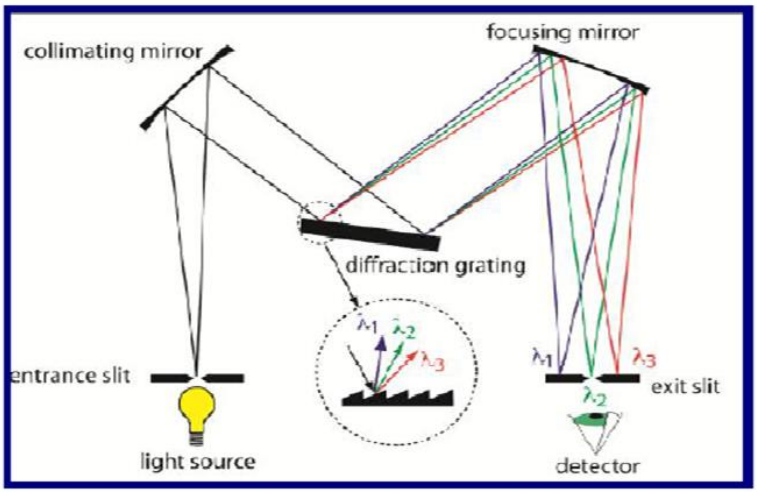

Fig 3.12: Constructions of monochromator

1. **Sample container:**

The containers (***cuvettes***) for the sample and reference solution must be transparent to the radiation which will pass through them. Quartz or fused silica cuvettes are required for spectroscopy in the UV region. These cells are also transparent in the visible region.

2. **Detector:**

A detector converts a light signal into an electrical signal. The photomultiplier tube is commonly used detector in UV-Vis spectroscopy. It consists of *photoemissivecathode* (a cathode which emits electrons when struck by photons of radiation), several *dynodes* (which emit several electrons for each electron striking them) and an *anode*. Another type of detector is linear photodiode array which is an example of a *multichannel photon detector*. These detectors are capable of measuring all elements of a beam of dispersed radiation simultaneously. Photodiode arrays are complex devices but, because they are solid state, have high reliability.

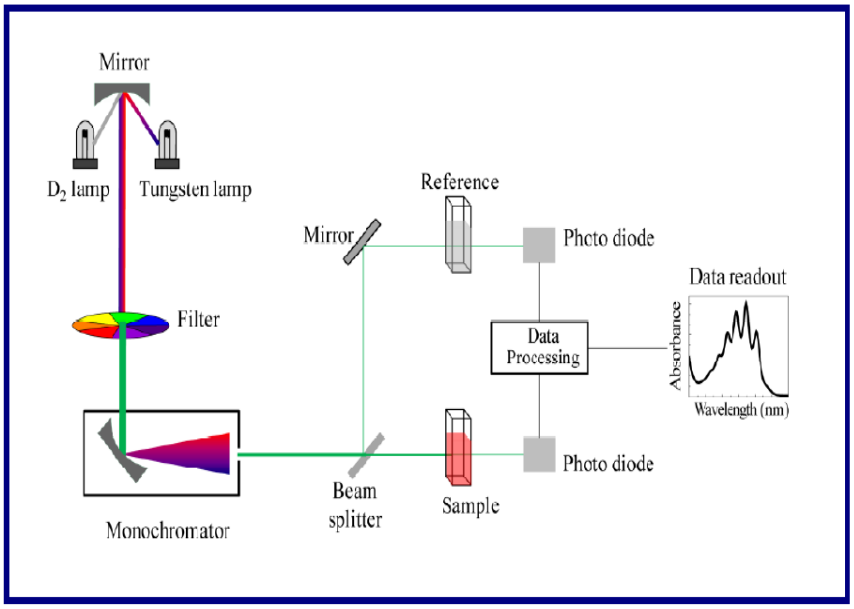

Fig 3.13: Configuration of Uv-Visible spectrophotometer.

Fig 3.14: Experimental set up of UV-Visible spectrophotometer.

3.2.4. Energy Dispersive Analysis of X−rays (EDAX):

- **Basic Principle:**

EDAX is an analytical technique used for elemental analysis or chemical characterization of a sample. It is based on the investigation of a sample through interactions between electromagnetic radiation and matter, analyzing X−rays emitted by the matter in response to being hit with the electromagnetic radiation. Its characterization capabilities are due in large part to the fundamental principle that each element has a unique atomic structure allowing X−rays that are characteristic of an element's atomic structure to be identified uniquely from each other.

To stimulate the emission of characteristic X−rays from a specimen, a high energy beam of charged particles such as electrons or a beam of X−rays, is focused with the sample being studied. At rest, an atom within the sample contains ground state (or unexcited) electrons in discrete energy levels or electron shells bound to the nucleus. The incident beam may excite an electron in an inner shell, ejecting it from the shell while creating an electron hole where the electron was. A position vacated by an ejected inner shell electron is eventually occupied by a higher energy electron from an outer shell and the difference in energy between the higher energy shell and the lower energy shell may be released in the form of an X−ray. The amount

of energy released by the transferring electron depends on which shell it is transferring from, as well as which shell it is transferring to. The number and energy of the X−rays emitted from a specimen can be measured by an energy dispersive spectrometer. As the energy of the X−ray is characteristic of the difference in energy between the two shells, and of the atomic structure of the element from which they were emitted, this allows the elemental composition of the specimen to be measured.

- **Experimental Set Up:**

Fig. 3.15 shows an experimental arrangement of EDAX attached to an SEM. It consists of four primary components:

1.Beam source

2. X−ray detector

3. Pulse processor

4. Analyzer

EDAX systems are most commonly found on scanning electron microscopes and electron microprobes. Scanning electron microscopes are equipped with a cathode and magnetic lenses to create and focus a beam of electrons. The energy of the electron beam has to be selected to give a compromise between the requirements of resolution and X−ray production efficiency. The X−radiation excited in the specimen was analyzed in two fully focusing crystal spectrometers. The EDS X−ray detector measures the relative abundance of emitted X−rays versus their energy. The detector is typically lithium drifted silicon, solid state device. When an incident X−ray strikes the detector, it creates a charge pulse that is proportional to the energy of X−ray. The charge pulse is converted to a voltage pulse by a charge−sensitive preamplifier. The signal is then sent to a multichannel analyzer where the pulses are sorted by voltage. The energy, as determined from the voltage measurement, for each incident X−ray is sent to a computer for display and further data evaluation. The spectrum of X−ray energy versus counts is evaluated to determine the elemental composition of the sample volume.

Elements of low atomic number are difficult to detect by EDAX. The Si (Li) detector is often protected by a Beryllium (Be) window. The absorption of the soft X−rays by the Be precludes the detection of elements below an atomic number of 11 (Na). In windowless systems, elements

with as low atomic number as 4 (Be) have been detected, but the problems involved get progressively worse as the atomic number is reduced **[1−2]**.

Fig 3.15: Experimental set up of Energy dispersive analysis of X−rays (EDAX).

3.2.5 Transmission electron microscope (TEM):

- **Basic Principle:**

Transmission electron microscopy (TEM) is a technique used for analyzing the morphology, defects, crystallographic structure, particle size and even composition of a specimen. In this technique a beam of electrons is transmitted through an ultra thin specimen, interacting with the specimen as it passes through. An image is formed from the interaction of the electrons transmitted through the specimen; the image is magnified and focused onto an imaging device, such as a fluorescent screen, on a layer of photographic film, or to be detected by a sensor such as a CCD camera. The transmission electron microscope (TEM) operates on the same basic principles as the light microscope but uses electrons instead of light. What you can see with a light microscope is limited by the wavelength of light. TEM use electrons as "light source" and their much lower wavelength make it possible to get a resolution a thousand times better than with a light microscope.

TEMs are capable of imaging at a significantly higher resolution than light microscopes, owing to the small De Broglie wavelength of electrons. This enables the instrument's user to examine fine detail even as small as a single column of atoms, which is ten thousands of times smaller

than the smallest resolvable object in a light microscope. TEM forms a major analysis method in a range of scientific fields, in both physical and biological sciences. TEMs find application in cancer research, virology, materials science as well as pollution and semiconductor research. At smaller magnifications TEM image contrast is due to absorption of electrons in the material, due to the thickness and composition of the material. At higher magnifications complex wave interactions modulate the intensity of the image, requiring expert analysis of observed images. Alternate modes of use allow for the TEM to observe modulations in chemical identity, crystal orientation, electronic structure and sample induced electron phase shift as well as the regular absorption-based imaging.

- **Experimental Set Up:**

TEM offers two methods of specimen observation-

1. Image mode

2. Diffraction mode

In image mode, the condenser lens and aperture will control electron beam to hit the specimen, the transmitted beam will be focused and enlarged by objective and projector lens and form the image in the screen, with recognizable details related to the sample microstructure. In diffraction mode, an electron diffraction pattern is obtained on the fluorescent screen, originating from the sample area illuminated by the electron beam. The diffraction pattern is entirely equivalent to an X−ray diffraction pattern. A single crystal will produce a spot pattern on the screen and polycrystal will produce a powder or ring pattern.

The microstructure, e.g. the grain size, and lattice defects are studied by use of the image mode, while the crystalline structure is studied by the diffraction mode.

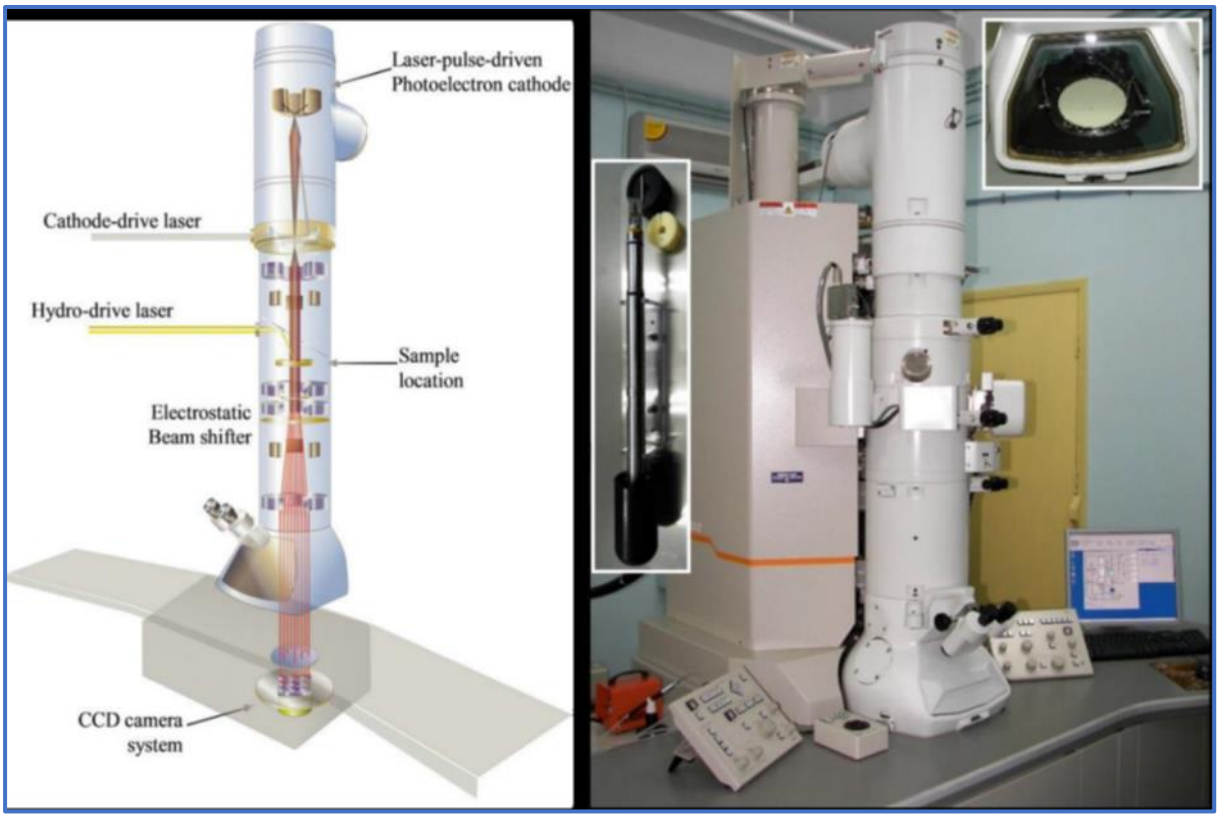

Figure 3.16 Left: Layout of optical components of basic TEM instrument.

Right: JEOL JEM-2100 HRTEM

- **Restrictions on samples:**

Sample preparation for TEM generally requires more time and experience than for most other characterization techniques. A TEM specimen must be approximately 1000 A^{o} or less in thickness in the area of interest. The entire specimen must fit into a 3 mm diameter up and be less than about 100 microns in thickness. A thin, disc shaped sample with a hole in the middle, the edges of the hole being thin enough for TEM viewing, is typical. The initial disk is usually formed by cutting and grinding from bulk or thin film/substrate material, and the final thinning done by ion milling. Other specimen preparation possibilities include direct deposition onto a TEM-thin substrate (Si3N4, carbon); direct dispersion of powders on such a substrate; grinding and polishing using special devices like tripod; chemical etching and electro-polishing; and lithographic patterning of walls and pillars for cross-section viewing. A focused ion beam (FIB) may be used to make cross-sections; however this capability is not currently available at HUJ.

- **Applications:**

  a. **Morphology**

The size, shape and arrangement of the particles which make up the specimen as well as their relationship to each other on the scale of atomic diameters.

b. Crystallographic Information

The arrangement of atoms in the specimen and their degree of order, detection of atomic scale defects in areas a few nanometers in diameter.

c. Compositional Information (if so equipped)

The elements and compounds, the sample is composed of and their relative ratios, in areas a few nanometers in diameter.

3.2.6. X-Ray Photoelectron Spectroscopy(XPS):

X-Ray Photoelectron Spectroscopy is one of the most powerful surface analytical techniques capable to provide accurate qualitative elemental analysis (for all elements except hydrogen and helium), quantitative composition and determination of chemical state such as binding and oxidation can also be done. The information should be originated within ~10 nm from the outer surface.

- **Principles of XPS:**

XPS is based on the photoelectric effect which is discovered by Hertz in 1887. In this case, electron emission from the surface is resulted due to the interaction of an x-ray photon of sufficient energy with the solid surface. The applied x-ray of 1-15 KeV energy is capable to induce electrons not only from the outer shells but also from the core levels of all elements of periodic table. The governing equation of this phenomenon is as follows:

$$h\nu = E_b + E_{kin} + W_f$$

Where, $\mathbf{E_b}$ is binding energy, $\mathbf{E_{kin}}$ is kinetic energy of photoelectron, $\mathbf{W_f}$ is work function of the instrument.

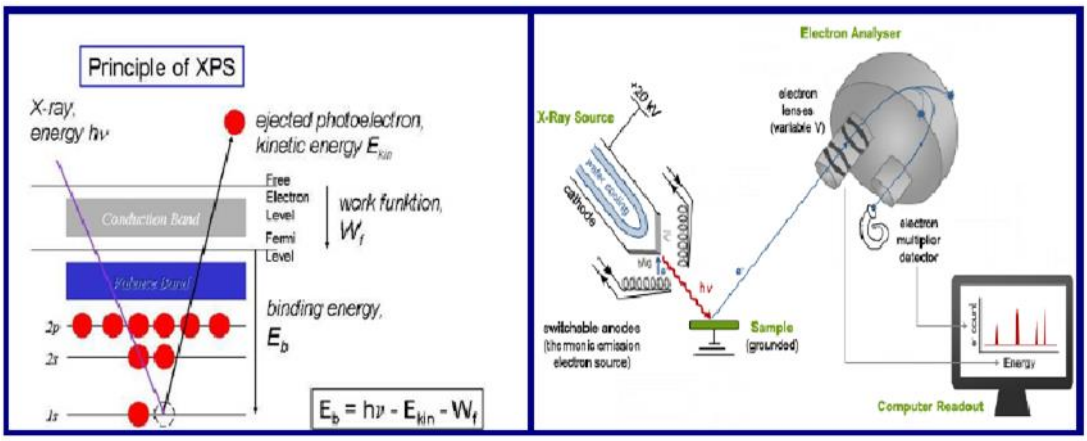

Fig 3.17: Basic principles and constructions of XPS.

- **Configuration of XPS instrument:**

The experimental set up contains mainly the following parts: (i) an X-ray source for XPS, (ii) an electron energy analyzer, combined with a detection system and (iii) a sample stage, all contained within a vacuum chamber. As for most techniques, the system is operated and controlled by a computer, usually provided with software allowing mathematical treatment as shown in Fig 3.18.

- **X-ray source:**

Since XPS is concerned with the analysis of core electrons from a solid surface, sources used in XPS must be able to produce photons of a sufficient energy to access a suitable number of core electron levels. Photons of this energy lie within the X-ray region of the electromagnetic spectrum. As a result, these are otherwise referred to as X-rays. X-ray tubes produce X-rays by directing a sufficiently energetic electron beam at some metallic solid. This metallic object is referred to as the X-ray anode, with the electron source being the cathode. Although any solid can in principle be used as an X-ray anode, Al has become that most commonly used in XPS due to the relatively high energy and intensity of Al-*K*α X-rays, the minimal energy spread of Al-*K*α X-rays and the fact that Al is an effective heat conductor.

- **Electron energy analyzer:**

Since information in XPS is derived from the *Ekin*of the electron emissions, effective analysis requires energy filter that exhibits both a high-energy resolution and a high transmission. The

former allows for the separation of closely spaced peaks, thereby optimizing speciation identification capabilities, while the latter allows for sensitivity to be maximized. The two primary energy filter configurations used in XPS named **Cylindrical Mirror Analyzer (CMA), Concentric HemisphericalAnalyzer (CHA).**

- **Detector:**

In XPS, it is not only important to measure the energy of the electron emissions but also the number of electrons produced. XPS spectra is plotted in units of energy versus intensity, with the energy defined by the energy analyzer used and the intensity defined by the number of electrons recorded by the detector. To obtain the best possible sensitivity, the detector must be capable of recording individual electrons, that is, operating in pulse counting mode. This signal is recorded in units of current (A), which are then represented in units of counts per second.

- **Sample stage:**

The mounting of the samples on the sample holder should be done in such a way that electrical conduction is guaranteed. This is achieved by using metallic clips or bolt-down assemblies. Alternatively a metal loaded tape may also be used. In the case of powders, the particles can be pressed into an indium foil or carbon tape.

- **Vacuum requirement:**

As XPS is a surface sensitive method, impurities can play a major role in the observed spectra. The criterion is that a good vacuum is needed to maintain the integrity of the surface. In general, 10^{-5}Torr is sufficient to allow the photoelectron to reach the detector without suffering collisions with other gas molecules. On the other hand, 10^{-9}Torr or lower is required to keep an active surface clean for more than several minutes. So, 10^{-8}-10^{-9}Torr provides a reasonable pressure range for XPS measurement. Sample analysis was performed on the SPECS with hemispherical energy analyzer (HAS 3500). Photoelectrons were excited using the monochromatic Mg Kα X-ray (1253.6 eV) or Al Kα X-ray (1486.6 eV) was used as the excitation source operated at 10 kV and with an anode current 17 mA. The photograph of the X-ray photoelectron spectroscopy is shown in the Fig 3.18.

Fig 3.18: Experimental set up of XPS

3.2.7. IV Characterization Apparatus:

IV setup as precision source/Measure Unit (SMU, KEYSIGHT B2902A) is used to measure current-voltage characteristics of any electronics device more accurately. It is also used to determine forward and reverse bias IV characteristics as well as leakage current measurement. SMU combines of a current source, a voltage source, a current meter, a voltage meter along with the capability to switch easily between these various functions into a single instrument.

An SMU is a precision power sourcing instrument that provides voltage sourcing and measurement resolution at or below 1 mV as well as current sourcing and measurement resolution below 1 μA. In addition, SMUs offer remote-sense capability and a four-quadrant output that incorporates both bipolar voltages and the ability to sink power. Finally, SMUs are optimized for sweeping both current and voltage to determine the IV characteristics of a device. As a result, SMUs have been widely adopted, especially in the semiconductor industry and are a common component in many automated test systems.

Virtually all research, design, development, and production applications require an instrument that can source power to a device that is being developed or tested. Many of these applications also require the ability to monitor the voltage and current being consumed by the device to characterize device behavior or to test for proper operation. Often, you can meet both of these requirements with a single programmable power supply that sources either a constant voltage or constant current as well as reads back the associated current or voltage. In these applications, milliamp sensitivity in current measurement often suffices.

Other applications require sourcing and measuring with more precision than you can find on a typical programmable power supply. For instance, consider ubiquitous electronic devices for which every μamp of current drawn reduces battery life. Manufacturers often need to characterize these devices during production for power draw in a variety of states. For these situations, a high-precision power supply offering μamp-level sensitivity works well.

Certain applications are especially demanding and require even higher precision and specific features. Semiconductor validation and characterization is an example of an application that requires current sensitivity into the nanoamp range and below. In addition, the demand for m a traditional programmable power supply insufficient. For these situations, where precision low-level sourcing and measuring is needed, a source measure unit (SMU) is the best choice. ore precision, higher speed, remote sensing of voltage and four-quadrant outputs can render.

This SMU connects to PC via IV measurement software by a LAN connection. This IV measurement software is used to measure a variety of function such as sweep measurement, sampling measurement, graphical display functions. It also have an ability to save test result into CSV file. Figure 3.19 shows the Photograph of SMU (KEYSIGHT B2902A) instrument with display of IV measurement software.

Fig. 3.18. The Keysight B2902A SMU at Thin Film and Nano Science Lab, JU

3.2.8 High Voltage DC power Supply:

In field emission instrument D.C voltage is applied between the cathode (sample under test) And the anode. For this experiment a 5 KV-0.5 A DC regulated power supply unit (model NTPL/91/03-04), which is manufactured by Neo Tele-Tronix Pvt.ltd, calcautta is used. The

input to the unit is 230V, 50 Hz, 1 Ph, AC supply and output is continuously vary from 0 to 5KV.

3.2.9. Electrometer, Multimeter:

Keithley electrometer (Model 671 and 6517A) is used to measure current voltage characteristics of the samples. The range of the voltage and current are ± 1000v and ± 1pA to ± 20mA respectively. Another Keithley electrometer (Model 6514) is used to measure field emission current range ±100nA to ±21 mA. Also several multimeter (RISH MULTI 15 S) are used during the experiment.

3.2.9 Fourier transform infrared spectroscopy (FTIR):

FTIR Spectroscopy, fourier-transform infrared spectroscopy, is concerned with the vibration of molecules. Each functional group has its own discrete vibrational energy which can be used to identify a molecule through the combination of all of the functional groups. This makes FTIR microscopy ideal for sample ID, multilayer film characterization, and particle analysis.

The electromagnetic spectrum consists of different regions corresponding to different energy (E), frequency (ν), and wavelength (λ) ranges as seen in Figure 1. The unit for near-, mid-, and far-infrared, the wavenumber (cm^{-1}), is derived from the inverse relationship between wavelength and frequency.

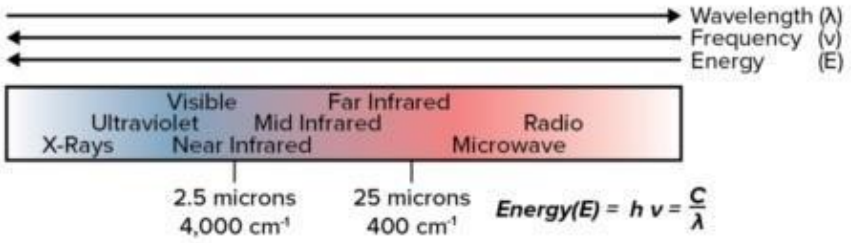

Fig. 3.12- Electromagnetic spectrum showing near and far infrared regions.

FTIR spectroscopy takes advantage of how IR light changes the dipole moments in molecules that correspond to a specific vibrational energy. Vibrational energy corresponds to two

variables: reduced mass (μ) and bond spring constant (k). For k constant, we can look at C-C, C=C, and C≡C showing an increase of 800 cm^{-1} across the series. Substituting atoms in a C-C bond with nitrogen and oxygen causes a shift of 100 cm^{-1}. By looking at the two series, it can be seen that bond strength alters the wavenumbers more than mass.

Since every functional group is composed of different atoms and bond strengths, vibrations are unique to functional groups, and classes of functional groups (e.g. O-H and C-H stretches appear around 3200 cm^{-1} and 2900 cm^{-1}, respectively). A correlation chart with various functional group vibrations can be seen. Since the collection of vibrational energy bands for all of the functional groups a molecule is unique to every molecule, these peaks can be used for identification using library searches of comprehensive sample databases.

Working principle and different parts of FTIR

The three major parts of an FTIR are the source, interferometer, and detector The source is typically a broadband emitter such as a mid-IR ceramic source (50-7,800 cm^{-1}), a near-IR halogen lamp (2,200 – 25,000 cm^{-1}), or a far-IR mercury lamp (10-700 cm^{-1}). The interferometer is the heart of FTIR and consists of a beam-splitter, a stationary mirror, a moving mirror, and a timing laser (box in figure 4). The beam-splitter splits the light from a source into two paths with half the light going to a stationary mirror and the other half going to a moving mirror. In many FTIR systems, the beam-splitter is placed at 45 degrees to the incident beam, but for high throughput applications, a low angle interferometer is preferred as the P and S polarizations converge close to the Brewster's Angle. Common beam-splitter materials are KBr (375 – 12,000 cm^{-1}) for mid-IR, Quartz (4,000 – 25,000 cm^{-1}) for near-IR, and Mylar (30 – 680 cm^{-1}) for far-IR. The beams from the moving and stationary mirrors are recombined back at the beam-splitter and steered toward the sample. The difference in the path of the mirrors causes constructive and destructive interference over the course of time it takes for the moving mirror to make a pass. The signal versus mirror position (and, thus, time) is called an interferogram. A laser is used to determine the position of the moving mirror using the precisely known wavelength of the laser (Figure 5). He-Ne lasers are the industry norm due to their excellent wavelength stability compared to solid-state or diode lasers. This laser stability allows for spectral additions, library searches, and other functions that need high wavenumber accuracy.

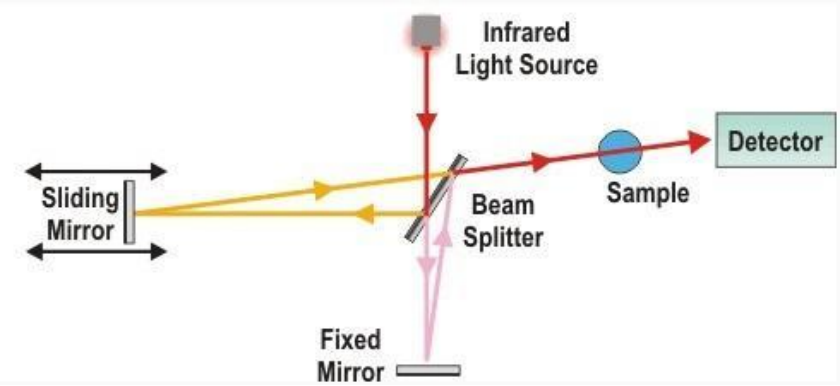

Fig. 3.13- Different parts and working of FTIR spectroscopy

Apparatus for synthesis of $CsCucl_3$.

- The surface morphology of the films was examined using Field Emission Scanning Electron Microscope (FESEM: HITACHI S-4800).
- X-ray diffraction analysis was performed by employing Bruker D8 diffractometer with Cu-Kα radiation of wavelength 1.5404 Å.
- FT-IR spectrum was recorded in shimadzu IRprestige-21 spectrometer.
- Dielectric behavior and impedance spectra were monitored using Agilent 4294A precision impedance analyser.
- Electrical polarization hysteresis curves (P-E loop) were obtained from the Precision Premier II ferroelectric tester of Radiant Technologies, Inc. using standard bipolar waveform.
- To detect output voltage, a digital storage oscilloscope (KEYSIGHT InfiNiiVision DSOX2012A, Digital storage oscilloscope, 100 MHz, 2 GSa/s, input impedance 1 M) was directly connected with the nanogenerator, whereas the piezoelectric current was calculated from the voltage across a known load resistance (RL) connected in series with nanogenerator.

Chapter 4

Highly Efficient and Flexible Piezoelectric Nanogenarator based on Lead free Perovskite Modified Self-Poled Poly (vinylidene fluoride) composite

Abstract

Piezoelectric nanogenerators (PNGs) have emerged as a practical energy alternative for the development of self-powered electronic systems and miniaturized power sources for small-scale wearable/portable devices. PNGs scavenge electric power at ambient from biomechanical movements and mechanical vibrations. Here, composite films made of polyvinylidene fluoride (PVDF) and cesium copper chloride (CsCuCl3) transform into a useful functional material for piezoelectric-based mechanical energy harvesters. The synthesized composite possesses high crystallinity and electroactive phase fraction of 92%. A noteworthy output performance was demonstrated by a piezoelectric nanogenerator (PNG) under a repetitive applied force. The concertation of perovskite filler plays a significant role in composites polymer to achieve benchmark level output responsiveness. An instantaneous output voltage and current of 230 V and 13 μA were displayed by PNG made with 4 wt%$CsCuCl_3$ in PVDF. Additionally, it demonstrated endurance under demanding circumstances and long cycle stability (1,000 cycles). Additionally, power from the PNG was used to power industrial LEDs and charge a capacitor. The results that were obtained are quite significant and reveal the viability of developing revolutionary smart devices employing this class of perovskites.

INTRODUCTION

Nowadays mankind is effortlessly reliant on non-renewable energy like fossil fuels, however, the repository of these sources is bounded in the earth. As a result of the diminishing of these fossil fuels, the prices are rising continuously, the majority of the non-sustainable energies emit CO_2 gas as a by-product which is a terrible impact on climate change and the human body, persistently contaminated in the environment. Conquering these issues, researchers continue to work on eco-friendly harvesting energies like solar energy, geothermal energy, Hydro energy, etc. But still, among the discoveries of research of renewable energy,

nanogenerator is excellent, this is minimal expenses, portable compare to other mechanical harvesting energies. Z. L. Wang and L. Sang first introduced the nanogenerator in 2006 [1]. Nanogenerator is a small size and light weighted device which converts into electricity by giving pressure or rubbing two materials, either giving the temperature to a specific material or delivering some sort of electromagnetic force between two materials that assist to create power. Nanogenerators can be partitioned into several parts – piezoelectric nanogenerator, triboelectric nanogenerator, pyroelectric nanogenerator, thermoelectric nanogenerator, electromagnetic nanogenerator, etc. Among the different piezoelectric materials, Piezoelectric polymers have great attention in energy harvesting applications due to flexibility and durability. Furthermore, PVDF is one of the best piezo-polymer which exhibits at least four distinct polymorphs, viz. α, β, γ, and δ phases, and the β phase has the largest dipole moment per unit volume and is the most sought-after phase for energy-harvesting applications [2]. Impregnation of the polymer matrix by perovskite is extremely tempting to promote more electroactive β-phase development and enhance PVDF's dielectric characteristics. The majority of systems have adopted high-temperature processed perovskites, which have several limitations and compatibility issues for self-powering wearable electronics, despite the obvious progress reported in this regard. This leaves a huge window of opportunity for development in this field through low-temperature, cost-effective protocols [3]. Due to their distinctive optical and electrical properties, all-inorganic halide perovskites with the chemical formula ABX_3 (A and B are two separate cations, and X is a halide) have already established their dominance in a variety of application systems [4]. Because of their piezo- and ferroelectric responsiveness, these perovskites not only provided optical excellence but also significant piezoelectricity.

We have successfully used all inorganic chemically treated $CsCuCl_3$ within the PVDF matrix for mechanical energy harvesting in this experiment. The production of all-inorganic

halide perovskite-PVDF based nanogenerators was only previously presented in two papers. Nevertheless, both pieces are on $CsCuCl_3$ [3, 4]. Adding perovskite filler boosts the desired electroactive β phase while also enhancing the hybrid film's overall dielectric constant and crystallinity. Since the final performance of the device is heavily dependent on these characteristics, improvement of them provides a strong piezo response from the hybrid as compared to pure samples. To enhance device performance, the perovskite content in hybrids was also changed. The improved hybrid's desired electroactive β phase rose by >92%, or approximately 2.5 times, over the pure PVDF film. Under straightforward hand hammering, the constructed PNG based on 4 wt% $CsCuCl_3$ loadings produced an output voltage (230 V) and current (13 μA). Under various types of external stimuli, PNG energy harvesting was seen. Without any outside bias, PNG energy can power a variety of commercially available LEDs. Another significant problem, the lack of electricity needed to power the electronic gadgets we use every day in some locations, was solved with the use of optimized PNG [6]. Here, we developed a portable charger that stores energy at the expense of the steps we took while moving about. The voltage created across the PNG maintained under the shoe bottom was gathered by this gadget and stored in a battery that may be used later to recharge portable electronics whenever necessary. This work's flexible and wearable devices will offer a chance to transform our civilization into a smart one, notably in terms of biomechanical movement detection and effective PNG energy harvesting.

Experimental section:

Materials

copper chloride ($CuCl_2$), cesium chloride (CsCl), hydrogen chloride (HCl), hexane. PVDF pallets (Mw ≈ 275000 g/mol), N, N-dimethylformamide (DMF) (Sigma Aldrich), Acetone (Merck India).

$CsCuCl_3$ nanocube synthesis

The perovskite based powdered cesium copper chloride was prepared by dissolving 0.67g(0.5 mmol) of copper chloride (CuCl2) in 2.5 ml of hydrogen chloride at room temperature. After consummate dissolution of copper chloride,0.84g (0.5 mmol) of cesium chloride (CsCl) was added gradually. The conflation was stirred for 45 min to ascertain the completion of reaction. The precipitated was filtered and washed with ethanol.

Preparation of PVDF/$CsCuCl_3$ thin film

PVDF pallets were added in acetone (6 ml) and DMF (4 ml) mixture. Afterwards, as synthesized $CsCuCl_3$ with different concentration (1, 2, 3, 4 and 5 wt% (w/v)) was added to the above solution and stirred for 2 h at 70C. A white yellow colored, homogeneous solution was prepared which was further solution drop casted on pre-cleaned glass slides. These coated substrates were kept in vacuum at 65 C for overnight. Thereafter, films were peeled off from the glasses and used for device fabrication and various characterizations.

Fabrication of piezoelectric nanogenerator

To fabricate piezoelectric nanogenerator (PVCS), firstly a PET substrate and an aluminium (Al) sheet (bottom electrode) were glued together. As prepared films were then placed on the bottom Al electrode followed by another Al sheet (top electrode) attached with it. Two copper wires were then connected with top and bottom electrodes. The effective area of PVCS is 1×1 cm^2.

Characterization:

The surface morphology of the films was examined using Field Emission Scanning Electron Microscope (FESEM: HITACHI S-4800). X-ray diffraction analysis was performed by employing Bruker D8 diffractometer with Cu-Kα radiation of wavelength 1.5404 Å. FT-IR

spectrum was recorded in shimadzu IRprestige-21 spectrometer. Raman spectra were recorded in a WITec ALPHA300 RS confocal Raman spectrometer employing an Nd: YAG laser (532 nm). Dielectric behaviour and impedance spectra were monitored using Agilent 4294A precision impedance analyser. Electrical polarization hysteresis curves (P-E loop) were obtained from the Precision Premier II ferroelectric tester of Radiant Technologies, Inc. using standard bipolar waveform. To detect output voltage, a digital storage oscilloscope (KEYSIGHT InfiNiiVision DSOX2012A, Digital storage oscilloscope, 100 MHz, 2 GSa/s, input impedance 1 M) was directly connected with the nanogenerator, whereas the piezoelectric current was calculated from the voltage across a known load resistance (RL) connected in series with nanogenerator.

RESULTS AND DISCUSSION

XRD profile of the as synthesized $CsCuCl_3$, presented in Fig. 1a shows diffraction peaks at 2θ = 15.41°, 21.82°, 25.07°, 30.65°, 33.02° and 42.05°corresponds to (100), (103), (110), (200), (203) and (213) planes respectively. Such positioning of the peaks agrees well with literature and confirms orthorhombic phase formation of $CsCuCl_3$. Using the Full-prof programme, XRD data is cleaned up, and the outcome is shown in Fig. 1b. It demonstrates that the cubic lattice system $CsCuCl_3$ is a member of the Pm 3m space group. Lattice constant is estimated to be 5.91Å. The phase purity of the synthesised product is confirmed by this refining. The VESTA created a drawing of the $CsCuCl_3$ unit cell's crystal structure, which is seen in the inset (Fig. 1b). Fig. 1c shows a VESTA-drawn array of three-unit $CsCuCl_3$ cells along the X, Y, and Z axes. Fig. 1d shows the morphology of the produced product [20]. The main particles in this picture are cube-shaped with ragged edges. These cubes have an average side dimension of 50 nm. This picture also implies that the product is morphologically homogeneous on a wide scale over the scanned region. Cs, Cu, and Cl are the sole component elements found in the EDX spectrum of the $CsCuCl_3$ cubes shown in Fig. 1.d No further peaks

associated to any impurity elements are seen, further confirming the phase purity of $CsCuCl_3$ and correlating with the aforementioned XRD finding. The EDS examination determined the stoichiometric ratio of the component elements to be 19:20:61, which is likewise consistent with the earlier findings.

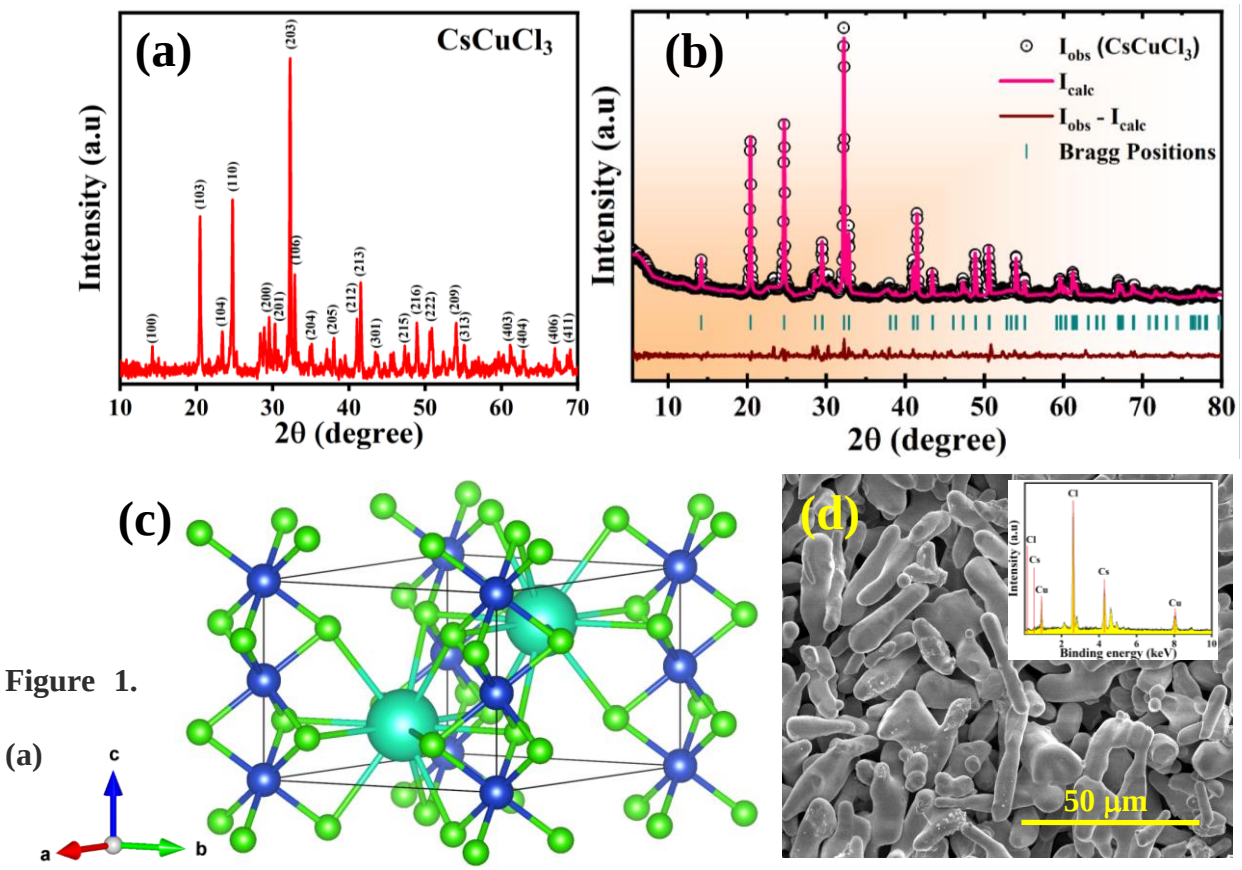

Figure 1.

XRD profile, (b) rietveld refinement, (c) crystal structure and (d) FESEM image of $CsCuCl_3$. (e) EDX image of $CsCuCl_3$

All of the samples underwent FTIR spectroscopy to determine if crystalline phases were present, and the findings are displayed in Fig. 2a. PVDF's non-polar α phase is indicated by the characteristics vibrational band at 1150, 976, 796, 764, 613, and 532 cm^{-1}, whereas the semi-polar β phase is shown by the characteristics band at 1234, 812 cm^{-1}. The required phase's

vibrational band peaks at 1279 cm^{-1}. In general, the low proportion of bare PVDF in the β phase restricts their use in energy harvesting applications. When used as filler in a PVDF matrix, $CsCuCl_3$ rods interact with the α phase chain to change it into the desired β phase. For bare PVDF, the absorption band strength of the typical peak of the -phase (Fig. 2a) is substantially greater, and it gradually reduced with the addition of $CsCuCl_3$ up to 4 wt% of $CsCuCl_3$. While the amount of $CsCuCl_3$ in the composite film increased, reaching a maximum of 4wt% of perovskites, the intensity of the band at 1279 cm^{-1} connected to phase

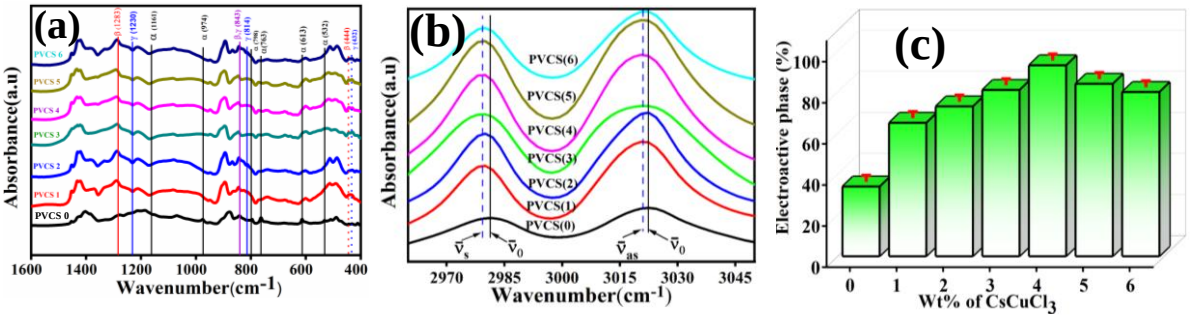

Figure:2 (a) FTIR spectra in the range 1600-400 cm^{-1} (b) 3050-2960 cm^{-1} (c) Dependency of electroactive β phase on $CsCuCl_3$ wt%.

gradually increased. Super-posed band at ~840 cm^{-1} is used to determine the relative proportion of electroactive phase content in the samples. Relative electroactive phase content (FEA) for all the samples is assessed using the following equation:

$$F_{EA} = \frac{A_{840}}{\frac{K_{840}}{K_{764}}A_{764} + A_{840}} \times 100\%$$

where A_{764} and A_{840} stand for, respectively, the absorbance intensities at 764 and 840 cm^{-1}. K_{764} and K_{840}, with respective values of 6.1 x 104 and 7.7 x 104 cm^2/mol, are absorption coefficients that correspond to the aforementioned bands. [8]. Up to 4wt% perovskite loading increment, the samples' electroactive phase content grew; beyond that, it declined (Fig. 2b). The maximum F_{EA} percentage for PVCS 4 is about 92%, compared to a maximum of 38% for

PVDF film. We listed the phase content of the samples against the composition of the perovskite to facilitate comparison in Table 1. The $CsCuCl_3$ compound's positive surface charge interacts with the PVDF chain's -CH_2-CF_2- dipole to increase the percentage of electroactive phase in the composites. Such contact is minimal because PVCS 3 and PVCS 5 contain less perovskite, which in turn restricts the conversion from α phase to β phase. More contact is produced by filler that is evenly distributed throughout the polymer matrix and has a relatively high perovskite loading (PVCS 4). Beyond 4 weight percent of filler, perovskite aggregates inside the polymer matrix and the surface charge interaction with the dipole is reduced. The FTIR spectrum in the region of 3050-2960 cm^{-1} in Fig. 2 clearly shows the interfacial interaction of $CsCuCl_3$ with PVDF dipole analysing the electroactive phase generation via interfacial contact, the absorption peaks at 2980 and 3023 cm^{-1} associated to the symmetric and asymmetric -CH_2- bond stretching, respectively, have tremendous significance.[3] The sole explanation for the shifting of these peaks is the disturbance of vibrational bands. When comparing composite films to PVDF alone, both peaks are blue-shifted, indicating interaction between the perovskite and PVDF dipoles. The effective mass of -CH_2 molecules was increased by an increase in interfacial interactions, which also caused the aforementioned molecules' vibrational frequency to decrease. Such contact serves as a dampening source. Under damped and undamped conditions, the angular frequency of the -CH_2 stretching vibration dipole is correlated with the damping constant. The amount of perovskite in the film is found to enhance the assessed values of damping constants. It is important to notice that F_{EA} and damping constant behave similarly to perovskite loading in this context. Such comparable behaviour points to a causal connection between the interaction of the diploes with $CsCuCl_3$ and phase development in the PVDF matrix. Analysis of these peaks also indicated that PVCS 4 had the largest β phase composition, which was supported by the FTIR data.

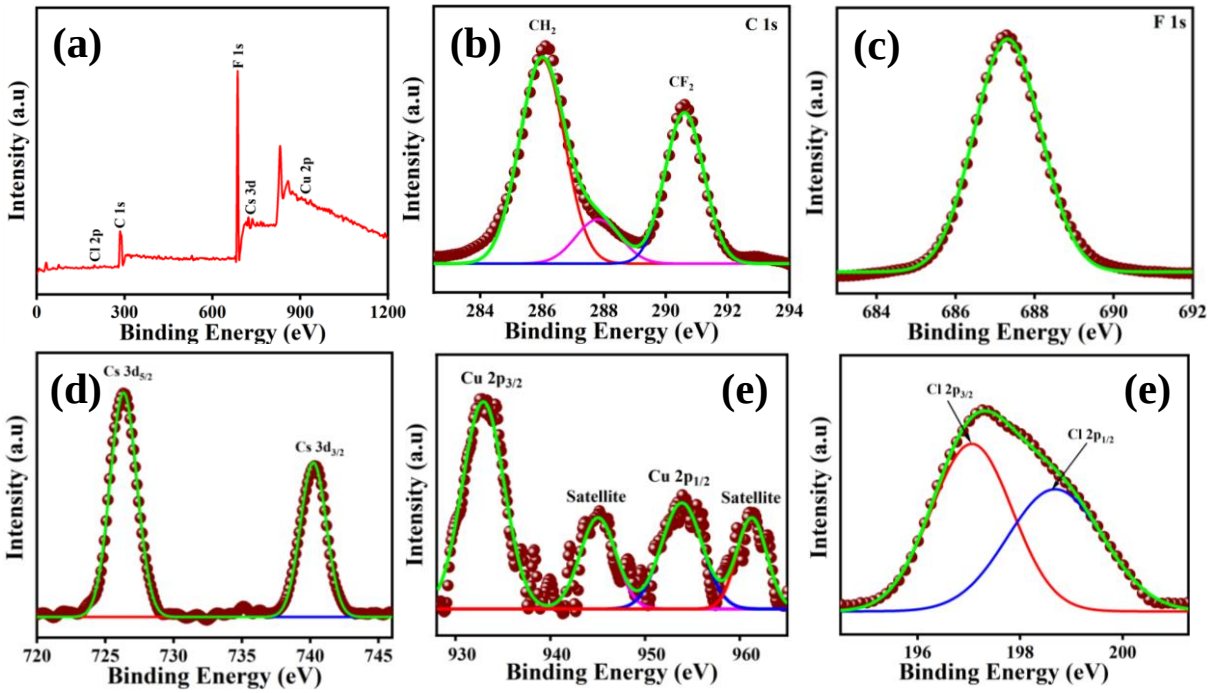

Figure:3 (a)-(e) XPS image of $CsCuCl_3$, Florine, CH_2-CF_2 Bond

Further confirmation of the chemical makeup and oxidation states of the components of Cscucl3, PVDF, and PVCS 4 is provided by x-ray photoelectron spectra (XPS). All of the spectra were charge-corrected using the C1s peak, which was located at 284.6 eV. The Cs and Cu XPS spectra of the $CsCuCl_3$ sample shown in the Figures 3. showed typical doublet characteristics for both metals. Peaks for Cs $3d_{3/2}$ and $3d_{5/2}$ are seen at 740.4 and 726.36 eV, respectively, whereas Cu $2p_{3/2}$ and $4p_{1/2}$ peaks are visible at 935.46 and 955.57 eV, respectively. Deconvolution of the Cl_3-related asymmetric gaussian curve yields two peaks at 197.05 and 199.05 eV, which are associated with the Cl_3 $2p_{3/2}$ and $2p_{1/2}$, respectively. These peaks' positions imply that all of the component elements (Cs, Cu, and Cl_3) are in their typical oxidation states, namely the 1, 2, and 1- states. The C1s peak in pure PVDF showed two components with energies of 286.1 eV and 290.5 eV, which correspond to the CH_2 and CF_2 bonds, respectively. Fluorine's 1s peak is a single, well-fitting Gaussian curve with a symmetric

peak at 687.2 eV. The typical peaks of $CsCuCl_3$ move to lower binding energies whereas a C1s and F1s peak for PVCS 4 is discovered to be pushed towards higher binding energies. From Fig. 3a-e, it is clear that the binding energies for PVCS 4 have changed in relation to the base samples. Such a change in binding energies may be attributed to the hybrid formation's internal electric field production, which has a considerable impact on the local binding energies of the base materials.

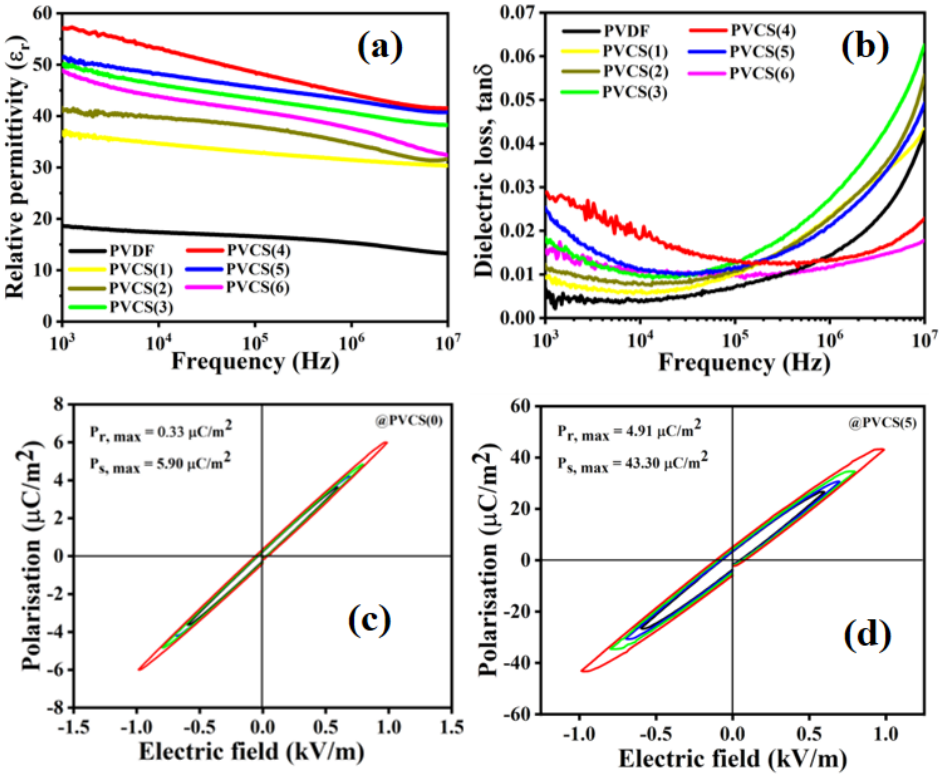

Figure 4 (a) variation of ε_r with frequency (b) variation of dielectric loss with frequency (c) and (d) P-E loop of PVDF and PVC 0 and PVC 4 hybrid films (inset shows variation in remanent and saturation polarization as a function of perovskite loading)

Figure 4c and d shows the P-E hysteresis loop of all the samples, monitored by sweeping the electric field (E) in a window of ± 1 kV/m at room temperature. The remanent polarization (P_r) for PVDF is 0.33 μC/cm^2. Under an applied field of 1 kV/cm, the saturation polarizations for PVDF and PVCS 4 attained 5.90 and 43.30 μC/cm^2 respectively. Remanent polarization, saturation polarization and coercive field values. Comparison of these loops suggests

maximum values of the remanent and saturation polarization for PVCS 4. Such increment in remanent polarization and saturation polarization in PVCS 4 indicates higher dipole moment per unit volume in PVDF chain (CH_2-CF_2) present in the hybrid. Much lower remanent polarization for PVDF than the hybrid is due to less dipole-dipole interaction. Pristine PVDF is largely composed of α phase having no dipole moment, while the composite is largely composed of electroactive β phase with higher dipole moment. Addition of perovskite in PVDF eases the dipole alignment in the hybrid system which ensued in the higher values of remanent polarization. Such high remanent polarization is expected to produce higher piezo output.

4 c shows the variation in the samples' saturation and remanent polarisation as a function of the amount of inserted perovskite. It is discovered that when the sample's perovskite concentration rises, remanent polarisation does as well. Under a specific electric field, it is discovered that the hybrid has a substantially better energy storage density than the PVDF. This improvement may be attributable to an increase in dielectric constant brought on by the uniform distribution of perovskites and an improvement in interface compatibility in the polymer matrix.

The dielectric behaviour of hybrids was similarly affected by the pairing of perovskites with PVDF. Figures show the dielectric constant (r), dielectric loss (tan), shown as functions of frequency for all samples, spanning from optical range 1 kHz to 10 MHz, respectively. This figure also suggests a rapid step down in ε_r values for the hybrid samples with increasing frequency. Perovskite incorporation in hybrid increases the interfacial space charge which ensures more space charge polarization and subsequently the ε_r value increases.

Ionic, electronic, interfacial, and dipolar polarizations all cause a sizable increase in r with respect to a constant applied voltage at low frequencies. However, due to a weakening of the interfacial / space polarisation, the aforementioned values are decreased at high frequency in the applied frequency window. The fluctuation of dielectric loss as a function of frequency is

seen in Fig. 4 a Pure PVDF exhibits a dielectric loss of 0.06 at 1 kHz, whereas hybrid films have a range of 0.008 to 0.03. Due to PVDF's relaxation loss, the dielectric loss of all the films rose over 10 kHz. This examined frequency window's nominal dielectric loss raises questions about the value of hybrid films. This could happen as a result of a strong polarisation effect and a long relaxation period for dipole orientation in the field's direction. However, the same values grow rapidly in frequency. The polarisation effect is negligible at high frequencies. Additionally, the dipoles self-assemble more quickly along the applied field. The relationship between a material's dielectric constant and piezoelectric coefficient is direct. The hybrid films' piezoelectric properties improve with higher remanent polarisation and piezoelectric constant. The inset of Fig. compares the dielectric constants and piezoelectric coefficient (d_{33}) of PVDF and hybrid films as a function of $CsCuCl_3$ wt%.

Films with a size of 1x1 cm2 were utilised to create nanogenerators in order to assess the piezo output voltage as a function of various base materials and the applied periodic force. We created a number of nanogenerators using both pure PVDF and hybrid samples. Fabricated nanogenerators using virgin PVDF are referred to as reference generators and given the designation PVCS 0. Other hybrid-prepared nanogenerators are designated as PVCS 1, PVCS 2, PVCS 3, and PVCS 4, PVCS 5, PVCS 6 where the associated numeric with PVCS denotes the weight percentage of $CsCuCl_3$ in hybrids. All devices' piezoelectric outputs are analysed without the use of any extra electrical poling. The open circuit voltage (Voc) and short circuit current (Isc) of each device are shown in Figures periodic hammering by hand with constant amplitude.

Variation in output power for different wt% of $CsCuCl_3$ i.e., for different PVCSs shown Fig 5 discloses maximum output power with power of 4.24 mW at 4 wt % of $CsCuCl_3$ loading in the

composite (PVCS 4). To quantify the instantaneous output power of the PVCS 4, dependence of output voltage and current on the load resistance (R_L) is studied. RL is varied from 10 KΩ to 10 MΩ while applied periodic pressure is kept constant (Fig.). Instantaneous voltage drops across the resistances increased gradually with the increment of RL and gets saturated at high resistance, equivalent to the V_{oc} at a high resistance. In contrast, short circuit current (Isc) is found to decrease with the increase of RL. Fig.# displays the load resistance vs. power graph. From the graph, maximum instantaneous power delivered at load resistance of 3.5 MΩ and reached to ~30 μW. This result suggests that, as an energy harvesting source PVCS 5 is sensitive over a wide range of load resistance. Furthermore, it agrees well with linear circuit theory which measures the internal resistance of PVCS 4 of 3.5 MΩ. To explain the observed piezoelectric performance and account for such noticeable differences among the devices, understanding of basic fundamental of non-polarised and piezo-electrically enhanced PVDF is crucial. PVDF, a nonconjugated linear fluorinated hydrocarbon, formed by repeating unit of –(CH_2–CF_2)– carries a vacuum dipole moment of pointing roughly from negative fluorine atom to positive hydrogen atom. Based on their macromolecular chain conformations of trans and gauge linkage, PVDF generally exhibits four different polymorphs namely α, β, γ and δ phase. Both packing of the molecules and chain conformations affect the orientation of dipole. α-phase is thermodynamically stable polymorph at ambient. Owing to anti-parallel packing of the chains in unit cell, dipole moments cancel out, rendering this phase as non-polar one. Without any electric poling or mechanical stresses PVDF film mostly results in α-phase. Although α phase does not exhibit piezoelectric features, it is usually a precursor of other active piezoelectric phases. In contrast to the above, β phase crystal structure possesses the hydrogen atoms are at one side and fluorine atoms on other side of the polymer chain. Because of the stronger electron affinity, fluorine atoms of the chain pull away the shared electron from hydrogen atoms. Electronegativity differences of these two atoms ensue net dipole moment in

a stacked direction inside β phase. Dipole moment per unit cell is maximum for β phase as compare to other phases. To obtain β phase, different strategies have been documented, mainly aiming on inclusion of filler and development of suitable processing route. When this stacked polymer chain is subjected to a mechanical stress, local dipole distribution changes and an electric field induces in the stack. Induced electric field gathers the charges at top and bottom electrode, presenting the principle of piezoelectricity. When these electrodes are connected with external load, piezo-potential prompts the electrons to flow through the load so as to screen the piezo-potential partially and attain a new equilibrium. In PVDF, piezoelectricity is mainly governed by volume electrostriction. It is noteworthy to mention here that output peak value is caused by the change in piezoelectric material content in the piezoelectric/polymer composite. Furthermore, presence of fillers in PVDF matrix might increase the local electric field and can enhance the domain mobility of the localized stress points, thus contribute in improving overall polarization. Here, $CsCuCl_3$ act as filler. It played vital role in transferring non-polar phase of PVDF to polar one, which helped the hybrid to acquire electroactive features. With the incorporation of $CsCuCl_3$ in PVDF, dielectric permittivity of the composite also improved. Increment in dielectric constant of the film ensued an improvement in piezo response since piezoelectric coefficient is directly proportional to the dielectric permittivity of the material. Further, presence of CsCuCl3 in PVDF also increased overall crystallinity of the hybrid and the interaction between perovskite and PVDF induced high yield of the β phase. Degree of crystallinity followed the similar kind of behaviour as the β-phase content. Relying these, PVCS 4 delivered highest piezo response among all. To access the impact of β phase constitution and thereby to get an account on the observed piezo response, we have further calculated the piezoelectric coefficient (d_{33}) of the all the samples. In d_{33} coefficient, first subscript denotes the direction of electric field and second subscript stands for the direction of mechanical deformation or stress. the d_{33} values and β phase content for all the samples at

different perovskite loading. d_{33} variation in the samples showed exactly similar nature as the β phase content. The maximum d_{33} value, 62.7 pC/N, is reached for the PCS 4 with highest β-phase content (~92%). d_{33} value of a sample is determined by the number of oriented dipoles; therefore, explanation of the observed behaviour is that higher electroactive β phase constitution implies larger availability of dipoles able to be oriented. For low β-phase content, orientation of dipoles is hindered in the samples due to the dispersion in an α-phase matrix. Maximum d_{33} value for PCS 4 is attributed to its highest β phase content among all synthesized samples as higher β phase infers larger availability of dipoles able to be oriented. Similar kind of results are also observed by the other researchers also. For a facile comparative view, we have also tabulated the β-phase content and d_{33} coefficient for the all samples in . For the practical usage a PVCS 4

For the practical usage a PVCS 4 was connected to a number of commercially available green light-emitting diodes (LEDs) using a bridge rectifier. Generated power from PVCS 4 under periodic compressive and releasing stress is sufficient to turn on 30 LEDs without any storage device, shown in Fig. Fig. 5g and h shows the output voltage in forward and reverse connection respectively which confirm that the output is due to piezo response. DC outputs signal for PVCS 4 presented in Fig. 6a also suggest a constant output voltage ~220 V.

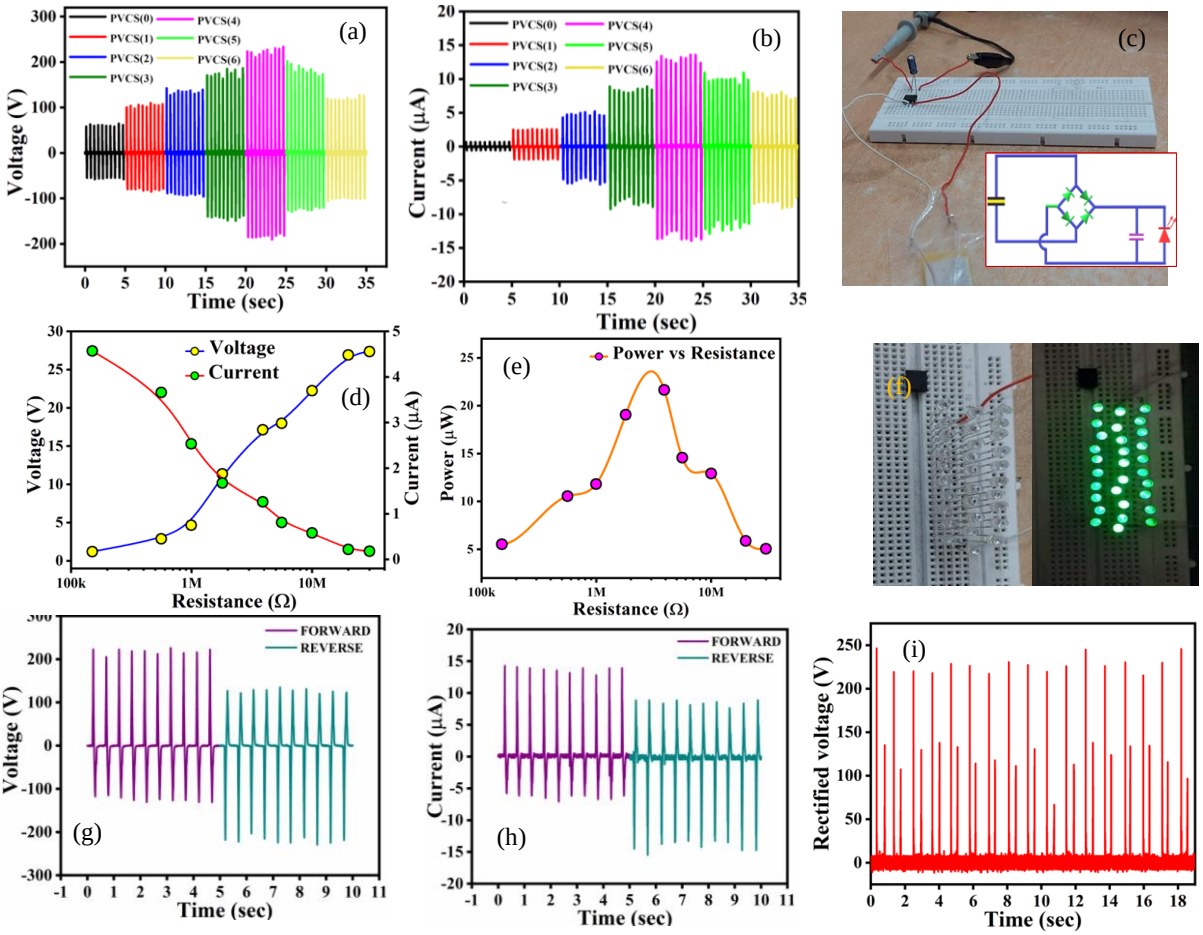

Figure :**5 (a) Output voltage (b) current of all the PNGs. (c)CCircuit diagram of PENG (d) Variation in output voltage and current vs resistance (e) output power variation with wt% $CsCuCl_3$ (f) equivalent diagram and glowing of 30 LED bulbs with constant hammering. Output voltage (g) forward connection (h) reverse connection (i) rectified DC output voltage of PVCS.**

Table 1

Device structure	Filler	Voltage (volt)	Current/current Density	Power/power density	Stability cycle	Ref.
Cerium Complex - PVDF	Cerium complex	32	-	-	-	[7]
ZnS/PDMS film	ZnS	35	-	2.43 μW/cm^3	-	[8]

CTAB modified Montmorillonite incorporated PVDF	CTAB modified	42	1.9 μA	50.72 mW/cm3	50	[9]
$BaTiO_3$-PDMS	$BaTiO_3$	126.3	77.6 μA/cm2	7 mW/cm2	-	[10]
PVDF/$Al2O_3$ decorated rGO	$Al2O_3$/rGO	36	3.4 μA	-	-	[11]
PVDF - $CH_3NH_3PbBr_3$	$CH_3NH_3PbBr_3$	5	0.06 μA	-	3600	[12]
P(VDF-TrFE)/boron nitride	Boron nitride nanotubes	22	0.64 μA	-	-	[13]
$ZnSnO_3$-PDMS	$ZnSnO_3$	20	1 μA/cm2			[14]
$BaTiO_3$ and graphitic carbon	PZT/MW-CNTs)	100	10 μA	-	600	[15]
$FAPbBr_3$ -PDMS	$FAPbBr_3$	8.5	3.8 μA/cm2			[16]
PVDF-$ErCl_3$. 6H2O	$ErCl_3$·6H2O	115V	32 μA	160 mW/cm2		[17]
$BaTiO_3$/P(VDF-TrFE)	$BaTiO_3$	6 V	2 μA/cm2	1.4 μW/cm2		[18]
$CsCuCl_3$-PVDF	$CsCuCl_3$	120 V	35 μA	4.24 mW	15000	[19]

To test the feasibility of the practical application of the PVCS, the PVCS is directly connected with 30 commercial LEDs in parallel but opposite directions without any storage units. When the PVCS is impacted by hand, the red LED is instantly lit, and the green LED is lit by reverse output after release as shown in Figure 6b and. Then, a typical rectifier was employed in order to convert the generated ac to dc output. Figure 6b shows the output voltage signal rectified.

To test the capacitor's charging capability from the PVCS, the capacitors of 1.0, 4.7, and 10 μF were charged by the rectified output with the PVCS, respectively; the concerning transient response is exhibited in Figure 6. It is observed that the charging voltages increased gradually and eventually reached the maximum value of 3.5, 3, and 2 V within 26, 38, and 48s, respectively. The above result indicates that the PVCS 4 can be seen as a promising power source device for tiny energy harvesting applications and self-powering electronic devices. Moreover, in order to prove the stability of the PVCS 4, a durability test was carried out over 1000 cycles. As shown in Figure 6a, no degradation in the output performance is observed even after 1000 cycles. The $CsCuCl_3$–PVDF-based nanogenerator shows exceptionally durable and reliable energy harvesting performance.

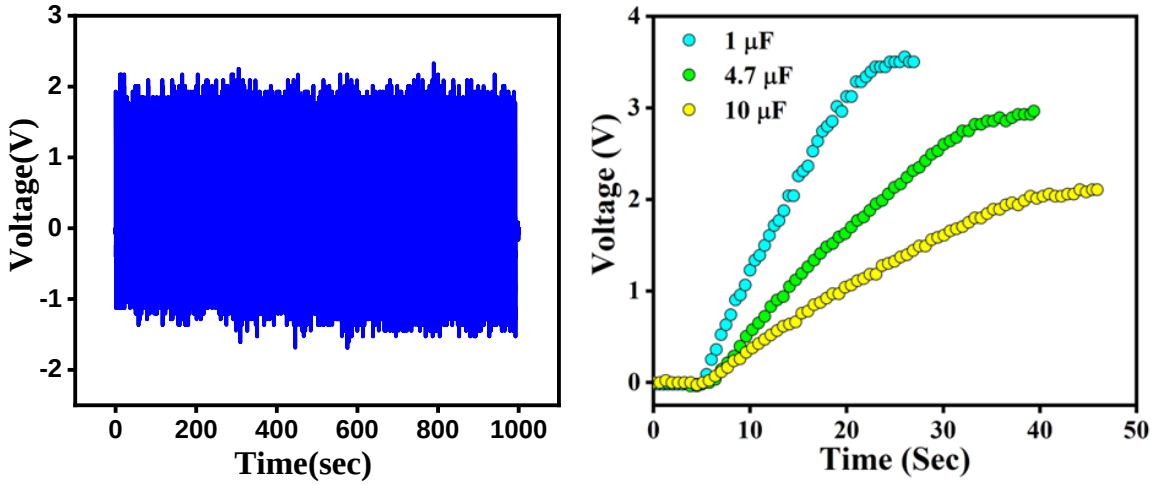

Figure 6: long cycle and capacitance charging of PVCS

Furthermore, different types of body movements such as, Toe pressing, finger bending, finger tapping, neck bending, Elbow Bending, Knee bending are available in our daily life. These are very ideal biomechanical energy sources for human based self-powered devices. We verified the viability of our fabricated PVCS to harvest the biomechanical energy for developing human

based self-powered devices. We performed different types of sensitivity of PVCS under various conditions, e.g., Toe pressing, finger bending, finger tapping, as shown in Figure 7 a-f

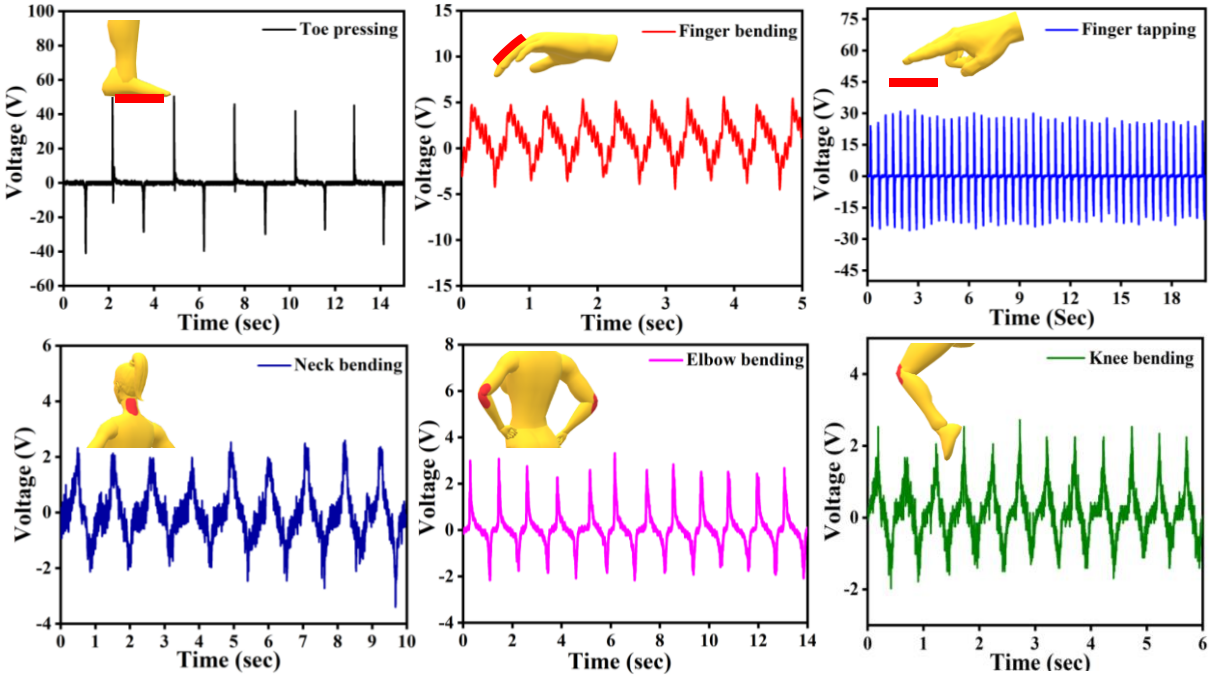

Figure 7: Output voltage generation from PVCS subjected to different deformations, such as (a)Toe pressing, (b)finger bending, (c)finger tapping, (d) neck bending, (e)Elbow Bending, (f)Knee bending with respective schematic structure

As can be seen, under toe pressing the generated voltage is quite higher than the other conditions. This could be due to the availability of more effective area for deformation under toe pressing condition. Under bending mode, the mechanically active surface area is less than finger tapping and toe pressing. Thus, the all bending mode shows low output voltage than the other two modes of human body movement, as shown in Figure 7. We also investigated other types of sensitivity of the PVCS under various conditions, e.g., finger bending, finger neck bending, Elbow Bending, Knee bending, comparatively weak signal (≈3 to ≈4 V) was observed for bending (at elbow) and elbow bending (≈6 V) than that obtained from finger tapping (≈31 V) and toe pressing (≈52 V) response. This is due to the more deformation of crystal structure in the nanocomposite with large effective area during walking/running. These features suggest

that the device can be used to harvest the biomechanical energy during hand folding, walking, and running conditions both in outdoor and indoor circumstances. It is well known that the generated output voltage of the PVDF based PVCS is closely related to the alignment of different dipoles of PVDF in presence of nanofillers. Furthermore, as we avoided any electrical poling, thus alignment of the dipoles arises from the applied stress, i.e., strain applied on the crystalline zone of the PVDF/$CsCuCl_3$nanocomposite. We could thus utilize the biomechanical energy from treadmill during running where people usually spend significant time in everyday's life. In this context, the harvesting capability of the PVCS was investigated under running/walking condition (PVCS is attached with shoes) in daily life, which generated an output voltage up to ≈55 V. this highly durable PVCS sheet could be placed as inner layer, may be an alternative source for storage of biomechanical energy to power up various portable electronic devices such as LEDs, LCD screen, and/or even charging of mobile phone.

Conclusion

In essence, we have created a piezoelectric nanogenerator employing PVDF and rod-shaped $CsCuCl_3$ nanoform. Maximum -phase was visible in the hybrid sample with 4 wt% perovskite, which was roughly 2-fold that of pure PVDF. Under repeated hand hammering, PVCS based on this sample delivered an instantaneous voltage of around 200 V. The same's performance was also tested using several fundamental human motions. When you bent PVCS 4 with your leg you got an output of 55 V. LEDs might also be lit up by PVCS 4 without the need for external bias. These findings emphasise the hybrid's potential use as a foldable and wearable energy harvester and, consequently, its incorporation into smart gadgets.

Reference

[1] 3 Zi, Yunlong, and Zhong Lin Wang. "Nanogenerators: An emerging technology towards nanoenergy." Apl Materials 5.7 (2017): 074103.

[2] Gaur, Anupama, et al. "Flexible, lead-free nanogenerators using poly (vinylidene fluoride) nanocomposites." *Energy & Fuels* 34.5 (2020): 6239-6244.

[3] Sahu, Manisha, et al. "Piezoelectric nanogenerator based on lead-free flexible PVDF-barium titanate composite films for driving low power electronics." *Crystals* 11.2 (2021): 85.

[4] Mondal, Suvankar, et al. "Human motion interactive mechanical energy harvester based on all inorganic perovskite-PVDF." *Nano Energy* 74 (2020): 104870.

[5] Ailneni, Ravi Charan, et al. "Influence of the wearable posture correction sensor on head and neck posture: Sitting and standing workstations." *Work* 62.1 (2019): 27-35.

[6] Guo, Wenzhe, et al. "Wireless piezoelectric devices based on electrospun PVDF/BaTiO 3 NW nanocomposite fibers for human motion monitoring." *Nanoscale* 10.37 (2018): 17751-17760.

[7] S. Garain, T.K. Sinha, P. Adhikary, K. Henkel, S. Sen, S. Ram, C. Sinha, D. Schmeißer, D. Mandal, ACS Appl. Mater. Interfaces 7 (2015) 1298–1307.

[8] A. Sultana, M.M. Alam, S. Garain, T.K. Sinha, T.R. Middya, D. Mandal, ACS Appl. Mater. Interfaces 7 (2015) 19091–19097.

[9] P. Biswas, N.A. Hoque, P. Thakur, M.M. Saikh, S. Roy, F. Khatun, B. Bagchi, S. Das, ACS Sustain. Chem. Eng. 7 (2019) 4801–4813.

[10] N.R. Alluri, A. Chandrasekhar, V. Vivekananthan, Y. Purusothaman, S. Selvarajan, J.H. Jeong, S.J. Kim, ACS Sustain. Chem. Eng. 5 (2017) 4730–4738.

[11] S.K. Karan, R. Bera, S. Paria, A.K. Das, S. Maiti, A. Maitra, B.B. Khatua, Adv. Energy Mater. 6 (2016) 1601016.

[12] Sultana, Ayesha, et al. "Organo-lead halide perovskite regulated green light emitting poly (vinylidene fluoride) electrospun nanofiber mat and its potential utility for ambient mechanical energy harvesting application." *Nano Energy* 49 (2018): 380-392.

[13] S. Ye, C. Cheng, X. Chen, X. Chen, J. Shao, J. Zhang, H. Hu, H. Tian, X. Li, L. Ma, W. Jia, Nano Energy 60 (2019) 701–714.

[14] K.Y. Lee, D. Kim, J.H. Lee, T.Y. Kim, M.K. Gupta, S.W. Kim, Adv. Funct. Mater. 24 (2014) 37–43.

[15] K.I. Park, C.K. Jeong, J. Ryu, G.T. Hwang, K.J. Lee, Adv. Energy Mater. 3 (2013) 1539–1544.

[16] R. Ding, H. Liu, X. Zhang, J. Xiao, R. Kishor, H. Sun, B. Zhu, G. Chen, F. Gao, X. Feng, J. Chen, Adv. Funct. Mater. 26 (2016) 7708–7716.

[17] N.A. Hoque, P. Thakur, S. Roy, A. Kool, B. Bagchi, P. Biswas, M.M. Saikh, F. Khatun, S. Das, P.P. Ray, ACS Appl. Mater. Interfaces 9 (2017) 23048–23059.

[18] S.H. Wankhade, S. Tiwari, A. Gaur, P. Maiti, Energy Rep. 6 (2020) 358–364.

[19] X. Zhou, K. Parida, O. Halevi, Y. Liu, J. Xiong, S. Magdassi, P.S. Lee, Nano Energy 72 (2020) 104676.

[20] T. Yang, Y. Zheng, Z. Du, W. Liu, Z. Yang, F. Gao, L. Wang, K.C. Chou, X. Hou, W. Yang, ACS Nano 12 (2018) 1611–1617

Chapter 5

Grand conclusion and Scope for future works

Conclusion

Alternative choices like solar energy, wind energy, tidal energy, etc. are now being worked upon in order to create mega-gigawatts of energy due to the supply of fossil fuels becoming limited and their detrimental effects on the environment. The widespread use of low-power electronic, optoelectronic, and sensor devices, which survive on considerably reduced, dispersed, and transportable power demands, is essential for many modern daily tasks. Such systems need low-cost, very effective, and reliable energy harvesting and storage options. For the growth of technology and the quality of human existence, numerous such devices are required for personal and portable electronics, healthcare, infrastructure monitoring, environmental protection, defence, and security. The demand for sensor networks itself is developing and is anticipated to reach a trillion dollars by the year 2022 as an example of the huge canvas of such expanding devices and corresponding low power needs. The majority of these types of sensor systems have power needs between nano and microwatts. The batteries are the typical portable power supply devices. These, however, are larger and hazardous to the environment. They also have challenges with recycling and a short lifespan. Therefore, new choices for self-sufficient and sustainable tiny power systems must be created. Given that a large portion of India is rural and has several sensing needs for agriculture, it is very desirable that such small power is harnessed locally.

The first chapter contains the fundamentals of nanoscience and technology, their applications, and the definitions of perovskite material and nanogenerators as well as their dielectric characteristics. The discussion of the researchers' work on various Perovskite-based nanogenerator types and perovskite dopes in PVDF or composite-based nanogenerators is covered in **the second chapter**. Their essay demonstrates a variety of cheap and simple

methods. In their publications, they demonstrate a variety of excellent daily applications**. The third chapter**, explained the primary synthesis process and characterization, including how the machine works and which equipment utilises our synthesis process and electrical characterization. **The fourth chapter** explains Polyvinylidene fluoride (PVDF) and caesium copper chloride ($CsCuCl_3$) hybrid films change into valuable functional materials for piezoelectric-based mechanical energy harvesters. A piezoelectric nanogenerator (PNG) constructed from a combination of PVDF and $CsCuCl_3$ displayed notable output performance. provides for high crystallinity and electroactive-phase nucleation of 92% in the PVDF Perovskite concertation was enhanced in composites to attain benchmark level output responsiveness. PNG constructed with 4wt% CsCuCl3 in PVDF demonstrated an instantaneous output voltage and current of 220 V and 13 μA. It also proved endurance under difficult conditions and long-cycle stability (1,000 cycles). Additionally, electricity from the PNG was utilised to power 30 LEDs and charge a capacitor. The results that were obtained are quite significant and reveal the viability of developing revolutionary smart devices employing this class of perovskites.

Future work

Over the past few years, many electronic device systems, particularly for small-scale applications, have been demonstrated. On the basis of this background, we offer a few suggestions for potential large-scale energy scavenging uses below.

1. **Multi-layered large-scale designs**: Piezoelectric nanogenerators' power output is the main barrier to the eventual commercialization of this technology. Therefore, we would like to suggest a flexible polymer-based multilayer large-scale design for the NGs. The layer-by-layer device design has been tried in the past to increase the device's piezoelectric power output. In such a vast area, transparent and flexible devices can be utilised as flags or drapes to capture

wind energy. Hybrids with CNTs or graphene can also be used to create similar kinds of systems. These load-bearing structures can be utilised to generate mechanical power on sidewalks or in jogging parks.

2. **Bio-compatible stretchable membranes:** As previously said, piezoelectric energy harvesting technology allows sensor networks, personal gadgets, and healthcare devices to operate on their power by capturing the energy from mechanical work schedules. We suggest employing piezoelectric ceramic nanostructures, such as BSTO (barium strontium titanate) nanofibers created using electrospinning, to design biocompatible stretchy membranes. These ceramics are lead-free. They are naturally non-toxic and biocompatible. Furthermore, they have greater piezoelectric coefficients than $BaTiO_3$ which has not been doped. These ceramic fibres can also be used to create hybrid systems by combining them with PDMS (stretchable matrix) and CNT/Graphene (mechanically strengthening materials). These stretchable matrices can be employed as biocompatible stretchable patches for monitoring blood pressure, blood sugar levels, heart rate, etc.

3. **Nanomaterials growth for Triboelectric nanogenerator (TENG):** Electrospinning creates several fascinating nanostructures for a range of uses. The power generating range has been elevated to the level of Kilowatts in the previous three to four years because of the development of (TENG). This nanogenerator operates based on electrostatic interaction and contact electrification. The electronegative series is typically used as the foundation for the material selection for this type of nanogenerator. Furthermore, compared to homogeneous flat surfaces, protruding/pointed structures have much greater power production efficiency. We suggest using electrospinning to create protruding structures, and then growing caterpillar-like needle-like pointed structures (needle structures) on top of them to create 3D hybrid networks, which will increase the device's power output.

4. **Nanostructured ceramics by electrospinning for piezo magnetic applications:** Investigating the potential linkage of the materials' piezoelectric and magnetic capabilities is another intriguing feature for future inventive applications of the nanogenerator investigation. In recent literature, active sensors have been developed using piezoelectric nanogenerators (PENG). We suggest using the NGs in magnetoelectric actuators as well as using them to detect weak magnetic fields.

We come to the conclusion that newer materials, nanoscale designs, and unique device ideas may be used to expand research on self-powered Nano systems in a number of new areas that are both technologically beneficial and scientifically interesting. We are optimistic that this study will eventually be able to meet the challenging demands of a widespread yet sparsely distributed source of energy for our contemporary environment, which is powered by electrical device systems.